

Functional role of parallel circuits in the hippocampus

Inauguraldissertation

zur

Erlangung der Würde eines Doktors der Philosophie
vorgelegt der
Philosophisch-Naturwissenschaftlichen Fakultät
Der Universität Basel

von

Annapoorani Udhayachandran

Von India

Basel, 2017

Original document stored on the publication server of the University of Basel
edoc.unibas.ch



This work is licenced under the agreement
„Attribution Non-Commercial No Derivatives – 3.0 Switzerland“ (CC BY-NC-ND 3.0
CH). The complete text may be reviewed here:
creativecommons.org/licenses/by-nc-nd/3.0/ch/deed.en

Genehmigt von der Philosophisch-Naturwissenschaftlichen Fakultät
auf

Antrag von

Prof.Dr.Pico Caroni
(Dissertationsleiter)

Prof.Dr.Silvia Arber
(Korreferent)

Basel, 08.12.2015

Prof. Dr. Jörg Schibler
(Dekan)

Table Of Contents

Acknowledgements.....	5
Preface.....	6
Abbreviations.....	7
1.Introduction.....	9
The Hippocampus.....	10
Hippocampal function.....	10
Hippocampus dependent learning paradigms.....	11
Contextual fear conditioning	
Morris water maze	
Familiar object recognition	
Hippocampal neuroanatomy.....	13
The mossy fiber projection.....	16
Hippocampal principal neuron subpopulations.....	18
Hippocampal interneurons and microcircuitry.....	20
Aims and rationale of the thesis.....	22
2.Results.....	24
Distinct hippocampal principal neuron subpopulations exhibit c-Fos plasticity upon provisional and definite learning	
 Abstract.....	25
 Introduction.....	25
 Results.....	27
 Discussion.....	40

**Alteration of specific connectivity in Lsi1 principal neuron subpopulation
results in partial learning.**

Abstract.....	44
Introduction.....	44
Results.....	48
Discussion.....	71
3.General Discussion and Outlook.....	74
4.Materials and Methods.....	78
5.Bibliography.....	88
6.Curriculum Vitae.....	100

Acknowledgements

First of all, I thank Prof. Dr. Pico Caroni for being my mentor and allowing me to work in his lab for my PhD. Thank you Pico for your guidance, discussions and support.

I thank the members of my thesis committee; Dr. Silvia Arber and Dr. Jan Pielage for their insightful inputs and comments, which helped me, shape my project to its current stage.

I would like to thank Flavio for teaching me the various techniques from slice culture to performing surgeries...Grazie mille Flavio for introducing me to "the world of neurocircuits" and for the discussions right from my PhD interviews! Thank you Arghya for your friendship, all the conversations from neuroscience to travelling to anything and everything. Thankyou Maria for all the pep talk and chat sessions. Thankyou Francesco and Sarah for all the scientific advice at various occasions especially during the starting days of my PhD. I would like to thank Kerstin, Mike, Smitha, Fernando, Ananya, Melissa, Komal, Sebastian, Matteo, Maria Spolidoro, Dominique, Manxia, Swananda, Roberta and all the other members of the Caroni group for a lively scientific environment, for all their support, useful comments and also for all the discussions scientific and otherwise.

Many thanks to the members of FAIM facility, animal house facility for all their support during the course of my PhD.

I would like to thank Appa, Amma and Dharini for their moral support, prayers and most importantly trusting my decisions and letting me pursue my interest. I thank all my family and friends for their encouragement and for being there for me in times of need. A special mention to Gobi Thaatha and Bhavesh anna. My sincere thanks to Late Prof. Dr. Abitha Devi for her extremely contagious scientific enthusiasm. A very big thank you to JB Ma'm for her constant support, motivation, for all the long conversations and time. Last but not the least I thank my husband, Vasanth who stood by me all the time, for understanding all the extended hours of work in the lab and many many more...Nandri Vachu for everything!

Preface

Learning and memory is a continuous and dynamic process. It involves an orchestra of distinct and dissociable events across various ensembles or circuits in the brain that are highly specialized to process specific aspects of the event. A proper functioning of these neuronal ensembles largely depends on the specificity of the connections between neurons that is established during development. Specificity of connections within the structure and between neurons in different structures are both important. Gaining insight into this microcircuitry allows better understanding of the role of each structure in learning and memory.

One of the primary structures involved in learning and memory is the hippocampal formation. Although the gross anatomy of hippocampus and its role in learning has been studied extensively, little is known about the microcircuits that underlie the computations involved.

In this thesis, I explore how the hippocampal principal neurons contribute to learning and memory. In the first part I investigated the roles of principal neuron subpopulations in various hippocampal learning paradigms such as one-time association learning, incremental learning and incidental learning using activity and plasticity markers. In the second part of the thesis, I explored how the selective connectivity contributes to the hippocampal memory formation. In order to do so, I have pharmacologically altered the selective connectivity during early stages of circuit development and have observed structural and behavioral alterations in these mice as adults. These two parts together could help understand the requirement of parallel microcircuits in hippocampal function.

Abbreviations

BSA	Bovine Serum Albumin
CA	Cornu Ammonis
CCK	Cholecystokinin
cFC	contextual Fear Conditioning
DG	Dentate Gyrus
DIV	Day in vitro
EC	Entorhinal cortex
EE	Environmental Enrichment
FOR	Familiar Object Recognition
FFI	Feed Forward Inhibition
GABA	Gamma Amino butyric acid
GC	Granule cell
IN	Interneuron
LMT	Large Mossy Fiber Terminals
L-NAME	N^{ω} -Nitro-L-arginine methyl ester hydrochloride
LV	Lentivirus
mGFP	membrane targeted Green Fluorescent Protein
MWM	Morris Water Maze
P	Postnatal Day
PC	Pyramidal cell
pCREB	phosphorylated cAMP Response Element-Binding protein
pERK	phosphorylated Extracellular signal-regulated kinases
PFA	Paraformaldehyde
PNN	Perineuronal net
PP	Perforant Path
PV	Parvalbumin
RFP	Red Fluorescent Protein
SC	Swim control
Str luc	Stratum Lucidum

Str.pyr	Stratum Pyramidale
Str.rad	Stratum radiatum
TA	Terminal Arborization
TE	Thorny Excrescences
v	Ventral
VIP	Vasoactive Intestinal Peptide

1.Introduction

1.1 The Hippocampus:

The Hippocampus is an integral part of medial temporal lobe of the brain. It is functionally relevant in both cognitive and emotional aspects of learning and memory in day-to-day activities. In the following sections, I would elaborate on the functional role of the hippocampus and its neuroanatomy.

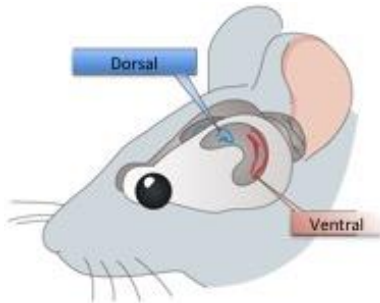


Figure 1: Position of hippocampus in mouse brain

Depiction of rodent hippocampus and its position in the brain. Each hippocampus is a C-shaped structure (only the left one is highlighted) located in the caudal part of the brain. The top portion close to the upper surface of the brain is the dorsal hippocampus whereas the caudal and inferior portion constitutes the ventral hippocampus. A cross-sectional view of dorsal and ventral hippocampus is depicted in blue and red respectively. (Modified from Bannerman DM et al., 2014)

1.1.1 Hippocampal function:

Hippocampus has been implicated in various memory formation since the case of patient HM. He lost the ability to form any new memories post bilateral removal of hippocampus and its adjacent parts owing to his seizures (Scoville and Milner, 1957). In general, different functions of the hippocampus are attributed to different regions along the dorso-ventral axis: memory and cognition to dorsal part and emotions to ventral part of hippocampus based on various lesion studies, gene expression data and connectivity to other regions (Fanselow and Dong, 2010). However, from recent studies across different species, it is evident that there are not only discrete transitions in the functional organization of the hippocampus along the long axis, but also there are some gradual transitions (Strange et al., 2014) that are superimposed.

The role of hippocampus in **spatial memory** has become more prominent since the discovery of place cells in the hippocampus and lesion studies in hippocampus that could impair spatial memory. Place cells are also thought to

work together with the grid cells (Hafting et al., 2005), head direction cells (Sargolini et al., 2006) and border cells (Solstad et al., 2008) in the entorhinal cortex to determine accurately the space and orientation of the animal in a given environment. It has also been shown that the entire hippocampus has place fields with dorsal encompassing small place fields (order of 1 meter) whereas ventral has much larger place fields (order of 10 meters) in rodents (Kjelstrup et al., 2008). Such graded and multi-scale representation of space provides hippocampus with computational advantages on spatial resolution and contiguity. Although it is not clear if there exists a similar gradient representation of space in primates due to technical limitations, fMRI studies in virtual reality setup show increased activation of posterior (dorsal in rodents) when complexity of the context increases whereas increased activation in anterior (ventral in rodents) in larger mazes (Baumann and Mattingley, 2013).

Declarative memory or explicit memory refers to memories that require a conscious recollection such as facts and verbal knowledge. It can be further divided into episodic (what, where and when an event occurs) and semantic memory (factual knowledge extracted from experience) (Tulving, 1972). Owing to hippocampal connectivity with amygdala (Pikkarainen et al., 1999; Pitkänen, 2000; Petrovich 2001; Kishi et al., 2006) and hypothalamus, hippocampus has also been implicated in **emotions**.

Apart from the above mentioned functions, due to its gradient connectivity with nucleus accumbens (Groenewegen et al., 1987) and mesolimbic dopamine system (Legault et al., 2000), hippocampal activity especially ventral, affects locomotion and goal directed behavior (Ruediger et al., 2012). Thus hippocampus, plays a critical role in the generation, recombination, and flexible use of information of all kind.

1.1.2 Hippocampus dependent learning paradigms:

In this section I discuss about some of the hippocampal dependent learning paradigms. Although these paradigms are dependent on hippocampus, they often include interaction of the hippocampus with other networks for example prefrontal cortex, midbrain neuromodulator systems.

Contextual fear conditioning:

Contexts are routinely encoded without awareness (Barrett and Kensinger 2010) as they serve as a basis for recollecting the past, interpreting the present and anticipating the future. To understand the neural circuitry of how context is encoded and retrieved, many studies have used associative learning (for example, Pavlovian fear conditioning). In Pavlovian contextual fear conditioning, the subjects are exposed to a noxious unconditioned stimulus (US) such as foot shock along with a harmless conditioned stimulus (CS) – the context. On re-exposure to the CS, if the animal had made the association of CS and US, it will demonstrate a fear response. In rodents, a fear response mainly is demonstrated by freezing behavior along with reduction of exploratory behavior. It is further accompanied changes in the activity of the autonomous nervous system and the release of stress hormones (Iwata and LeDoux 1988; LeDoux 2000). It has been shown that animals that have been shocked upon immediate placement in a context do not show context conditioning (Fanselow, 1990). Hence it is important to encode the context before presenting the unconditioned stimulus. Hippocampus has been shown to be involved in contextual fear memory acquisition and recall through lesion studies (Philips and LeDoux, 1992). However, this contextual fear conditioning memory is hippocampal dependent for about a month post the acquisition.

Further secondary experiences post acquisition of contextual fear conditioning can modify or eliminate the fear memory associated to the context. This is achieved through the process of reconsolidation and extinction respectively. Reconsolidation happens upon a short duration re-exposure with or without modified US and / or CS that can strengthen or change the existing memory trace (Nader 2003, Suzuki et al., 2004). When the CS is repeatedly presented without US or if CS is presented for longer durations without US then there is a behavioral suppression of fear and it is called extinction (Myers and Davis 2002, Phelps et al., 2004). Protein synthesis is essential for reconsolidation and extinction memory. However, blocking protein synthesis affects the original fear memory in reconsolidation whereas during extinction it affects only the formation of new extinction memory and the original fear memory remains untouched (Eisenberg et al., 2003, Pedreira and Maldonado, 2003, Suzuki et al., 2004).

Morris water maze:

Morris water maze is widely used to study spatial learning and memory in rodents (Morris et al., 1982). Rodents in a pool of opaque water have to find the escape platform using the spatial cues presented outside the pool. Unlike the contextual fear conditioning which is one-time associative learning, water maze requires multiple exposures over a few days to the maze for efficient learning. Hence water maze is classified as incremental learning. Many hippocampal lesion (partial and complete) studies show the importance of hippocampus in water maze learning and reference memory. (Morris et al., 1982, Moser et al., 1995). Additionally, different parts of hippocampal longitudinal axis have been shown to participate in different stages of water maze and serve different functions (Ruediger et al., 2012).

Familiar object recognition:

It is a test to determine if animals can recognize and discriminate the familiar object and novel object. It is often reported as Novel object recognition (NOR). Since this test does not involve any subjective or reinforcement learning, it is a form of declarative memory. This paradigm consists of two sessions – acquisition and test session. The animal is introduced to two identical objects during acquisition. In the test session, a novel object replaces one of the identical objects and the discrimination index is calculated by the time spent with the novel object and familiar object. This paradigm is fairly simple and hence used in various species to test for memory – from rats to humans (Zola et al., 2000, Mumby and Pinel, 1994, Clark et al., 2001, Nemanic et al., 2004, Reed and Squire, 1997, Manns et al., 2003). All the above-mentioned studies elucidate the involvement of hippocampus and parahippocampus in the familiar object recognition memory.

1.2 Hippocampal neuroanatomy:

The rodent hippocampal formation is a C-shaped structure located in the medial temporal lobe. It mainly comprises of three regions that are constituted by different principal neuron (excitatory) cells: Dentate gyrus (DG) is primarily composed of granule cells and mossy cells, Cornu Ammonis (CA) further is divided as CA1, CA2 and CA3 which is constituted by pyramidal cells that

possess special characteristics in each region and subiculum that has its own pyramidal cells and it connects the hippocampus proper to the entorhinal cortex. The flow of information from entorhinal cortex (EC) to hippocampus proper and then back to entorhinal cortex is largely unidirectional, with each stage adding to unique feature of the information. This closed loop constitutes the classical trisynaptic circuitry of the hippocampus. Layer II of the entorhinal cortex (lateral and medial) projects to the granule cells in the DG through “Perforant Path” (PP) which then through the mossy fiber axons projects to CA3 pyramidal neurons that in turn projects to CA1 pyramidal neurons via Schaffer collaterals which finally projects back to entorhinal cortex (Layer III and Layer V) *en route* subiculum. Moreover, CA3 also sends and receives input from CA3 through associational connections. The PP innervates the CA3 and CA1 pyramidal cells directly apart from the granule cells in DG. Additionally, EC Layer III sends direct inputs largely to CA1 and subiculum. Since regions with largely parallel organization (EC layer III, DG, CA1) and the strongly recurrent excitatory networks (EC Layer II and V, CA3) are sandwiched between one another (figure 2: right), the neuronal representations can be iteratively segregated and integrated respectively at successive regions (Buzsáki., 2010). There is a differential flow of information within each of these regions and between the regions brought about by the interplay of the above-mentioned excitatory networks and the interneurons (explained in detail in 1.2.1) present within each of its region. This further allows some spatio-temporally discrete dynamics for intrahippocampal processing and for effective communication of hippocampus to neocortex facilitating various types of network oscillations. As shown in figure 2, all regions of the hippocampus possess a high degree of lamination, which facilitates the spatio-temporal dynamics of information processing.

The DG has three layers: superficially closest to the hippocampal fissure is the cell free layer- molecular layer which is primarily comprised of granule cell dendrites that receives inputs from the entorhinal afferents and it also contains some pre/parasubicular fibers and some interneurons; the principal cell layer is called the granule cell layer that is deep to the molecular layer and consists of densely packed granule cell somas; the last one is the polymorphic cell layer and it has a variety of cells the primary one being the mossy cells. Mossy cells send its input through commissural/associational fibers (Blackstad 1956, 1958).

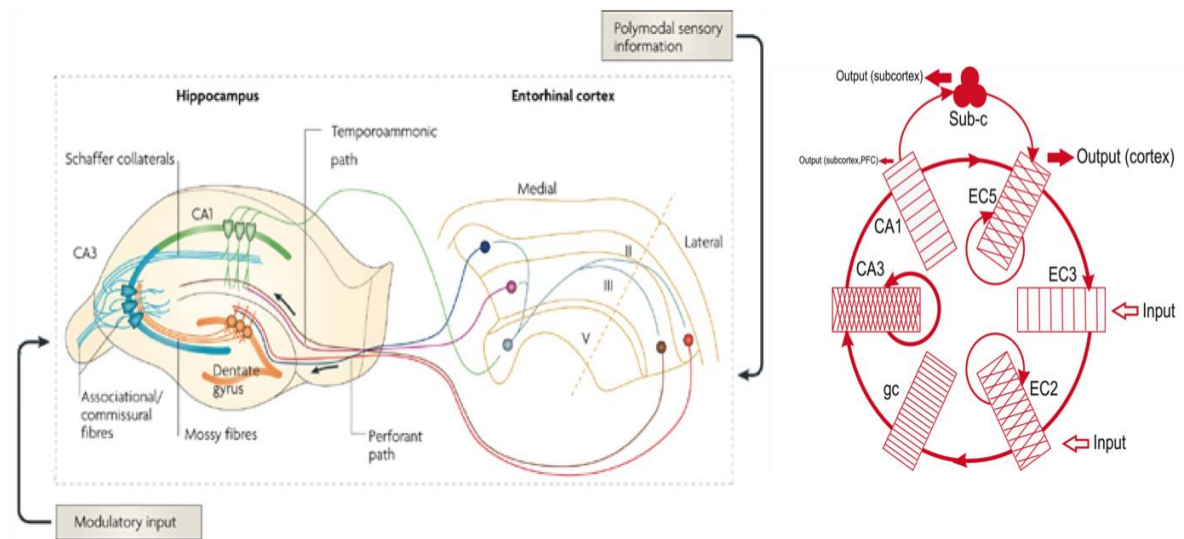


Figure2: Basic anatomy of the hippocampus (left) and Organization of excitatory hippocampal network (right).

The entorhinal projections to the hippocampus proper and back to entorhinal cortex are elaborated. Note that there is a high degree of lamination in the inputs received from EC and within the hippocampus. On the right is the main excitatory path in Hippocampus-EC feed forward loop. (From Neves et al., 2008 and Buzsáki, 2010)

The principal cellular layer in CA1, 2 and 3 is the pyramidal cell layer, which is primarily comprised of pyramidal cell somas and also has the axo-axonic cells and basket cells. CA1 pyramidal layer is more tightly packed than CA2 and CA3. The cell-free layer located deep to the pyramidal cell layer is the stratum oriens that has mainly the basal dendrites of pyramidal neurons and several classes of interneurons. Some of the CA3-CA3 associational fibers and some CA3 to CA1 Schaffer collaterals are located in the stratum oriens. A cell free layer called stratum lucidum exists exclusively below the CA3 pyramidal cell layer. It mainly contains the mossy fiber axons of the granule cells that innervate CA3. The layer superficial to stratum lucidum in CA3 and to that of the pyramidal cell layer of the CA2 and CA1 is the stratum radiatum. It contains the CA3 to CA3 associational connections and CA3-CA1 Schaffer collaterals. The stratum radiatum and stratum oriens have the following interneurons: PV NPY, Ivy and CCK cells. The most superficial layer of the hippocampus is the stratum lacunosum-moleculare (SLM) where the fibers from entorhinal cortex and afferents from nucleus reunions terminate. SLM also has O-LM interneurons, CCK and neurogliaform cells.

1.2.1 The mossy fiber projection:

The dentate granule cells project via its unmyelinated axons majorly to CA3 and some CA2 (Kohara et al., 2013). These axons were termed as mossy fibers by Ramon y Cajal owing to its similarity to the mossy fibers in the cerebellum. These axons have unique, large (>3 μm upto even 8 μm) and complex en passant presynaptic terminals called the large mossy fiber terminals (LMTs). Each granule cell gives rise to 11-15 LMTs and each CA3 neuron receives input from ~45 granule cells (Amaral et al., 1990; Acsady et al., 1998). The LMTs form highly irregular, complex, interdigitated attachments with CA3 pyramidal cells through finely branched spines called thorny excrescences. These thorny excrescences consist of a single neck connecting to about 1-15 spine heads (Hamlyn 1962; Amaral 1978; Stirling and Bliss 1978; Amaral and Dent 1981; Chicurel and Harris 1992). Typically, thorny excrescence is contacted by a single LMT, however each LMT can contact several thorny excrescences from the same CA3(Chicurel and Harris 1992; Kamondi et al. 1998). In the proximal portion of CA3 (CA3c) thorny excrescences are found both in the apical and basal dendrites (owing to the infrapyramidal bundle of mossy fiber axons). However, in CA3b and CA3a, thorny excrescences are prevalent only in the apical dendrites that traverse through stratum lucidum. A single LMT can have as many as 37 individual synaptic release sites onto the CA3 pyramidal neuron that can generate large postsynaptic currents. LMTs are hence called as a “detonator synapse” as they can powerfully activate a particular subset of the CA3 network (Henze et al., 2000). In addition, mossy fiber axons form small en-passant varicosities that synapse onto GABAergic interneurons along CA3. These mossy fiber axons also extend longitudinally towards the ventral hippocampus at the CA3/CA2 border for about 2mm. However, this is more in the dorsal and almost absent in the most ventral part. (Amaral and Dent 1981, Lavenex et al., 2007).

Further LMTs can exhibit “satellites” that are connected to the main core through 10-200 μm processes (Galimberti et al., 2006). These satellites can establish contacts onto the same pyramidal neurons in CA3, thus mediating the feed forward excitation (FFE). The LMTs can have filopodial extensions originating from its complex core. These LMT filopodial extensions and the *en passant* varicosities along the axons can establish synapses with GABAergic

interneurons that in turn makes inhibitory synapses on CA3 pyramidal neurons eventually inhibiting the CA3 (Acsady et al., 1998, Szabadics and Soltesz, 2009). This constitutes the feed forward inhibition (FFI) component of the LMTs. FFI mediated by LMTs can control the excitability of the CA3 pyramidal neuron by preventing excessive depolarization and burst (Lawrence et al., 2003 and 2004, Torborg et al, 2010). However unlike other FFI in the cortex, mossy fiber driven feed forward inhibition does not substantially influence the timing of single action potentials in CA3 firing (Torborg et al., 2010).

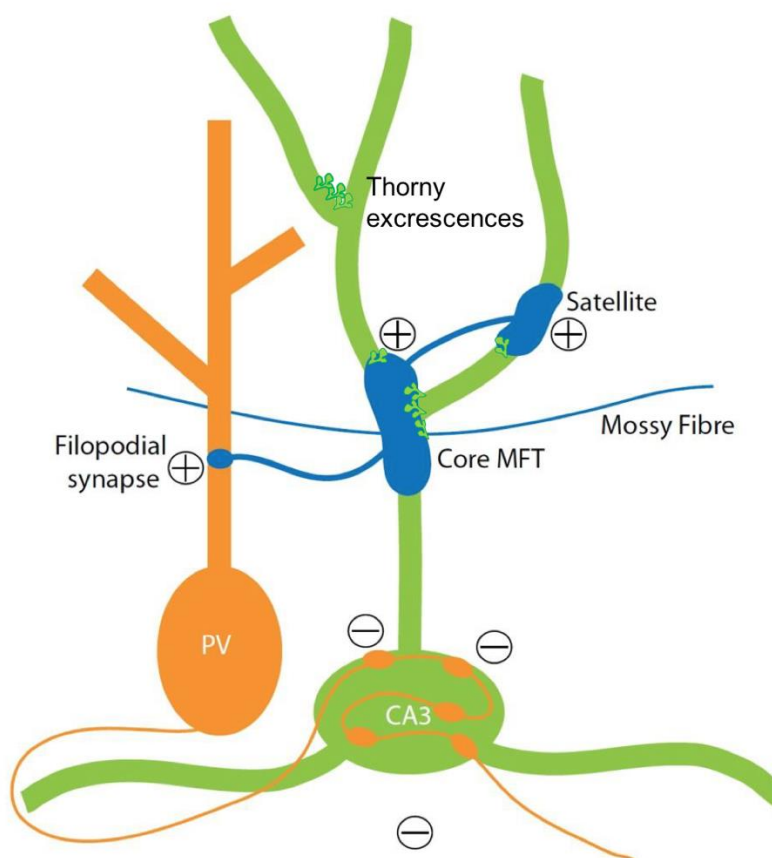


Figure3: Schematic microcircuitry in CA3.(Modified from Donato et al, 2013). The LMTs are able to mediate feed forward excitation through its core and satellite synapses onto CA3 pyramidal cells. Note the presence of thorny excrescences, a special synapse found exclusively in stratum lucidum of CA3 where the LMTs are usually present. LMTs also mediate feed forward inhibition by recruiting PV + interneurons through filopodial synapses.

Since there is recruitment of inhibitory neurons at various stages of the DG to CA3 (regulation of granule cell firing by hilar mossy cells, Granule cells- CA3 transmission through FFI, CA3 back projection through feed back inhibition) as well as a powerful excitatory drive by the LMTs through thorny excrescences ,

fine tuning of this circuit results in activation of specific granule cells that further enables strong excitation of specific subsets of CA3. Apart from this, the thorny excrescence itself can undergo modifications during stress (Stewart et al., 2005), hibernation (Magarinos et al., 2006) , age (Ojo et al., 2013) and learning (Sandi et al., 2003; Stewart et al, 2005). Additionally, it has been shown that the thorny excrescences are severely reduced in NCAM –KO mice (Cremer et al., 1997) and in Alzheimer patients (Tsamis et al,2010). Moreover recently, it has been demonstrated that in a transchromosomal mouse line Tc1, an animal model of down syndrome, defects in DG-CA3 synapses (structural complexity and electrophysiological properties) was central to the cognitive disabilities (Witton et al., 2015).

1.2.2 Hippocampal principal neuron subpopulations:

Neuronal circuits are organized in a way to process specific kinds of information. Neurons within these networks can form preferential connections forming microcircuits for efficient processing. Hippocampus principal neurons have been identified to contain at least two subpopulations of principal neurons that are generated during distinct time windows and are preferentially connected among themselves across the three main subfields (DG, CA3, CA1). These neurons were labeled distinctly Thy1-mGFP reporter lines (Lsi1 and Lsi2) and were further established to have matched patterns of gene expression, and windows of neurogenesis and synaptogenesis (Deguchi et al., 2011). These two subpopulations together contribute to about 45% of the total hippocampal principal neurons.

Additionally, granule cells of these two subpopulations also were found to have different number of highly plastic synapses called the Terminal Arborization (TA) along the mossy fiber axons. Lsi1 had 1 TA and Lsi2 had >2TA and the remaining mossy fibers exhibit no detectable TAs (Galimberti et al., 2010), Apart from this they also show distinct structural modification upon behavior – upon fear conditioning there is increase in filopodia in the LMTs in Lsi1 (Ruediger et al., 2011) whereas Lsi2 LMTs increase the number of satellites of the LMTs upon Enriched environment for 3 weeks (Bednarek et al., 2011).

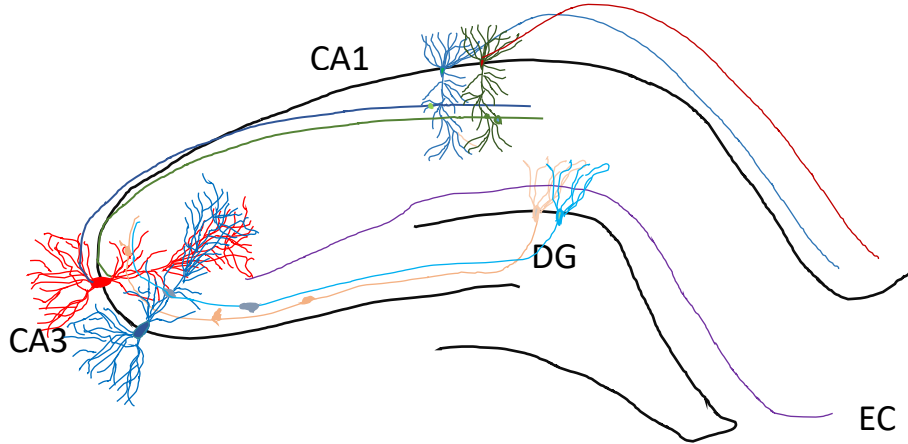


Figure4: Hippocampal trisynaptic circuitry with matched subpopulation of principal neurons. Lsi1 is preferentially connected to Lsi1(red) from DG-CA3 and from CA3 to CA1and similarly Lsi2 to Lsi2(blue).

There have been several other independent studies demonstrating the existence of different principal neuron subpopulations in the hippocampus. Early-born CA3 pyramidal neurons have been reported to have unique morphophysiological properties during development and as adults (Marissal et al., 2012). Although they have been classified as the hub cells that initiate network events during development, their role in adult remains to be discovered. The pyramidal cells in the deep and superficial layer of CA1 have altered firing rates, burst frequency, localization of place fields. Additionally, the deep and superficial layers had mismatched preferred phase of firing during REM sleep (Mizuseki et al., 2011). Further in ventral CA1, Parvalbumin expressing basket cells(PVBCs) inhibits the deep layer more than the superficial while superficial pyramidal cells sends more frequent excitatory inputs to PVBCs. Interestingly PVBCs received preferential excitation from PFC projecting pyramidal cells and preferentially innervates the amygdala projecting pyramidal cells thus creating distinct microcircuits in CA1(Lee et al., 2014). It has also been shown that principal neurons in CA1 and subiculum can be differentiated according to their bursting properties. These cell types exhibit differential plasticity by engaging mGluRs and mAChRs in addition to distinct morphological characteristics (Graves et al., 2012).

Apart from the above-mentioned differences in principal neuron subpopulations, there exists a difference at the genetic level that divides the

hippocampus CA3 septo-temporally and proximo-distally into nine non-overlapping domains of robust cohort of transcripts (Thompson et al., 2008).

Although it is clear that the cells in hippocampus are not homogenous, the microcircuits they form and the recruitment of the different classes of principal neurons in various functions of the hippocampus still remains to be addressed.

1.2.3 Hippocampal interneurons and microcircuitry:

GABAergic inhibitory interneurons are generated mostly in medial and caudal ganglionic eminence (MGE and CGE) while the rest of them are from lateral ganglionic eminence and preoptic area. These interneurons then undergo radial and tangential migration to reach their specific locations across the different regions in the brain (Anderson et al., 1997; Pleasure et al., 2000). Interneurons target the principal neurons and other interneurons at distinct sub-compartments leading to microcircuit formation. Depending on their subcellular specificity, interneurons have distinct effects on the principal neurons (Miles et al., 1996) and hence can dynamically recruit the principal neurons during defined phases of behavior including learning and memory formation (Nitz and Mc Naughton, 2004, Lapray et al., 2012). Perisomatic targeting interneurons like PV+ and CCK+ basket cells impinge on soma, axon initial segment and proximal dendrites and eventually regulate the output of the pyramidal cells directly. Since one interneuron can synapse on many pyramidal cells, activation of a perisomatic targeting interneuron can effectively inhibit large populations of pyramidal cells (Cobb et al., 1995, Miles et al, 1996). On the other hand, the dendrite targeting interneurons like SOM+ interneurons affect the input integration into the pyramidal cells and hence control efficacy and plasticity of glutamatergic inputs from different sources (Freund and Katona, 2007).

There are about 21 different classes of interneurons defined in hippocampal CA1 based on the location of their cell body and neurites, the expression of marker proteins, and electrophysiological properties (Klausberger and Somogyi, 2008). Although there is a plethora of interneurons, PV+ interneurons are among the extensively characterized interneurons as they are easily identifiable (fast spiking and posthoc labeling through immunohistochemistry) and can be genetically targeted efficiently through high selectivity of PV promoter for further manipulations. PV+ interneurons are also

highly interconnected among themselves (Muller et al., 2005) and along with their fast spiking nature, they contribute maximally to generate network synchrony. Through optogenetic manipulations and electrophysiology it is proved that PV+ interneurons by its strong influence on pyramidal cell firing affects the theta activity in CA1 whereas SOM+ interneurons have a weak influence on theta (Royer et al., 2012, Stark et al., 2012, Amilhon et al., 2015). The firing rate of PV+ basket cells altered according to the behavioral state of the rats with a strong increase in firing rate during sharp wave ripples (Lapray et al., 2012). Additionally, PV + interneurons are reported to form opposite, reversible and sustained network configurations with a low-PV network configuration (based on immunohistochemistry) in initial phases of learning and exploration whereas a high PV network configuration after learning and consolidation (Donato et al., 2013).

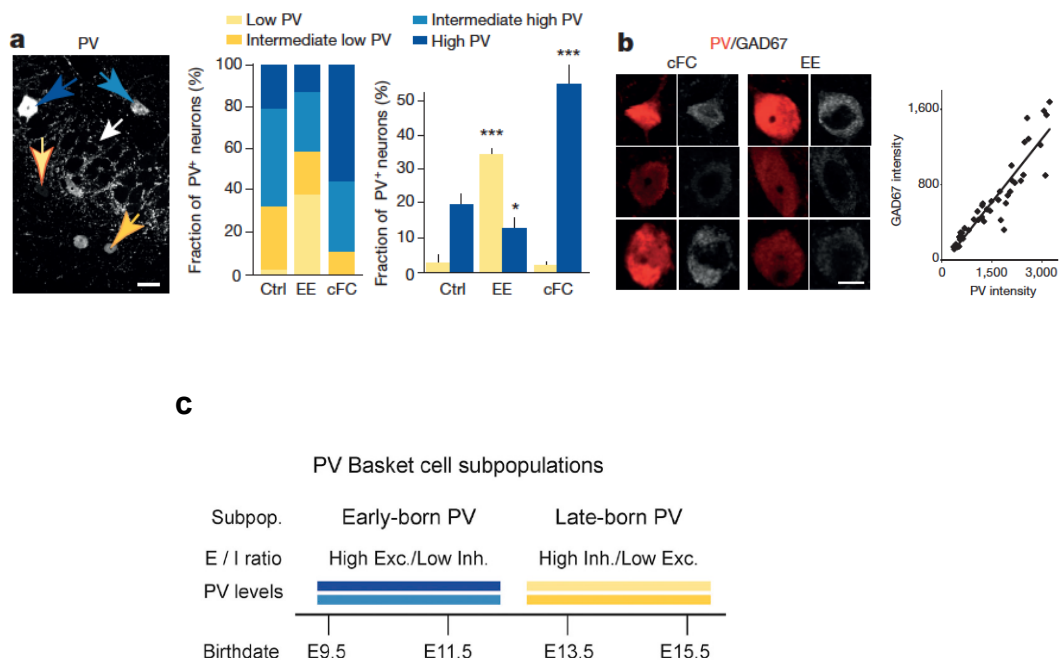


Figure5: Distinct plasticity in hippocampal PV basket cells and Schema for PV subpopulations. (Adapted from Donato et al., 2013 and Donato et al., 2015) Differential PV levels observed through immunohistochemistry. Experience dependent changes on PV network activity in hippocampal CA3 with changes in extreme PV levels upon enrichment and fear conditioning (a). PV intensity and GAD67 intensity are very well correlated. Schematic representation of PV levels in early and late born fractions (c).

High PV and low PV network configurations are mediated by two distinct subpopulations of PV+ interneurons. The PV+ interneuron subpopulations were defined by their time of neurogenesis and their altered induction of plasticity. Early born PV subpopulations were regulated through excitation while the late born PV through inhibition (Donato et al., 2015). This implies that there is a bidirectional involvement of PV+ interneurons during learning as PV+ interneurons regulate learning through network synchronization and learning induces plasticity in PV+ interneurons.

Aim and rationale of the thesis

The hippocampal formation is one of the primary structures involved in episodic and spatial memory. The rodent hippocampus has three main subdivisions: the dentate gyrus (DG), Cornu Ammonis 3 (CA3) and Cornu Ammonis 1 (CA1). Previous studies in the lab there are three or more principal neuron subpopulations in the hippocampus. Subpopulations Lsi1 and Lsi2 are revealed by mGFP expression in Thy1-mGFPreporter lines. Together, Lsi1 and Lsi2 constitute about 50% of total hippocampal principal neuron populations, and account for the earlier half of neurogenesis. Notably, Lsi1 and Lsi2 principal neurons are genetically matched and preferentially connected with themselves across hippocampal subdivisions: DG-CA3 (mossy fiber input), CA3-CA3 (recurrent collaterals), CA3-CA1 (Schaffer collaterals) [Deguchi Y et al., 2011], thus establishing partially separate parallel circuits in the hippocampus. This selective connectivity is achieved by matched window of neurogenesis and synaptogenesis.

In this thesis, the main question I address is what could be the role of parallel circuits (Lsi1 and Lsi2) in the hippocampus and how does selective connectivity contribute to their role. Although there are several studies that elucidate the role of hippocampus in learning and memory, they treat hippocampus as a single unit. The discovery of segregated pathways in the hippocampus implies that these could in principle allow differential processing of incoming information with little or complete absence of interference. Moreover, if these principal neuron subpopulations have distinct functional role or similar/additive role has not been found.

In order to ascertain the functional role of the principal neuron subpopulations, I have used different hippocampal dependent learning paradigms that could be largely grouped as temporary or provisional learning and definite learning. Further analysis of activity and plasticity markers post behavior helped to elucidate the possible functionality of these subpopulations. Since the selective connectivity was found to be temporally dependent, temporally regulated molecular cues that mediate DG-CA3 connections were tested using slice cultures and were further used to disrupt connectivity *in vivo*. The results obtained from the above-mentioned experiments are demonstrated in detail in the following sections.

2.RESULTS

2.1 Distinct hippocampal principal neuron subpopulations exhibit c-Fos plasticity upon provisional and definite learning

2.1.1 Abstract:

In this study, I investigated the role of hippocampal principal neuron subpopulations in learning and memory by testing for plasticity markers post behavior in general vs specific subpopulations namely Lsi1 and Lsi2. c-fos expression has been used extensively as a marker of plasticity for all the paradigms tested in this study. The analysis was done in CA3, CA1 and DG in ventral hippocampus. I demonstrate that Lsi1 pyramidal cells are recruited for temporary or provisional learning whereas Lsi2 pyramidal cells are recruited for definite learning. Additionally, I also show that short-term plasticity is observed in both the subpopulation, but only one of them is selectively recruited for long-term consolidation of each type of learning. Further, there can be a transient recruitment of both subpopulations in some learning phase for example in case of initial days of water maze or one trial extinction. However once the learning is definite, then it is taken over by one subpopulation. It also is interesting that during definite learning, there is increase in filopodia in the large mossy terminals of the subpopulation that is recruited for the provisional learning. Filopodia from LMTs recruit the PV neurons and mediates feed forward inhibition in CA3 (Ruediger et al., 2011,2012) which could imply that there is selective inhibition of one subpopulation and recruitment of the other in definite learning.

2.1.2 Introduction

Hippocampus is an important and integral part for learning and memory. It also exhibits various types of structural plasticity. Although the connectivity between neurons in a circuit are defined during development, there can be experience dependent structural modifications like gain/loss of synapses or rearrangement of pre-existing synapses. This process constitutes the structural plasticity as a result of which the properties of neuronal networks can be altered. There is a very small percentage of synapses that turns over spontaneously in baseline conditions and this forms the substrate for learning dependent plasticity. The remaining synapses are largely undisturbed throughout life (Holtmaat and Svoboda, 2009). For long-term memory formation, neurons undergo induction of new mRNA and protein synthesis after learning in order to modify their morphology or receptor densities. Although there are a lot of molecules that are

involved in the regulation of synaptic plasticity some of them have been used extensively as molecular markers. These molecular markers include immediate early genes like c-fos, Arc, zif268 (Sheng and Greenberg, 1990) and phosphorylated activity markers like pCREB, pERK1/2, CAMKII, protein kinase C (Trifilieff et al., 2006). Advanced techniques have allowed *in vivo* imaging of axonal and dendritic modifications over time and over different regions in the brain (Gu et al., 2014; Makino and Komiyama, 2015).

Further the inhibitory interneurons modulate the plasticity in the excitatory neurons and their synapses directly by inhibition or disinhibition (Hangya et al., 2014, Kepcs and Fishell, 2014). The strength of the input to GABAergic inhibitory interneurons can be altered depending on the experience (Ruediger et al., 2011; Chen and Nedivi, 2013; Donato et al., 2013). Although there are a variety of interneurons, the role PV basket cells have been extensively explored in learning. There is a shift to a low-PV-network configuration (based on immunohistochemistry) upon incremental trial and error learning that could facilitate consolidation and retrieval associations established by comparatively weak synaptic networks, whereas there is a shift to a high-PV-network configuration that promotes establishment of strong memories by comparatively strong synaptic networks upon contextual fear conditioning (Donato et al., 2013). Further this high PV and low PV network configurations is achieved by increased excitation and increased inhibition on to early born and late born PV neurons respectively (Donato et al., 2015). Other interneurons that are investigated include SOM and VIP that mediate disinhibition of pyramidal neurons upon learning. In summary, experience dependent structural plasticity occurs in both pre and post synapse and plays an important role in mediating learning and memory.

In this study, I looked at differences in structural plasticity in different subpopulations of principal neurons post various learning paradigms that results in high or low PV network configuration in CA3 and CA1 regions. Combining behavioral paradigms and confocal microscopy, I studied the behavioral function of hippocampal principal neuron subpopulations and analyzed the effect of learning and memory in Lsi1 and Lsi2 neurons.

2.1.3 Results

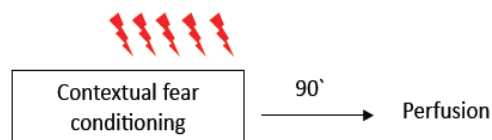
Differential recruitment of c-fos in contextual fear conditioning and Morris water maze

In this study, c-fos recruitment post two different behaviors namely contextual fear conditioning (cFC) and Morris water maze (MWM) were analyzed in specific subpopulations using the Lsi1 and Lsi2 Thy1mGFP lines. cFC is a form of definite learning whereas MWM is a form of incremental or trial and error learning where multiple trials over few days is essential before forming a definite memory. So the initial days of water maze can be considered as temporary learning, following which the mice form a definite memory.

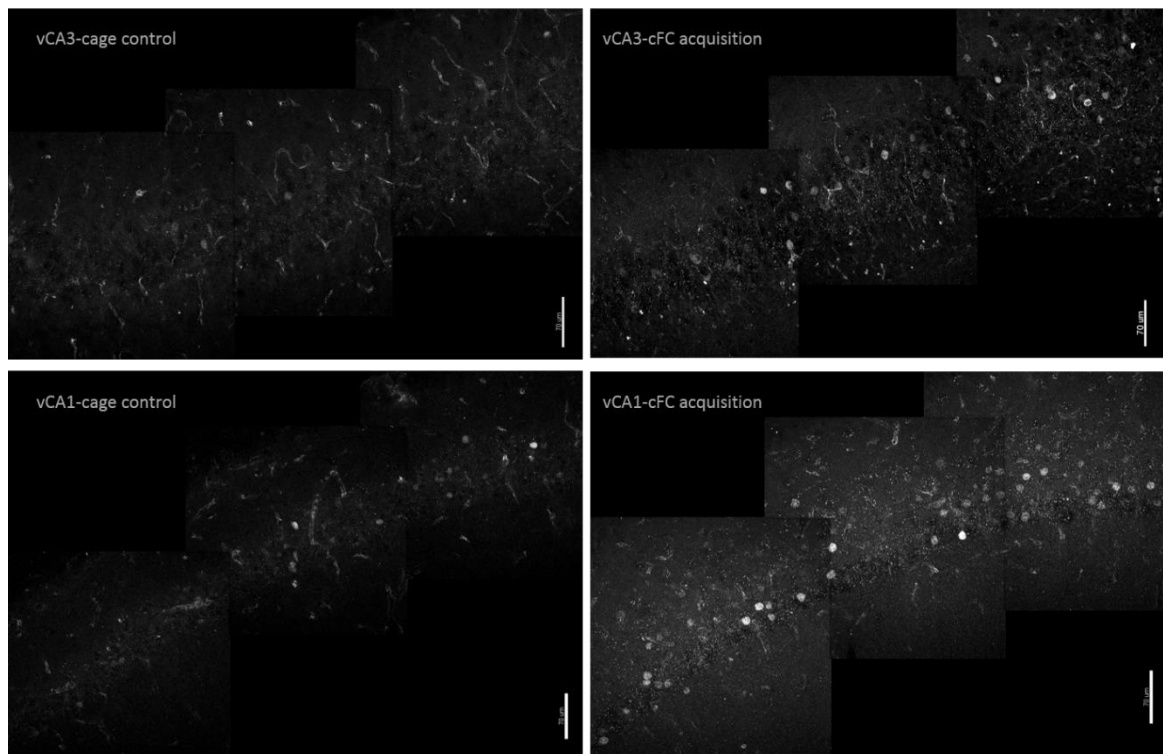
In cFC, mice are exposed to noxious unconditional stimuli-US (foot shock) within an otherwise harmless conditioned stimulus-CS (context). Re-exposure to the same context will elicit freezing in mice. Upon cFC acquisition, c-fos levels in CA3b and CA1b of ventral hippocampus increases in general population compared to the baseline (mean %cfos+/NeuN+ : CA3: baseline- 1.81121 ± 0.282706 , cFC - 4.2091 ± 0.4878 ; CA1: baseline- 1.6499 ± 0.5661 , cFC- 5.230564 ± 0.8253 Fig 2.1d). However, when the subpopulation specific c-fos expression is analyzed, only Lsi2 shows a larger increase than general population in c-fos expression compared to the baseline (mean %GFP+cfos+/GFP+: CA3: baseline- 1.7457 ± 0.06441 , cFC- 5.3284 ± 1.2590 ; CA1: baseline- 0.7118 ± 0.6475 , cFC- 4.3302 ± 1.5528 Fig 2.1d) and Lsi1 population remains unaltered upon cFC compared baseline (mean %GFP+cfos+/GFP+: CA3: baseline- 1.08927 ± 1.027355 , cFC- 1.3669 ± 1.0017 ; CA1: baseline- 0.6291 ± 0.6598 , cFC - 0.9771 ± 0.8466 Fig 2.1d). Generally even at baseline, the deep layer of CA3b had more c-fos expression than the superficial layer (mean % of total cfos cells: deep- 71.5491 ± 6.8143 , superficial – 28.4510 ± 6.8143). Thus contextual fear memory acquisition results in c-fos expression exclusively in Lsi2 principal neurons and not in Lsi1 neurons in both CA3 and CA1 region of the ventral hippocampus. It is interesting to note that CA3 and CA1 follow similar pattern of activation. It is also interesting that upon induction of c-fos post acquisition of cFC the increase in c-fos also was in the deep layer of CA3 (mean % of total cfos cells: deep- 67.4822 ± 3.9280 , superficial – 32.2573 ± 3.70124). In contrary to CA3, in CA1 c-fos is distributed equally in both superficial and deep layer (mean

% of total cfos cells: deep- 51.8817 ± 8.9425 , superficial – 48.11831 ± 8.9425) and the same distribution is maintained post acquisition (mean % of total cfos cells: deep- 50.2181 ± 4.8163 , superficial – 49.8471 ± 4.7185). The distribution of Lsi1 and Lsi2 cells in the ventral also follows a differential pattern in CA3 and CA1 owing to their neurogenesis schedule. (mean % of total cfos cells CA3 Lsi1: deep- 81.2721 ± 9.4326 , superficial – 18.8588 ± 9.4326 ; CA3 Lsi2 : deep- 77.3908 ± 7.1806 , superficial – 22.6092 ± 7.1806 ; CA1 Lsi1: deep- 56.7579 ± 14.3390 , superficial – 43.2426 ± 14.3390 ; CA1 Lsi2 : deep- 58.4709 ± 2.8374 , superficial – 41.5291 ± 2.8374 (fig2.1e)

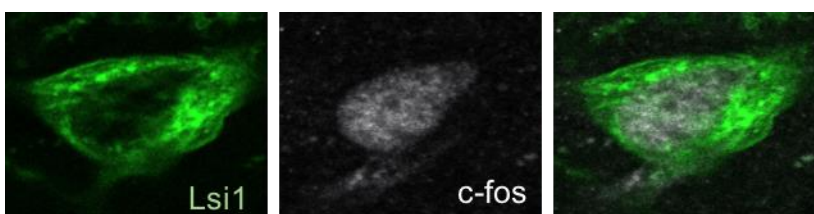
a



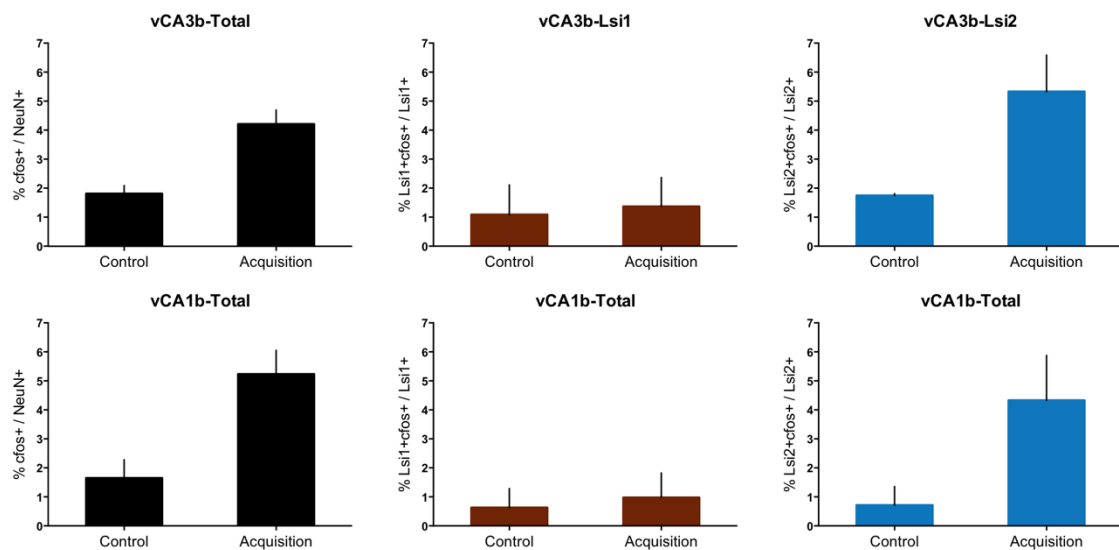
b



C



d



e

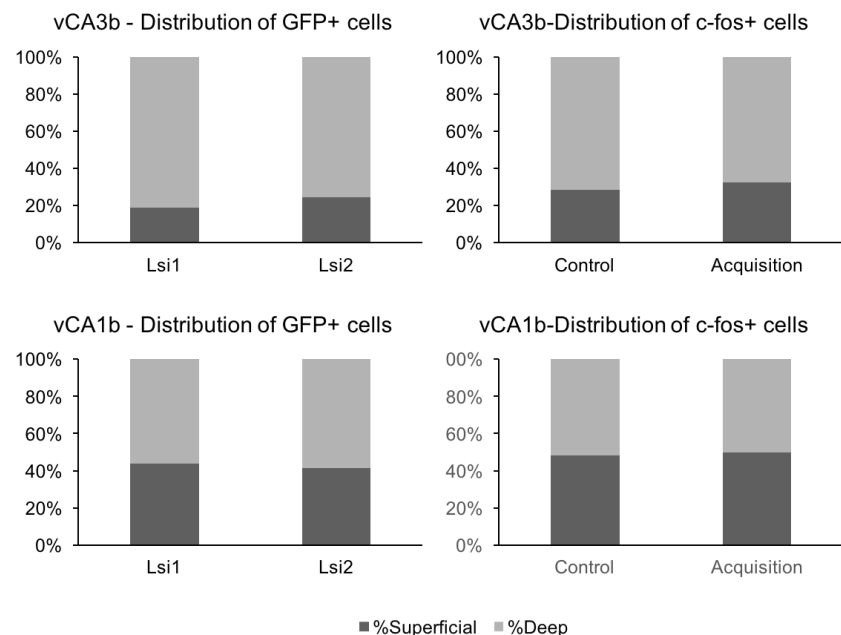


Fig 2.1 Analysis of c-fos upon contextual fear conditioning (cFC) – Acquisition reveals c-fos induction in Lsi2 and not in Lsi1.

- a) Protocol for testing c-fos induction upon cFC. b) Representative images of c-fos induction upon cFC acquisition from ventral hippocampus- region CA3 and CA1.
- c) Representative image of Thy1-mGFP+ pyramidal cell which is also cfos+.
- d) Quantification of c-fos positive pyramidal neurons in CA3 and CA1 in ventral hippocampus- total population (% cfos positive neurons over NeuN positive neurons); Lsi1 and Lsi2(GFP+cfos+ cells over total GFP cells analyzed) (total N=7-9, p=0.0006 for CA3 and CA1) (#Lsi1 CA3: Control- 310cells, cFC- 552 cells, #Lsi1 CA1: Control- 287 cells, cFC- 306 cells; #Lsi2 CA3: Control- 172, cFC- 184 cells, #Lsi2 CA1: Control- 269cells, cFC- 272 cells). e) Distribution of Lsi1 and Lsi2 and cfos positive cells across deep and superficial layers in ventral CA3 and CA1.

In MWM task, mice are taken to a pool of opaque water and they have to find the escape platform with the help of spatial cues. This is an incremental learning task with 4 trials per day (inter-trial-interval: 5minutes). Earlier studies in our lab demonstrated that ventral hippocampus completed its learning in the first four days of Morris water maze after which the dorsal plays a crucial role to fine tune the spatial map (Ruediger et al., 2012). Hence c-fos analysis was done after second, third and fourth day of MWM task. c-fos recruitment in the general population ramps up over the first 3 days and is stabilized in the general population in CA3b of ventral hippocampus (mean %cfos+/NeuN+: CA3: swim control- 2.7551 ± 0.4891 , day2- 5.9980 ± 0.4244 , day3- 10.7145 ± 1.4696 , day4- 10.7077 ± 1.50274 fig2.2 c). Upon subpopulation specific analysis, when the task is still exploratory on day 2 only Lsi1 shows increase in c-fos expression but not Lsi2 ; on day 3, when the goal is determined by the ventral hippocampus, there is a partial increase in both Lsi1 and Lsi2 and finally on day4, when the ventral hippocampus has completely learnt, the increase is found only in Lsi2 and not in Lsi1 (mean %GFP+cfos+/GFP+ CA3: Lsi1 swim control- 0.6289 ± 1.08934 , day2- 6.1596 ± 0.3379 , day3- 3.494385 ± 0.843799 , day4- 0.5051 ± 0.8748 , Lsi2: swim control- 3.4251 ± 0.128041 , day2- 2.5669 ± 0.7221 , day3- 5.7556 ± 0.8873 , day4- 9.2689 ± 1.6406 fig 2.2c). Thus initial stages of MWM task that is more exploratory results in c-fos expression exclusively in Lsi1 neurons whereas when learning becomes definite, c-fos expression is restricted to Lsi2 neurons.

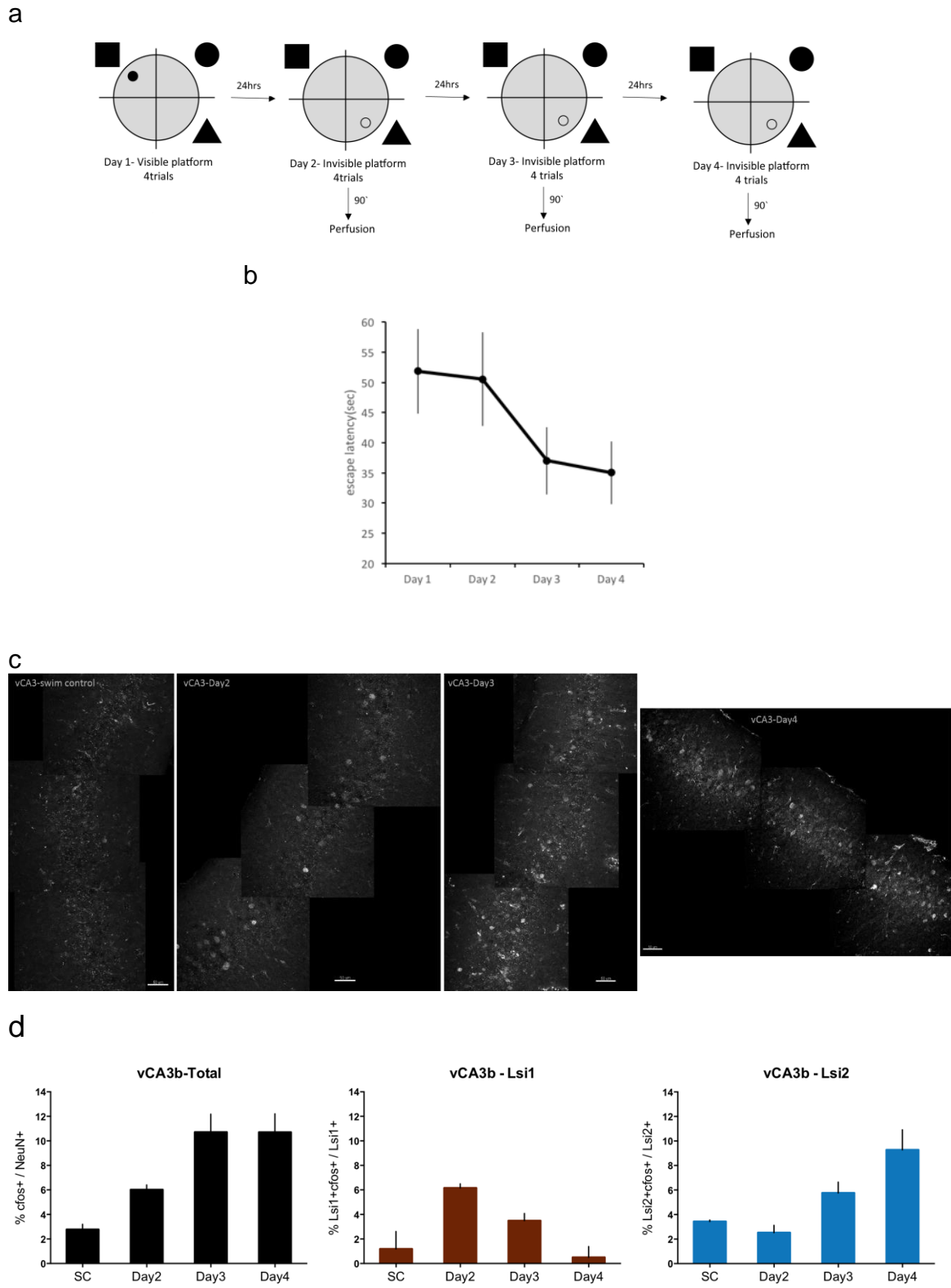


Fig 2.2 Analysis of c-fos upon MWM task –reveals initial c-fos induction in Lsi1 and then in Lsi2.

a) Schema for MWM task. b) mean escape latency to find the platform (N=22 for day1 and day2, N=11 for day3 and N=6 for day4).c) Representative images of vCA3b

In swim controls and upon cfos induction on day2,3 and 4. d) Quantification of c-fos induction upon MWM task in ventral hippocampus CA3 total population (% cfos positive neurons over NeuN positive neurons); Lsi1 and Lsi2(GFP+cfos+ cells over total GFP cells analyzed ; N= 5-10 mice per day, p value: sc and day2 <0.0001; day2 and day3 = 0.0025; # Lsi1 : sc- 232 cells, day2- 369 cells, day3- 369 cells, day4- 114 cells ; # Lsi2 : sc- 235 cells, day2- 328 cells, day3- 133 cells, day4- 173 cells).

With the above experiments, it is clear that although there is increase in c-fos expression in the general population, there is a clear distinction in its expression with respect to specific subpopulation upon different behaviors.

Analysis of early activity markers upon cFC reveals similar expression early on but differential expression later in hippocampal principal neurons

Since c-fos expression was observed at 90 minutes after the learning task, early activity markers like pCREB and pERK were analyzed at 15 minutes to identify if there were differences from the beginning between hippocampal principal neuron subpopulation. CREB phosphorylation and ERK phosphorylation has been described to be involved in the regulation of novel protein synthesis for long term plasticity.

In baseline, there is expression of pCREB in almost all the cells. However upon cFC acquisition, there is comparatively less increase in the intensity of pCREB in CA3b than in CA1b of ventral hippocampus (mean %pCREB+/NeuN+: CA3: baseline- 22.8030 ± 2.0608 , cFC- 49.6303 ± 10.4008 ; CA1: baseline- 25.015 ± 5.0841 , cFC- 76.06 ± 20.5061 Fig 2.3c). When the subpopulation specific pCREB expression is analyzed, both Lsi1 and Lsi2 shows similar increase in the intensity of pCREB at fifteen minutes post cFC acquisition (mean %GFP pCREB+/GFP+: CA3 Lsi1: baseline- 11.5217 ± 2.1521 , cFC- 54.5752 ± 14.327 ; CA1: baseline- 22.5 ± 9.1924 , cFC- 80.575 ± 15.6766 ; Lsi2 CA3: baseline- 26.2575 ± 3.8580 , cFC- 56.4921 ± 1.605117 ; CA1: baseline- 24.7641 ± 0.3335 , cFC- 73.2478 ± 14.9001 Fig 2.3c). Thus contextual fear memory acquisition results in increased pCREB levels in CA3b and CA1b of both Lsi1 and Lsi2. Hence the selection of c-fos expressing population is determined later in time.

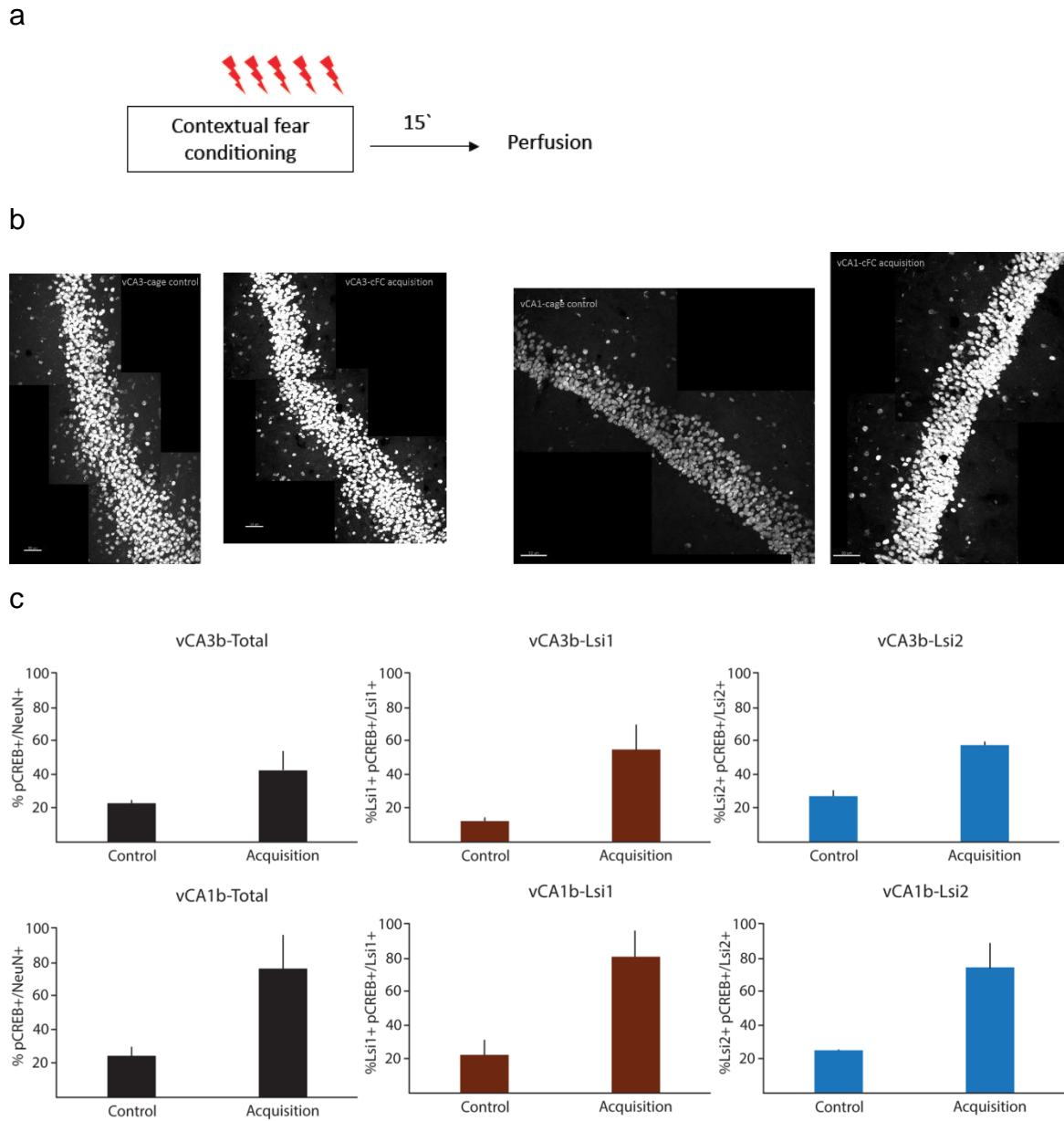


Fig 2.3 Analysis of pCREB upon cFC – reveals early pCREB induction in Lsi1 and in Lsi2. a) Protocol for testing pCREB induction. b) Representative images pCREB induction upon cFC in ventral CA3 and CA1. Note that the baseline for CA3 and CA1 are different. c) Quantification of pCREB upon cFC acquisition- total population (% pCREB positive neurons over NeuN positive neurons); Lsi1 and Lsi2 (GFP+pCREB+ cells over total GFP cells analyzed) (N= 5 mice) (#Lsi1 CA3: Control- 99 cells, cFC- 58 cells, #Lsi1 CA1: Control- 113 cells, cFC- 93cells; #Lsi2 CA3: Control- 137 cells, cFC- 114 cells, #Lsi2 CA1: Control- 113cells, cFC- 132 cells).

In stark contrast to pCREB expression in baseline, pERK1\2 is highly selective and expressed only in some neurons. Upon cFC acquisition there is increase in number of cells that express pERK1\2 in the general population (mean %pERK1\2+/NeuN+: CA3: baseline- 1.10618 ± 0.3292 , cFC- 3.5311 ± 0.3734

Fig 2.4d) .Similar to pCREB, pERK1\2 also increases in both Lsi1 and Lsi2 subpopulations in CA3b (mean %GFP+pERK1\2 +/GFP+: CA3 Lsi1: baseline- 0 , cFC- 1.8476 ± 0.7146 ; Lsi2: baseline- 0 , cFC- 1.5838 ± 0.3791 fig2.4d). Interestingly in the general population 90 minutes post acquisition pERK1\2 levels reach baseline (mean %pERK1\2+/NeuN+: CA3: baseline- 1.10618 ± 0.3292 , cFC - 1.1201 ± 0.6730 Fig) whereas it shows an increased activity only in Lsi2 and not in Lsi1 (mean %GFP+pERK1\2 +/GFP+: CA3 Lsi1: baseline- 0 , cFC- 0; Lsi2: baseline- 0 , cFC- 2.43 ± 0.6641 fig 2.4d).

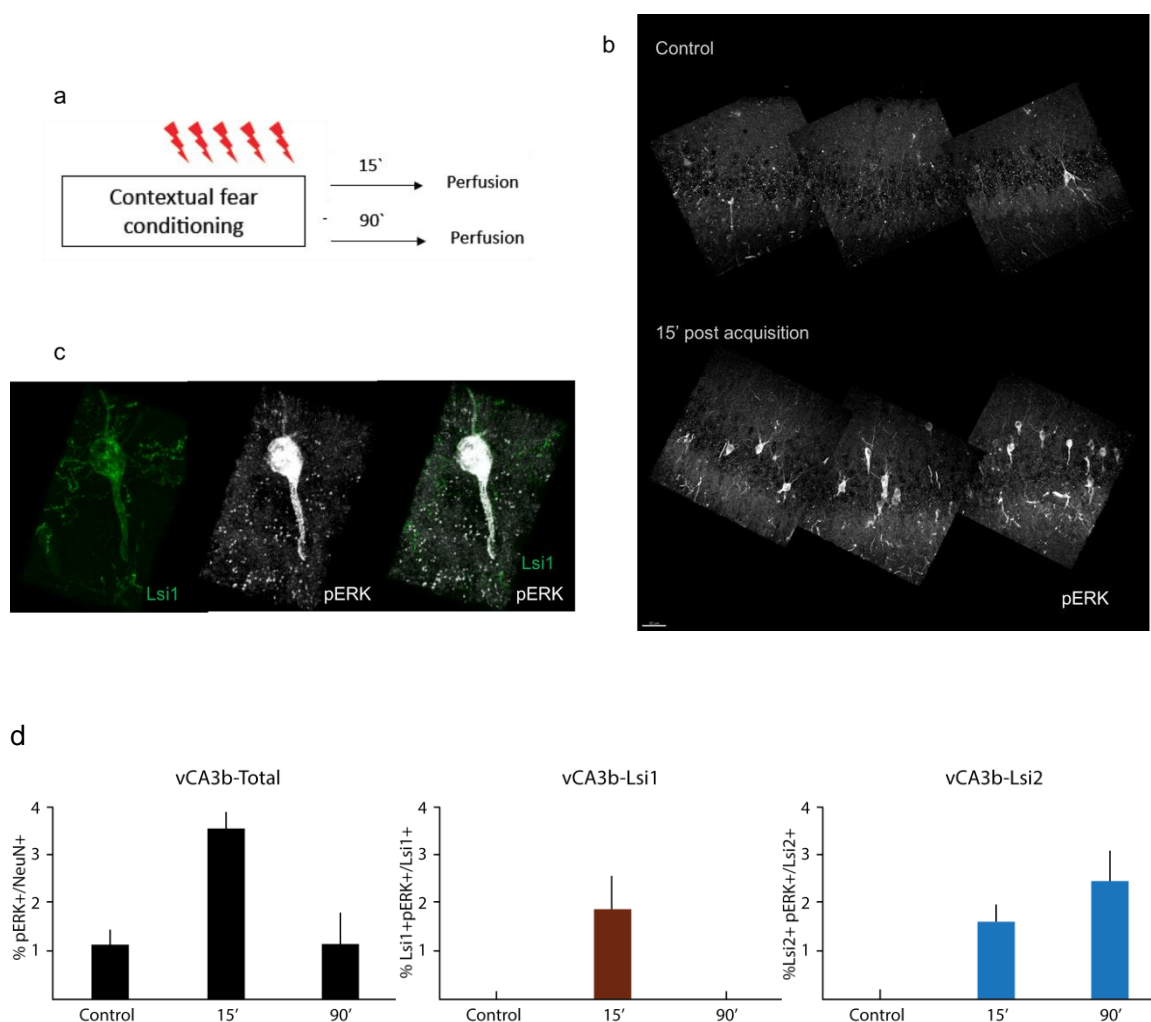


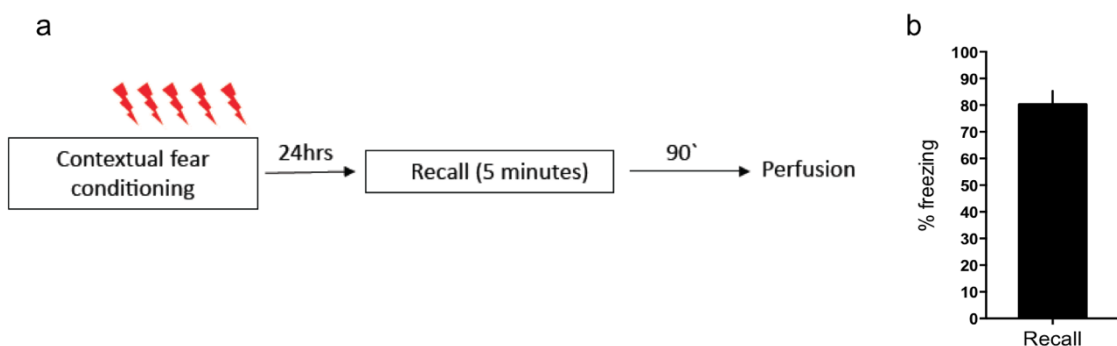
Fig 2.4 Analysis of pERK upon cFC – reveals early pERK induction in Lsi1 and in Lsi2 and a sustained activation in Lsi2 only. a) Protocol for testing pERK induction. b) Representative images ERK induction upon cFC in ventral CA3. c) Example of Lsi1+ pERK+ cell. d) Quantification of pERK upon cFC acquisition in ventral CA3 - total population (% pERK positive neurons over NeuN positive neurons); Lsi1 and Lsi2 (GFP+pCREB+ cells over total GFP cells analyzed) (N= 4 mice) (#Lsi1: Control- 105 cells, cFC 15' - 234 cells, cFC 90' – 98 cells; #Lsi2: Control- 108 cells, cFC 15' - 130 cells, cFC 90' – 119 cells).

Although there is presence of early pCREB and pERK1\2 in Lsi1 neurons 15 minutes' post cFC learning, at 90 minutes there is no c-fos induction in Lsi1 neurons.

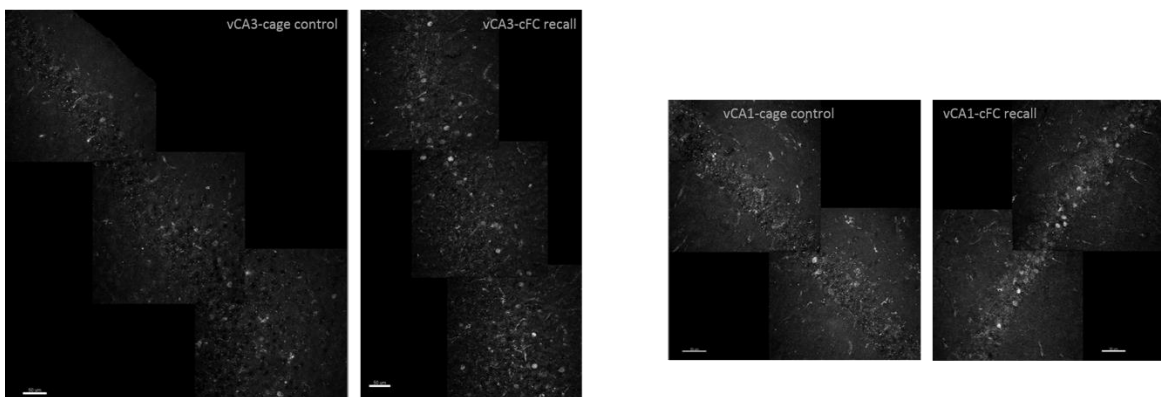
Analysis of c-fos expression in one trial extinction learning shows c-fos induction in both Lsi1 and Lsi2 principal neuron subpopulations.

As mentioned earlier, upon cFC acquisition only Lsi2 shows increase in c-fos expression. In order to identify if there is any additional subpopulation recruitment during one trial extinction learning which is transitory, mice were re-exposed to the training context 3 days post acquisition of fear memory for 30 minutes. Since it is just an extended recall, c-fos expression post 24-hour recall (5 minutes) was used as a control.

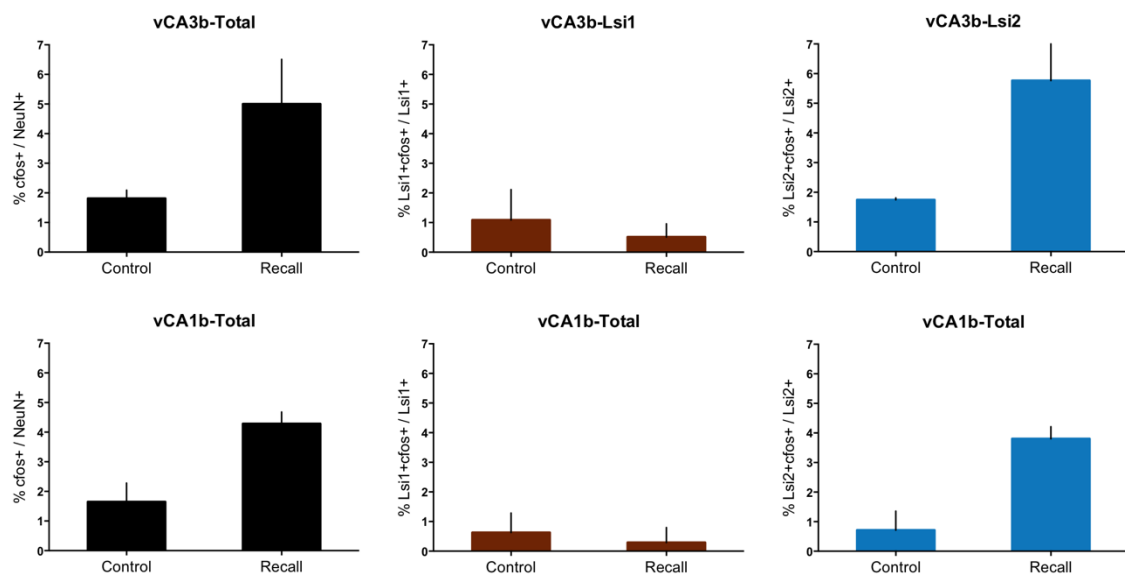
Similar to acquisition, during recall as well c-fos expression is seen exclusively in Lsi2 pyramidal neurons in both CA3 and CA1 of the ventral hippocampus (mean %cfos+/NeuN+: CA3: baseline- 1.81112 ± 0.2827 , cFC- 5.0027 ± 1.5076 ; CA1: baseline- 1.6499 ± 0.5661 , cFC- 4.2848 ± 0.3964 ; mean %GFP c-fos+/GFP+: CA3 Lsi1: baseline- 1.0893 ± 1.0273 , cFC- 0.5130 ± 0.4471 ; CA1: baseline- 0.6291 ± 0.6598 ,cFC- 0.2924 ± 0.5064 ; Lsi2 CA3: baseline- 1.7457 ± 0.0644 , cFC- 5.7661 ± 1.8192 ; CA1: baseline- 0.7120 ± 0.6475 ,cFC- 3.8024 ± 0.4125 Fig 2.5c).



C



d



e

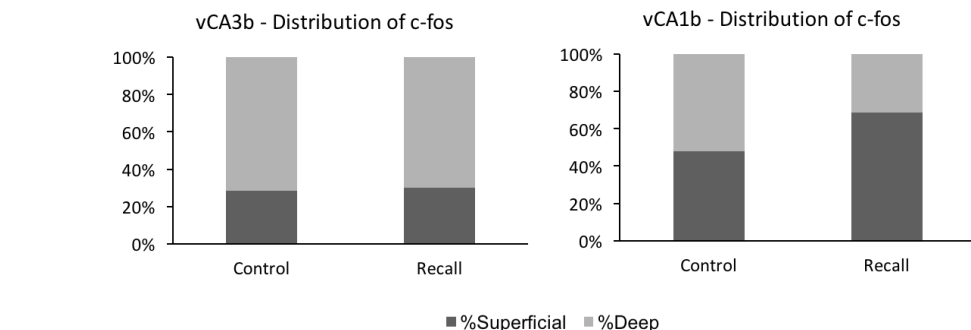


Fig 2.5 Analysis of c-fos upon contextual fear conditioning (cFC) – Recall also shows c-fos induction in Lsi2 and not in Lsi1.

a) Protocol for testing c-fos induction upon cFC recall. b) Behavioral response upon five minutes recall.(N=7) c) Representative images of c-fos induction upon cFC acquisition from ventral hippocampus- region CA3 and CA1. d)

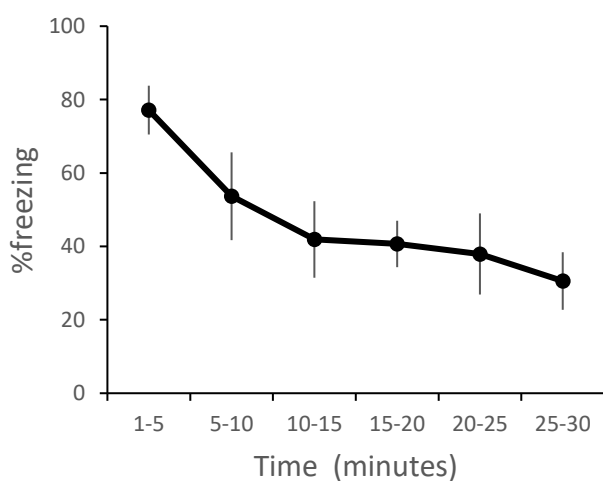
Quantification of c-fos positive pyramidal neurons in CA3 and CA1 in ventral hippocampus- total population (% cfos positive neurons over NeuN positive neurons); Lsi1 and Lsi2(GFP+cfos+ cells over total GFP cells analyzed) (total N=7, p=0.0012) (#Lsi1 CA3: Control- 298 cells, cFC- 334 cells, #Lsi1 CA1: Control- 286 cells, cFC- 343cells; #Lsi2 CA3: Control- 172, cFC- 172 cells, #Lsi2 CA1: Control- 172 cells, cFC- 159 cells). e) Distribution of c-fos+ cells across deep and superficial layers of ventral CA3 and CA1 respectively. Note that upon recall, induction of cfos+ cells are more in superficial layer in contrast to acquisition.

Additionally upon one time massed extinction learning, that is transitory learning, Lsi1 also shows a partial increase in cfos expression (mean %cfos+/NeuN+: CA3: baseline- 1.8902 ± 0.3669 , cFC- 5.3408 ± 0.9925 ; mean %GFP c-fos+/GFP+: CA3 Lsi1: baseline- 1.089 ± 0.8676 , cFC- 4.3761 ± 1.4642 ; Lsi2 CA3: baseline- 1.7457 ± 0.0644 , cFC- 5.7768 ± 0.9543).

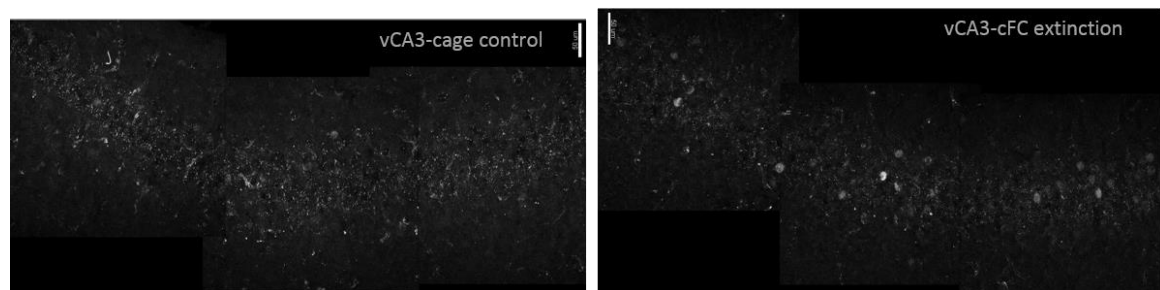
a



b



c



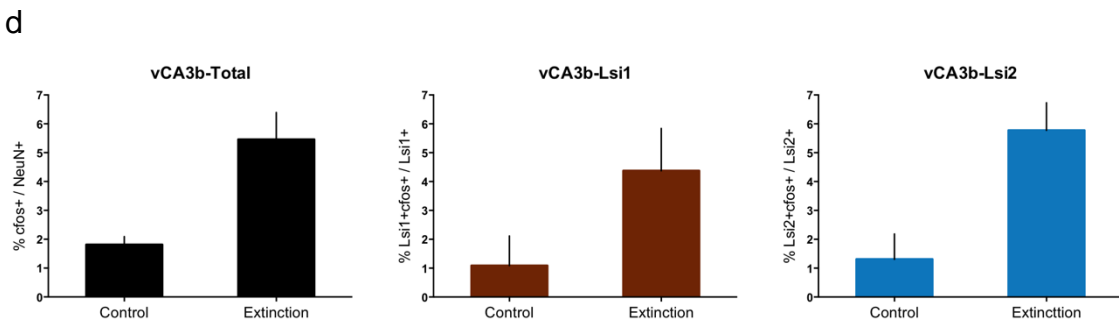


Fig 2.6 Analysis of c-fos upon one trial extinction –shows c-fos induction in both Lsi2 and Lsi1. a) Protocol for testing c-fos induction upon cFC one trial extinction. b) Freezing response upon one trial extinction elucidated in 5 minute bins (N=7) . c) Representative images of c-fos induction upon cFC acquisition from ventral hippocampus- region CA3 and CA1. d) Quantification of c-fos positive pyramidal neurons in CA3 and CA1 in ventral hippocampus- total population (% cfos positive neurons over NeuN positive neurons); Lsi1 and Lsi2(GFP+cfos+ cells over total GFP cells analysed) (total N=7, p=0.0012) (#Lsi1 CA3: Control- 298 cells, cFC- 236 cells ; #Lsi2 CA3: Control- 172, cFC- 160 cells).

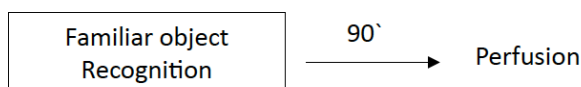
In summary, fear acquisition and recall results in c-fos expression solely in Lsi2 principal neurons and not in Lsi1 neurons, however transient learning of fear memory extinction results in additional partial expression of c-fos in Lsi1 principal neurons.

Analysis of c-fos expression in familiar object recognition of normal and enriched mice show exclusive c-fos expression in Lsi1 principal neurons.

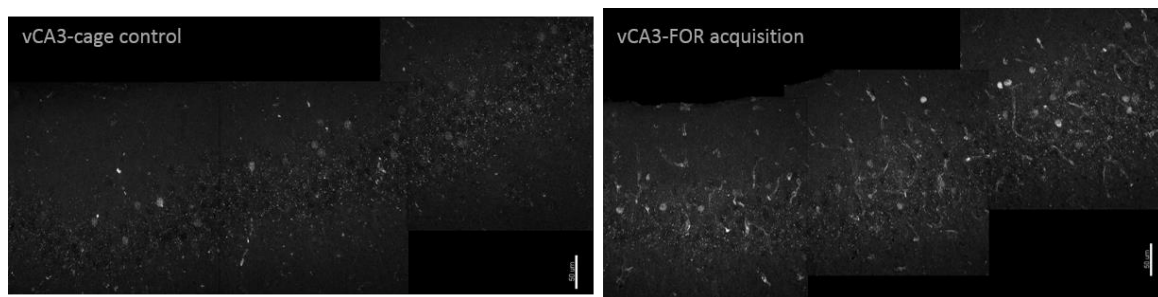
Incremental learning and fear conditioning induced c-fos in distinct hippocampal principal neuron subpopulation. In order to see if there is any specific c-fos induction in incidental learning, mice were exposed to two similar novel objects and perfused ninety minutes later. Exposure of mice to the novel context showed increase in c-fos in the general population almost similar to cFC acquisition in ventral CA3b (mean %cfos+/NeuN+: CA3: baseline- 1.4397 ± 0.7269 , FOR- 5.0994 ± 1.3402). Nonetheless, unlike in cFC Lsi2 does not have any change in c-fos expression post FOR but only Lsi1 had an increase in c-fos (mean %GFP c-fos+/GFP+: CA3 Lsi1: baseline- 1.0721 ± 0.8676 , FOR – 7.1081 ± 2.3658 . Lsi2 CA3: baseline- 1.7457 ± 0.0644 , FOR – 1.8622 ± 1.9535).

Consequently, mice were taken for acquisition of FOR one week post environmental enrichment. One-week enrichment has been already showed to improve the discriminatory index during the recall phase (Donato et al., 2013). There was a general increase in baseline owing to the enrichment, however FOR post enrichment resulted in increase in c-fos in Lsi1 (mean %cfos+/NeuN+: CA3: baseline- 3.0951 ± 0.8868 , FOR- 4.7174 ± 0.4243 ; mean %GFP c-fos+/GFP+: CA3 Lsi1: baseline- 1.2195, FOR – 7.15 ± 2.2627 . Lsi2 CA3: baseline-4.6153, FOR - 3.9216 ± 2.7730). So, acquisition of another exploratory task, familiar object recognition also results in expression of c-fos exclusively in Lsi1neurons and not in Lsi2.

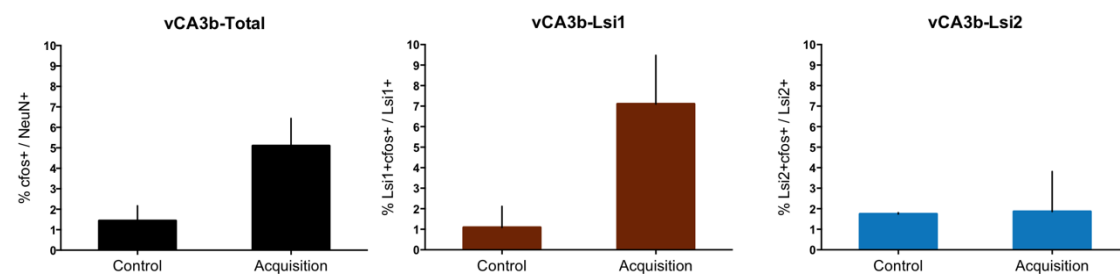
a



b



c



d

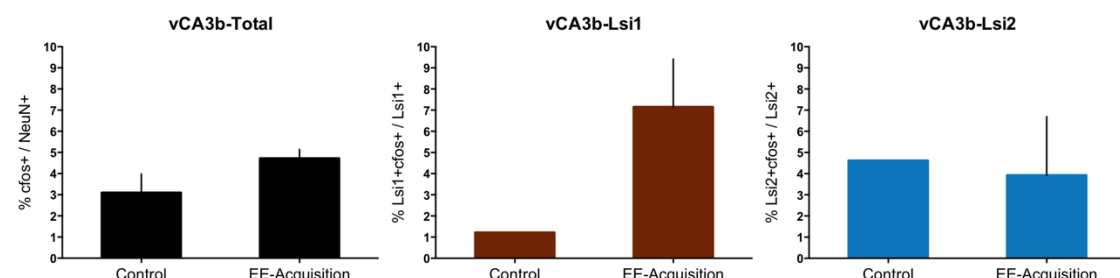


Fig 2.7 Analysis of c-fos upon familiar object recognition –Acquisition shows c-fos induction in Lsi1 and not in Lsi2.

a) Protocol for testing c-fos induction upon acquisition of familiar object recognition. b) Representative images of c-fos induction upon FOR acquisition from ventral hippocampus- region CA3. c) Quantification of c-fos positive pyramidal neurons in CA3 in ventral hippocampus- total population (% cfos positive neurons over NeuN positive neurons); Lsi1 and Lsi2(GFP+cfos+ cells over total GFP cells analyzed) (FOR: total N=10, p=0.0012, #Lsi1 CA3: Control- 298 cells, FOR - 234 cells, #Lsi2 CA3: Control- 172 cells, cFC- 258 cells). d) Quantification of c-fos positive pyramidal neurons in CA3 in ventral hippocampus after 1 week of Environmental Enrichment- total population (% cfos positive neurons over NeuN positive neurons); Lsi1 and Lsi2(GFP+cfos+ cells over total GFP cells analyzed) FOR 1 week EE: total N=4, #Lsi1 CA3: Control- 82 cells, FOR - 134 cells, #Lsi2 CA3: Control- 60 cells, cFC- 136 cells).

2.1.4 Discussion

Levels of c-fos+ neurons are low under baseline conditions and are readily enhanced upon learning. Hence, c-fos was used as a marker to identify the function of Lsi1 and Lsi2 hippocampal principal neuron subpopulation. This study shows that c-fos expression in CA3 and CA1 of ventral hippocampus is distinctly represented in hippocampal principal neuron subpopulations in different learning and memory tasks. Tasks that are transitory or exploratory in nature usually employ Lsi1 principal neurons whereas tasks that are more definite results in c-fos expression in Lsi2 principal neurons.

Under baseline conditions there was minimal c-fos activity in Lsi1 and Lsi2 PCs. However, upon contextual fear conditioning, only Lsi2 (and not Lsi1) exhibited induction of c-fos. This is true post acquisition, recall and extinction. It has been shown that for long term consolidation, there is reactivation of c-fos 15 hours post acquisition (Karunakaran S et al., 2015 submitted). Even during this re-induction, it is Lsi2 and not Lsi1 that shows increase in c-fos expression. So every time the fear memory is activated, Lsi2 subpopulation has induction of c-fos. This correlates very well with the memory engram hypothesis that indicates defined populations of neurons correspond to specific memory trace (Josselyn, 2010; Liu et al., 2012; Guenthner et al., 2013). Interestingly, Lsi2 is not recruited only in fear memory but also in later stages of Morris water maze, when the learning becomes definite. As we already know, that Lsi1 and Lsi2 form parallel circuits within the hippocampus, it might well be that the Lsi2 circuits are involved when the learning is definite.

On the other hand, Lsi1 is recruited upon novel context exposure and initial days of water maze, and during acquisition of one trial extinction memory. It is very intriguing that although there is c-fos induction in Lsi1 in FOR, there is no induction of c-fos in the swim controls used in MWM. When swim controls are sacrificed on day 1, then there is one-fold increase in c-fos only in Lsi1 and not in general or Lsi2 subpopulations (data not shown here). Swim controls generally do not have any goal are targeted movement in MWM. This clearly shows that active exploration of the context is required for c-fos induction in the general population however, just being in the novel context could prime the Lsi1 CA3 cells. Even when c-fos levels in general population is at baseline, it can happen that one subpopulation could be primed. This is also true for pERK at 90 minutes post acquisition. Although pERK in general population returns to baseline by then, pERK activity in Lsi2 persists and this also is accompanied by increase in c-fos expression only in Lsi2.

As for one trial extinction memory, it has been long known that there could be two distinct population of neurons are involved – one representing the original fear memory and another for encoding the acquisition of extinction (Debiec et al., 2002, Tronson et al., 2009). From this study, it is clear that Lsi2 encodes fear memory and Lsi1 likely encodes the extinction memory. However, it is not known now if repeated massed extinction could lead to initial c-fos induction in Lsi1 and when the extinction memory becomes definite then Lsi2 is recruited again.

One of the most interesting finding of this study is that there could be paradigms when both the subpopulations are simultaneously recruited — in extinction learning and on day 3 of MWM. These two instances reflect the multiple components employed during learning a pre-exposed task where active comparisons between online learning and previously acquired learning is represented.

Additionally, in contextual fear conditioning or later stages of Morris water maze (definite learning tasks), there is induction of filopodia (FFI-Feed Forward Inhibition) only in Lsi1 mossy fibers and they contact the PV+ interneurons (Ruediger et al., 2011 and Ruediger et al., 2012). Coincidental with the increase in FFI, it was also observed that PV network shifts to high PV network configuration. In contextual fear learning for example, although there is increase

in early activity markers, pCREB and pERK at 15 minutes' post acquisition in both the subpopulations, only Lsi2 has c-fos 90 minutes' post acquisition. Intriguingly, Lsi1 FFI connectivity is induced in between these two time points i.e., at 60 minutes. Also in MWM, the FFI growth begins at day 3 of training in Lsi1 and reaches the highest on day 4 (Ruediger et al., 2012). The c-fos expression also shows a partial decrease in Lsi1 neurons on day 3 whereas completely lost in Lsi1 on day 4. So in high PV dependent learning tasks, Lsi2 neurons express c-fos but not Lsi1.

When learning is more exploratory and gathering/editing information (second day of MWM task, one trial extinction) and not accompanied by any reinforcements (FOR), there is no FFI induction and c-fos expression observed in Lsi1 principal neurons. Moreover, these tasks are generally correlated to low PV induction except FOR which again can be influenced largely by induction of low PV (for example environmental enrichment, second day of MWM) (Donato et al., 2013). Interestingly, MWM task or enrichment also shows increase in synaptic plasticity in Lsi1 neurons (Donato et al., 2013). An important note about the distribution of c-fos+ cells in deep and superficial layers post fear conditioning is that they are different in acquisition and recall. During recall, there are additional cells that are recruited in the superficial layer of CA1. This could mean differential recruitment of PV basket cells during recall (Lee et al., 2014). Further investigation on the relationship between PV network and subpopulations could provide greater insight to mechanisms of learning.

To summarize, this data provides the evidence in support of differences in hippocampal principal neuron subpopulations (Lsi1 and Lsi2) recruitment during different types of learning. Further studies with genetic access to these cells could more specifically, elucidate their role in learning and if Lsi1 and Lsi2 subpopulations are restricted to only hippocampus or could be in multiple regions in the brain.

2.2 Alteration of specific connectivity in Lsi1 principal neuron subpopulation impairs learning.

2.2.1 Abstract

In the following study, I investigate the role of selective connectivity in hippocampal function. It is known from previous studies that some temporally regulated extrinsic cues guide the formation of synapses in DG-CA3 junction (Deguchi et al., 2011). neuronal Nitric Oxide Synthase (nNOS) was taken as a candidate temporal regulator as it peaks in expression during synaptogenic windows across various structures in the brain (Ogilvie et al., 1995, Murray et al. 2009). When I block nNOS during the appropriate synaptogenic windows, there is mismatched connectivity between Lsi1 principal neuron subpopulation in the hippocampus. Interestingly, Lsi2 principal neuron subpopulation were not affected by L-NAME treatment. I also have done an extensive structural analysis of the pre and post synapse in order to determine the alteration in selective connectivity. Moreover, mismatched connectivity further results in alteration in recruitment of the principal neurons in the memory engram that further results in poor learning and memory. For example, in contextual fear conditioning these mice with mismatched connectivity freeze less to the training context and generalize more to the training context. These mice also have altered PV plasticity. In summary my data suggests that the parallel circuits are used for different types of learning and when their preferential connectivity is disrupted, learning is impaired.

2.2.2 Introduction

Neurons are interconnected to form defined neuronal circuits that underlie various behaviors. The formation of proper neural circuits requires precise control and organization of cell-cell interactions throughout development. This includes migration of neurons, axon guidance, arborization of neurites (axons and dendrites), and recognition of correct synaptic partners, formation and stabilization of synapses followed by elimination of improper synapses. During development neurons express unique array of molecules that help in defining the specificity of neuronal circuits. This specificity includes topographic, cellular and subcellular specificity. In most of the brain regions, dendrites from principal neurons extend to specific laminae, receive inputs precisely from distinct principal neurons or interneurons selectively at specific neuronal subcompartment.

Guidance molecules like semaphorins, plexin, Slit, hedgehog, cadherins etc., either diffuse over short distances or bind to extracellular matrix owing to the distinct pattern formation of extracellular matrix that results in formation of laminar/sub-laminar architecture. However, different type of cells including excitatory neurons, inhibitory neurons local and projection neurons are located in each lamina/region. Hence. In some cases, the expression levels of molecular cues that are transcriptionally controlled can identify appropriate synaptic partners, for example, Drosophila teneurins (ten-a and ten-m) mediate synapse formation between the Olfactory receptor neurons and projection neurons (Hong et al, 2012). Additionally, changes in intracellular signaling upon contact with potential synaptic partners also aid in cell-type specificity. CA3 dendrites elicited distinct calcium transients upon contact with axons from excitatory (stronger calcium transients) vs inhibitory neurons (Lohmann and Bonhoeffer, 2008). Even within the excitatory principal neurons, it is clear that there can be subpopulations that are preferentially connected in the hippocampus (Deguchi et al., 2011; Druckmann et al., 2014).

Temporal regulation in microcircuit development:

All the developmental steps from neurogenesis to establishment of synapses as described in the previous section are temporally regulated. Developmental studies have elucidated how spatial and temporal patterning of molecular cues controls neuronal fate. The temporal identity of the cell can be dictated by extrinsic or intrinsic cues. In case of intrinsic regulation, once the progenitor cell reaches the right place, it becomes completely independent of the external cues and the cell fate is controlled by temporally induced cell-intrinsic molecules. For example, using the same temporal cues, distinct Drosophila neuroblasts generate different neuronal cell types: according to their time of birth, the differentiated progenitors maintain the transcriptional profile that aids in determining the cell fate (Isshiki et al, 2001). Extrinsic regulation on the other hand is mediated by a set of extrinsic temporal cues once the progenitor reaches the appropriate position. As stated initially, throughout development there is temporal regulation of the neurons in order to achieve accurate connections ie., from their time of neurogenesis until synapse formation and maturation with appropriate partners.

In principle, the timing of neurogenesis can influence the neuronal connectivity and result distinct functions of neurons in the circuit. There are several examples from various brain regions that elucidate this aspect. In the olfactory system, the early and late born mitral cells are distributed differentially across the dorsoventral axis of odorant receptor map with late born mitral cells that send more projections to olfactory tubercle than their counterparts. This implies that distinct olfactory cortical regions are involved in information processing from different odorant receptor region (Imamura et al., 2011). In the spinal cord, the extensor and flexor premotor neurons are generated from the same progenitor cells but at different stages of embryonic development with proprioceptors targeting the dorsally located extensor premotor neurons leaving out the laterally located flexor premotor neurons (Tripodi et al., 2011). In hippocampus as well, there are distinct populations of principal neurons that match in the time of neurogenesis and synaptogenesis and are preferentially connected to each other (Deguchi et al., 2011). Recently, it has also been shown that GABAergic PV neurons are distinctly regulated by excitation or inhibition according to their time of neurogenesis (Donato et al., 2015). Further synaptogenesis and synapse maturation have a temporal regulation as well. There are several developmental check points constituting of activity regulated transcription factors (Ben-Ari and Spitzer, 2010) during synaptogenesis and synapse maturation that ensures the proper formation of neural circuits. Any disruption in these could ultimately result in neurodevelopmental disorders. Although building the synaptic network is not always a rigid process, the delay in time caused for the compensatory pathways to rescue the synaptogenesis may cause impairment and ultimately result in neurodevelopmental disorders.

In the hippocampus, as stated above it has been shown that time of synaptogenesis plays an important role in specifying the preferential connectivity with subpopulation of principal neurons. When heterochronic organotypic slice cultures were done with different combination of age and subpopulation, only when the time of synaptogenesis matched between the dentate and CA3 matched, the synapses could be formed irrespective of whether they were from the same subpopulation or different subpopulation of principal neurons (Deguchi et al., 2011). Hence, synaptogenesis is extrinsically regulated in the hippocampus principal neuron subpopulation. There could be several cues that constitute the

extrinsic regulation in the mossy fiber synaptogenesis like Ephexin5 that regulates excitatory synapse formation (Margolis et al., 2010), presynaptic organizers (Wnt-7a, neuroligins, FGF22 & FGF7, SynCAM, PSA-NCAM) or postsynaptic organisers (agrin, Narp, Neurexin, EphB, nNOS).

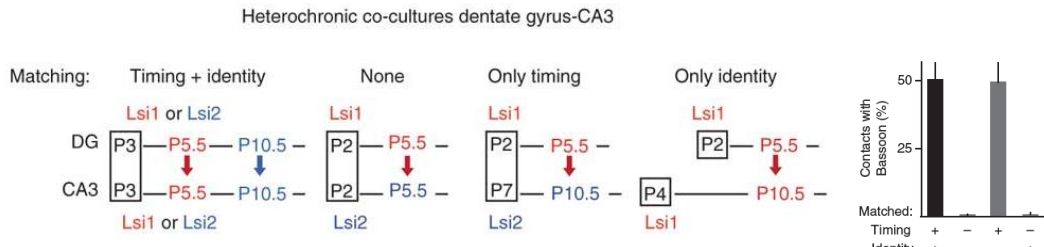


Figure 1: Temporal dependency of DG-CA3 synapse formation: Schema of heterochronic co-cultures to study mossy fiber synaptogenesis (left) and quantitative analysis of Lsi1 or Lsi2 synaptic contacts (right). Matched timing of synaptogenesis in CA3 and Dentate were enough to form synapses. (Deguchi et al., 2011)

Additionally, the extrinsic cue could also be early synchronous and spontaneous activity observed in developing hippocampus (Ben-Ari et al., 1989) that further induces molecular changes. This activity constitutes the giant depolarizing potential (GDPs) and are mediated by hub cells in CA3. These coordinated early activity also exists in cortex and precedes the sensory experiences. Later during critical period, the experience - dependent electrical activity aids the refinement of synaptic connections and is primarily marked by the maturation of inhibition in cortical circuits and heightened levels of synaptic plasticity. This critical period is well characterized in sensory cortices and duration varies according to the region of interest (Hensch, 2005). Thus there are a lot of time dependent modifications that ultimately lead to the formation of functional circuits that further underlies behavior.

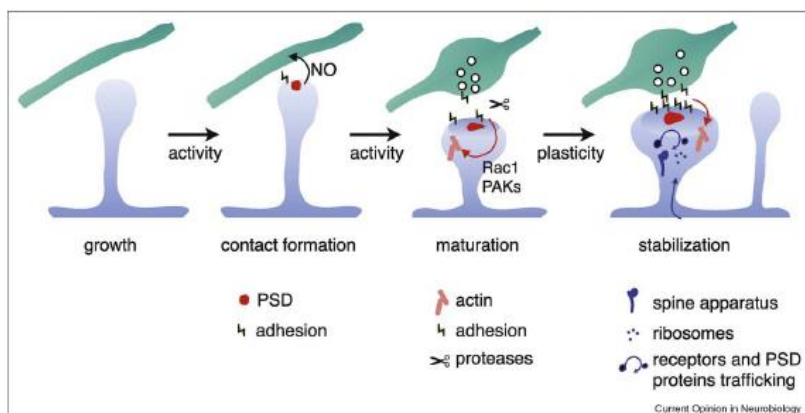


Figure2: A schematic diagram of putative molecular steps leading from spine growth to its stabilization elucidating role of nitric oxide in synaptogenesis .(Yoshihara et al.,2009)

neuronal Nitric Oxide Synthase is involved in retrograde nitric oxide signaling during synaptogenesis (Nikonenko et al.,2008) and it peaks during developmental synaptogenesis (Ogilvie et al., 1995 Murray et al. 2009). In hippocampus, nNOS is in the postsynapse both in development and in adult neurons. However, there are some highly intense nNOS positive pyramidal like cells seen in the early phases of development. Given that the dentate gyrus provides the main input to the hippocampal feed-forward circuit, and that the morphology and structural plasticity of its mossy fiber terminals in CA3 have been characterized in some detail, we exploited this synapse to investigate the role of nitric oxide signaling in shaping synaptogenic time windows using developing hippocampal slice cultures.

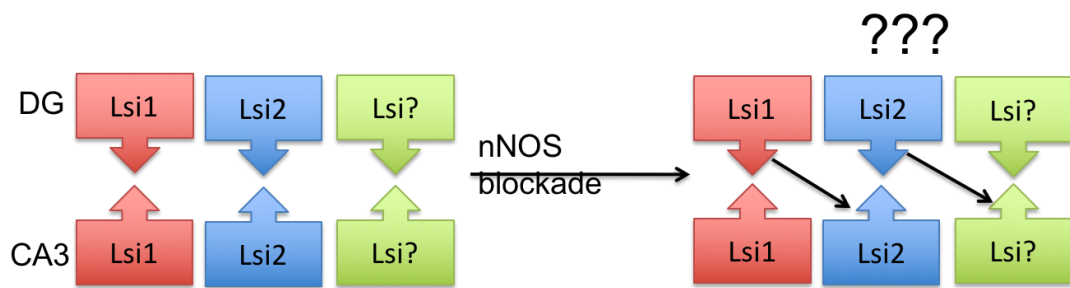


Figure3: Working hypothesis: Nitric oxide signaling could shift the synaptogenesis and hence by blocking this signaling pathway during respective synaptogenesis of Lsi1 and Lsi2, mismatched connectivity

2.2.3 Results:

2.2.3.1: Nitric oxide signaling allows selective access to hippocampal Lsi1 neuron function

Blocking Nitric oxide signaling during synaptogenesis in organotypic slice cultures specifically delays Lsi1 but not Lsi2

During the window of synaptogenesis, both in Lsi1 and Lsi2 there are a number of collaterals that arise at different points along the length of the granule cell axons. Mostly at these same points the mossy fibre synapses are formed. Not all collaterals turn into mossy terminals and some of them are lost. *In vitro*

time lapse experiments with 24 hour interval shows that once these mossy terminals are formed, they have to be stabilized as some of them are lost even after it is formed. Lsi1 and Lsi2 follow the same steps for mossy fiber synapse formation but Lsi1 is slightly ahead of Lsi2 in time (fig. 2.2.1).

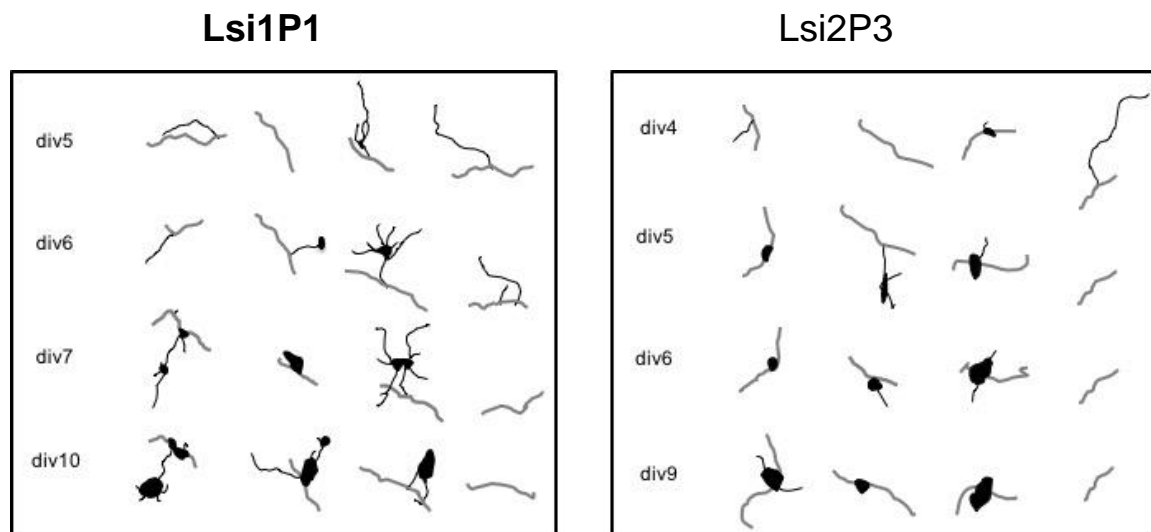


Figure 2.2.1: Developmental timelapse of LMTs in Lsi1 and Lsi2. Example traces of 24hr time lapse. Collaterals are formed at different positions along the axon. They either develop into mossy terminal or is lost. Both Lsi1 and Lsi2 follow the same pattern during development, in the terms of collateral sprouting followed by LMT formation and stabilization. The difference between them is that Lsi1 is ahead of Lsi2 during development.

To test if nNOS could be a temporal regulator of synaptogenesis in the hippocampal DG-CA3, L-NAME treatment was done in organotypic slice cultures from both in Lsi1 and Lsi2 during their respective synaptogenic window (Lsi1P1 div5-6, Lsi2P2 div5-6). 24hour time-lapse imaging was done for 4 days - The axons those were healthy from the first time point to the recovery were traced. In Lsi1 there were a proportion of collaterals that remained as collaterals and did not form terminals until there was L-NAME in the medium. Upon withdrawal of the drug most of them recovered after 3 days. Lsi2 was immune to nNOS blockade. (figure 2.2.2)

Are the rules for synaptogenesis different for different subpopulation?

It was unclear if nNOS blockade interfered with the collateral dynamics (collaterals seemed to be frozen) or with the process of synaptogenesis itself in

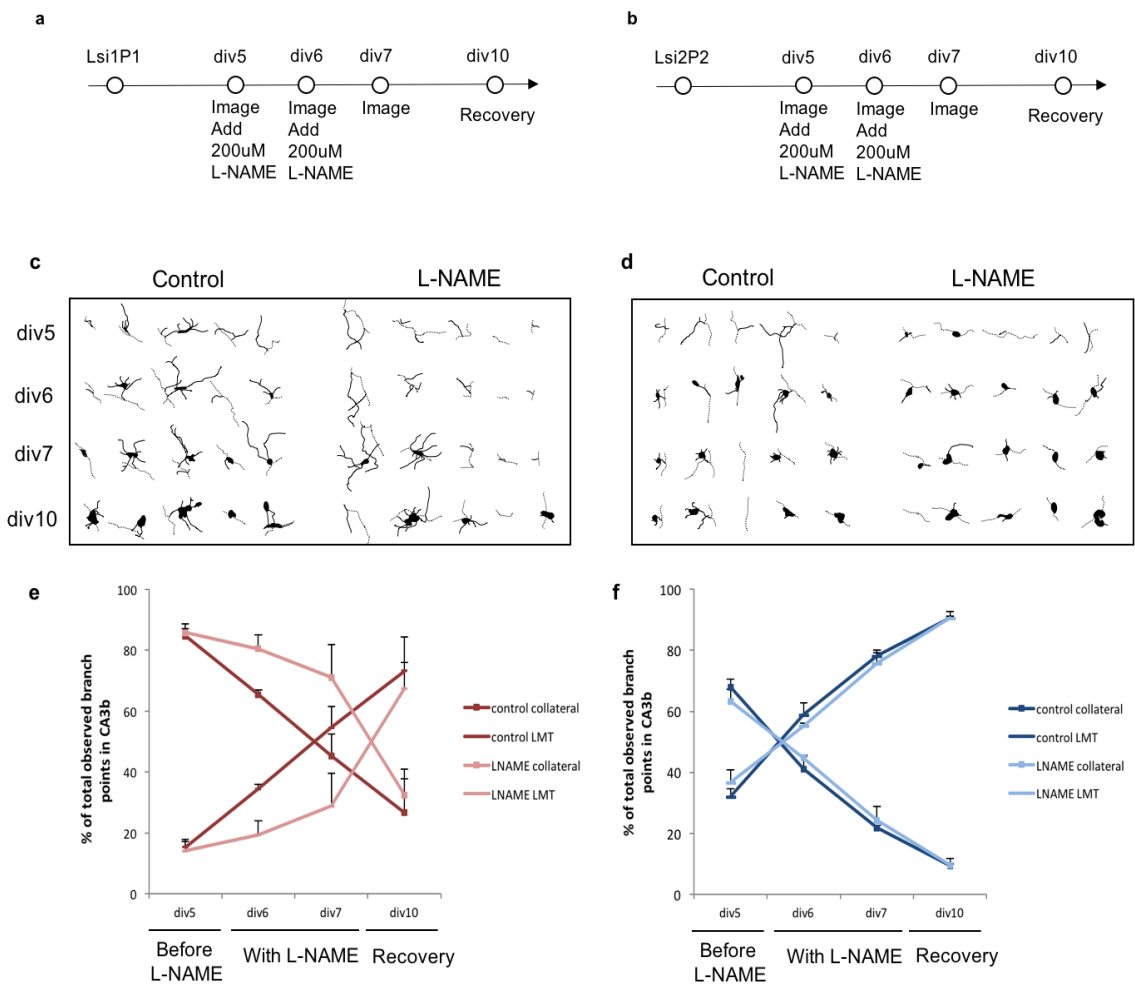


Figure 2.2.2: nNOS blocking prevents differentiation of collaterals into LMTs in L21 and not in L15. a) and b) Protocol for 24 hr time lapse imaging in Lsi1 and Lsi2 respectively.c) and d) Example traces of branch points traced. e) and f) Quantification of number of collaterals and LMTs from CA3b (N=3-5 pups with atleast 3 slices each).

Lsi1. In order to clarify this, time-lapse imaging at a higher resolution- for every 3 hours for two days of L-NAME treatment in both Lsi1 and Lsi2 was performed. Interestingly in Lsi1 L-NAME group few collaterals remained as collaterals but they were dynamic; few of them formed terminals that had high turnover rate. Most of the dynamic terminals and collaterals that did not make terminals during the treatment, recovered 3 days post withdrawal of L-NAME. Additionally, in Lsi1 even when the treatment was extended beyond the synaptogenic window, the effect of nNOS blockade still persisted (fig 2.2.3d). As long as L-NAME was in the medium during synaptogenic window, the stability of Lsi1 synapses were affected irrespective of the day of slice culture preparation (Postnatal day1 (P1),

P2 or P3) (figure 2.2.3b and e). However, the number of collaterals without any synaptic modification were dependent on the day of slice culture. Surprisingly Lsi2 was insensitive to L-NAME treatment both in Lsi1 and Lsi2 synaptogenic window even when the collateral and terminal dynamics was analyzed at much higher resolution (figure 2.2.3c and f).

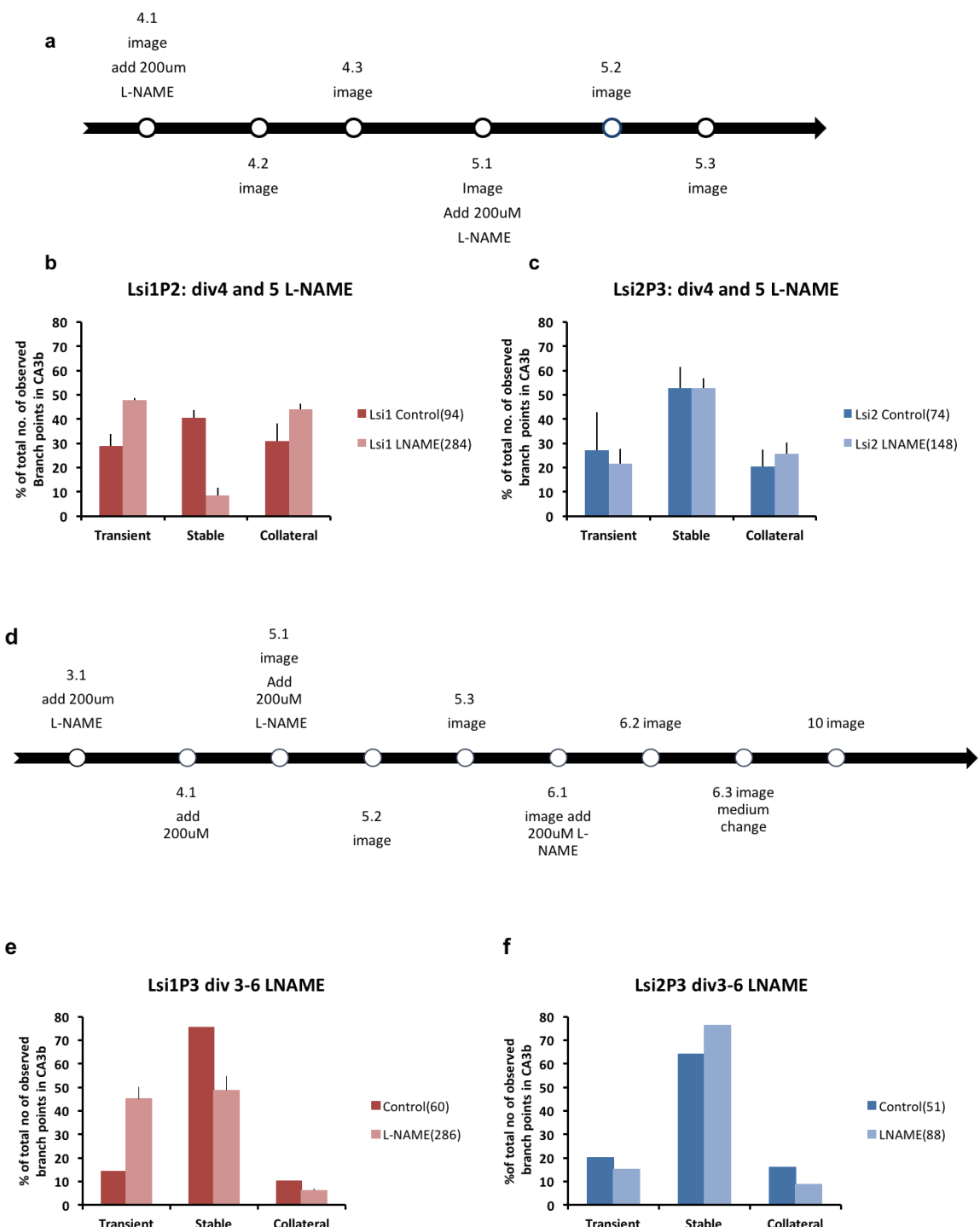


figure2.2.3: Lsi1 only responds to L-NAME treatment with altered stability of synapses. a) Protocol for imaging organotypic slice cultures during

synaptogenic window of Lsi1 and Lsi2 respectively. Time interval between consecutive imaging on the same day was 3 hours. First imaging (4.1) was done before adding L-NAME to the medium. Medium was changed immediately after the last imaging(5.3). b) and c) Quantification of stable and transient synapses along with the number of collaterals expressed as % of total number of observed branch points in CA3b.N= 3-6 pups with 2-4 slice cultures per pup. Total Number of branch points observed is represented within bracket in each graph. Note that the stability of synapses is affected only in Lsi1 and not in Lsi2. d)Protocol for extended imaging of organotypic slice culture encompassing synaptogenic window of Lsi1 and Lsi2.e) and f) Quantification of stable and transient synapses along with the number of collaterals expressed as % of total number of observed branch points in CA3b.N= 2-3 pups with 2-4 slice cultures per pup. Total Number of branch points observed is represented within bracket in each graph. Note that again, the stability of synapses is affected only in Lsi1 and not in Lsi2.

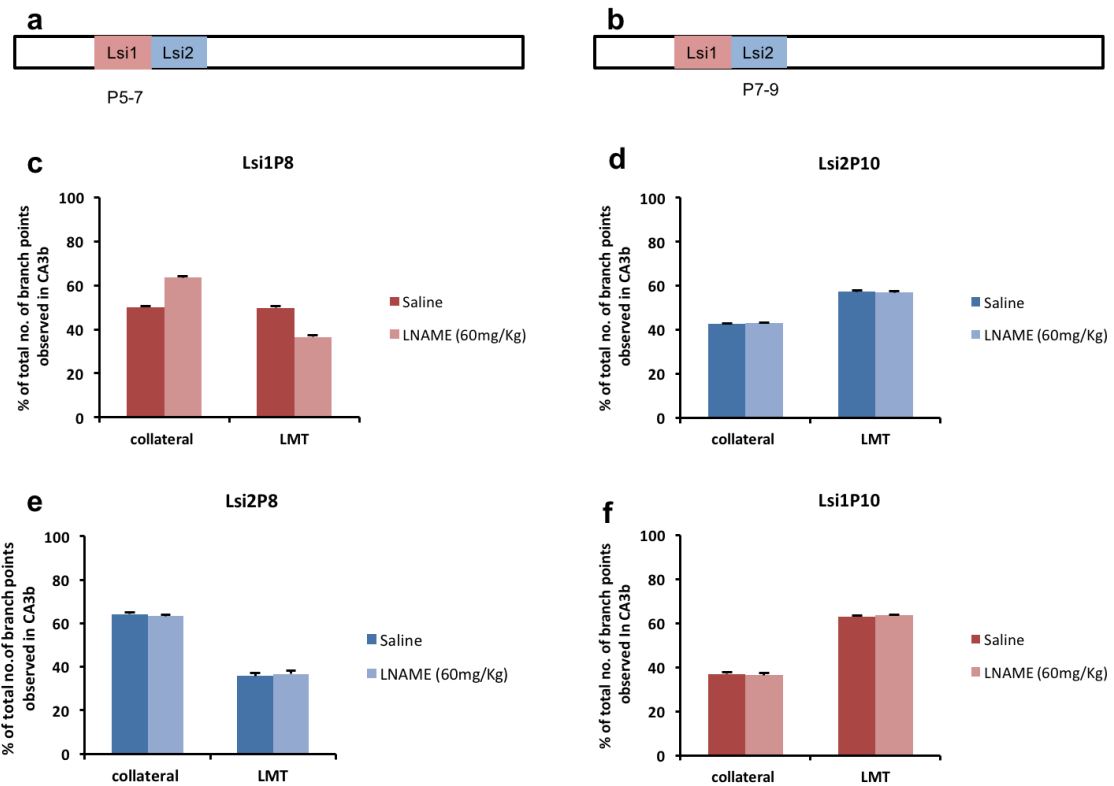
In summary, nNOS blockade affected only the synapse stability of Lsi1 and not of Lsi2 in their respective synaptogenic windows and in extended time windows.

In vivo study also shows delayed synaptogenesis only in Lsi1 upon nitric oxide signaling blockade

Post the initial screening with slice culture, nNOS blockade was further used *in vivo* to test for any effect on synaptogenesis. The synaptogenic window for DG-CA3 synapses in Lsi1 and Lsi2 is between postnatal day5 - 7 and postnatal day 7-9 respectively (Deguchi et al., 2011). Like in the slice cultures, every 24 hours L-NAME was injected intraperitonealy during the chosen window of synaptogenesis.

Collateral to LMT ratio was quantified per animal in CA3b region 24hrs after the last L-NAME treatment ie, on P8 and P10 respectively. Even in *in vivo* nNOS blockade, only Lsi1 treated in Lsi1 synaptogenic window had higher collateral to LMT ratio (fig 2.2.4b). Lsi1 in Lsi2 synaptogenic window did not have an increase in collateral to LMT ratio (figure2.2.4f). Lsi2 remained unaffected in both the synaptogenic windows.

Figure 2.2.4 Analysis of collateral and LMT *in vivo* post L-NAME shows that Lsi1 treated in P5-7 window only has a higher collateral to LMT ratio. a) and b) Description of Lsi1 and Lsi2 synaptogenic window. c-e) Quantification of number of Collaterals and LMTs in CA3b region expressed as % of total number of observed branch points in CA3b.N=3-4 pups per condition per treatment.



A further detailed analysis of the P5-7 window and an extended P5-9 window was done using neurolucida tracing. This also shows a decrease in number of LMT in both P5-7 and P5-9. Like in the extended slice culture experiment, upon P5-9 treatment also the effect on collaterals is much reduced than in P5-7, however the number of LMTs are reduced post L-NAME treatment.

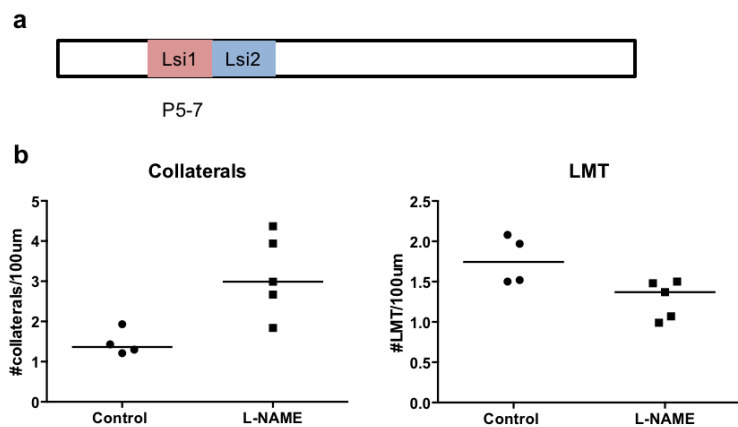
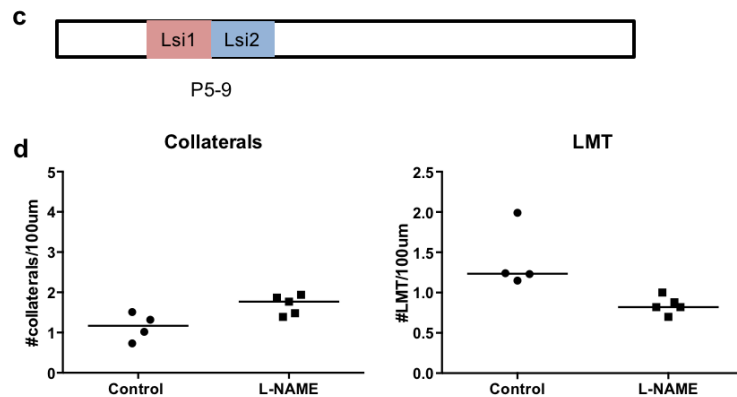


Figure 2.2.5 Detailed analysis of collaterals and LMTs of Lsi1 in CA3b. a) and c) shows the days of treatment. b) and d) Quantification of collaterals and LMT upon L-NAME treatment expressed as number of collaterals/LMTs per 100um axonal length. b) N=4 pups for control (Total 318 axonal segments analyzed); N=5 pups for L-NAME (Total 636 axonal segments analyzed). d) N=4

pups for control (Total 465 axonal segments analyzed); N=5 pups for L-NAME (Total 255 axonal segments analyzed).



Further analysis of active zone density with and without L-NAME treatment was performed in order to identify any alteration in synaptic plasticity. Anisomycin, protein synthesis inhibitor was used for testing the synaptic recovery as an indication of synaptic plasticity (Bednarek and Caroni, 2011). Active zone density in this case was calculated as follows (number of bassoon-pGUR1 colocalisation) / volume of LMT. This study also clearly indicates that there is a delay in the recovery of synapses at 9 hours post L-NAME treatment in Lsi1 and not in Lsi2 in its respective synaptogenic windows (figure 2.2.6). Since these are still developing synapses, the recovery is quicker in controls in Lsi1 and Lsi2.

Blocking nitric oxide signaling in adults also specifically alters the synaptic plasticity of Lsi1 and not other principal neuron subpopulations

In order to check if the Lsi1 synapses can be altered post development, synaptic recovery in LMTs of Lsi1, Lsi2 and randomly labelled granule cells were tested upon anisomycin treatment. In this experiment, bassoon density was calculated as number of bassoon puncta per LMT volume. In general, the synaptic dip is quicker in Lsi2 and in general population (12 hours) than in Lsi1 (24 hours). However, L-NAME treatment advances the synaptic destabilization time only in Lsi1(at 6 hours) (fig 2.2.7c). There was no change in Lsi2 and randomly labelled LMTs with L-NAME treatment compared to their respective controls (fig 2.2.7d).

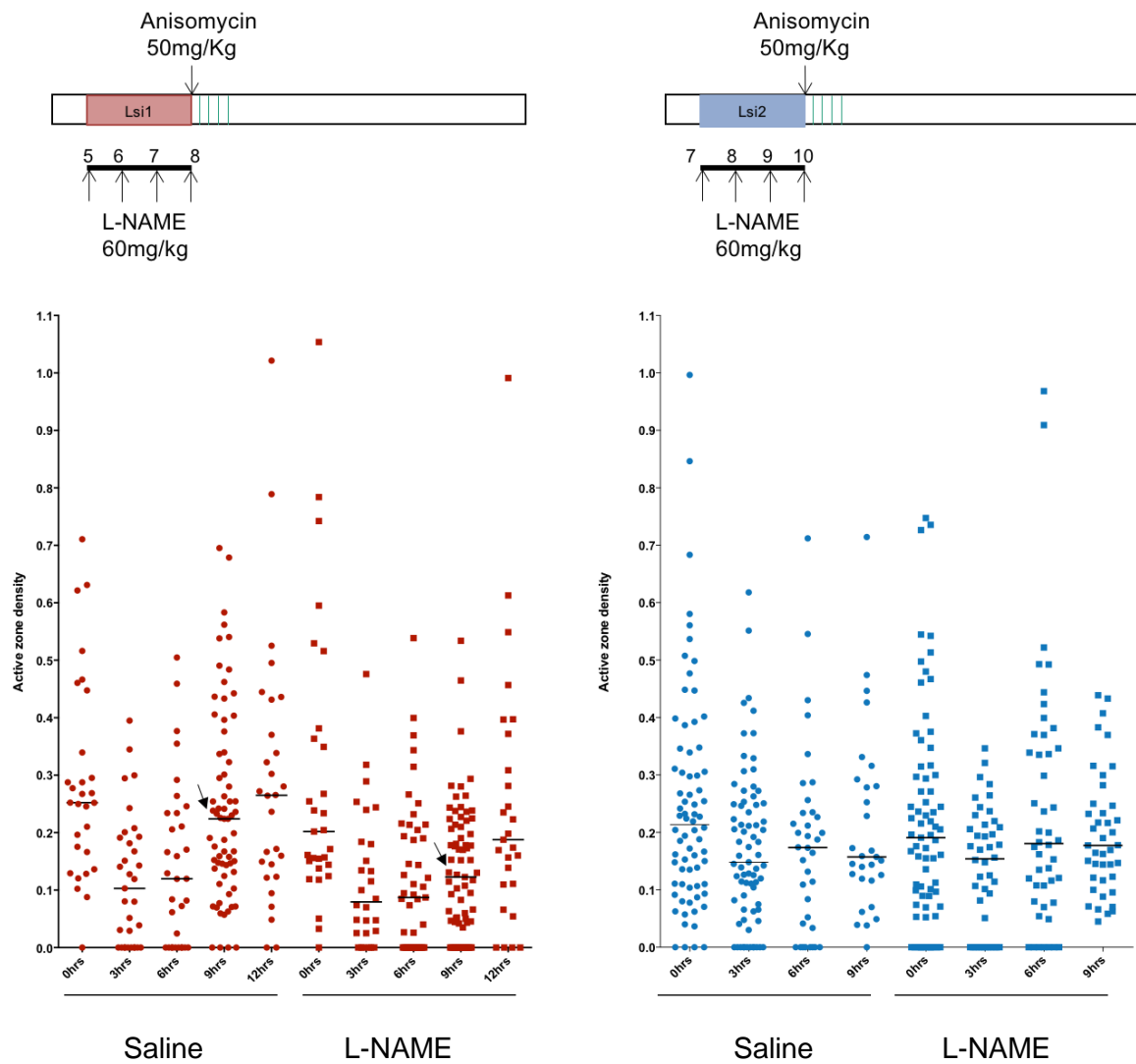
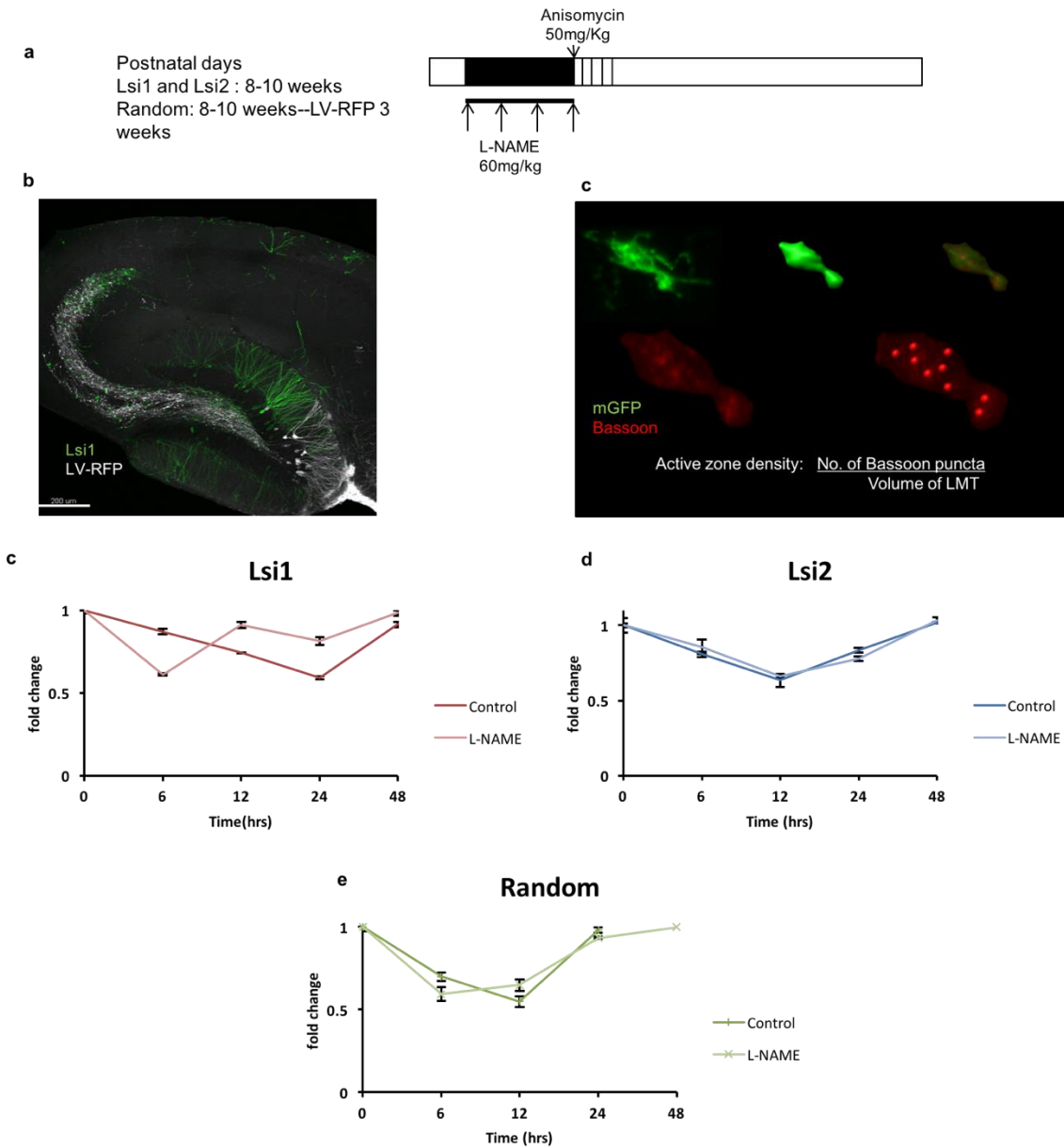


Figure 2.2.6 Active zone density analysis with anisomycin upon L-NAME treatment also shows delay in synaptic recovery in Lsi1. Quantification of active zone density per LMT (N=2-3 pups per condition). 9 hours post anisomycin shows a delay in synaptic recovery in L-NAME treated pups in comparison to the control.(p value< 0.0001)

In summary, only Lsi1 synapses are altered upon L-NAME treatment in *in vivo* as well both during development and in adult. Lsi2 synapses are immune to any change upon L-NAME treatment.

Figure 2.2.7 Synaptic plasticity in Lsi1, Lsi2 and randomly labelled LMTs

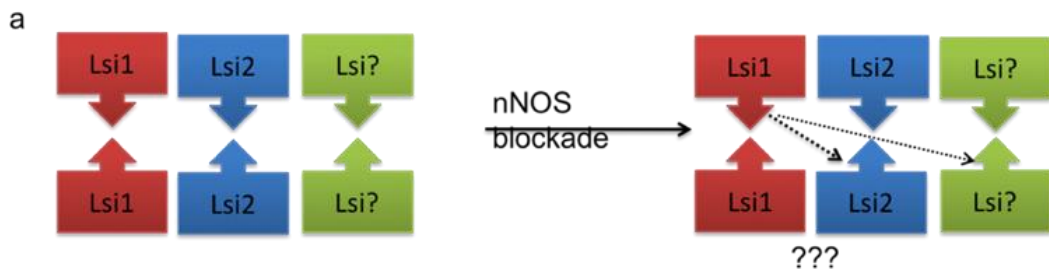
a) Schema for L-NAME treatment followed by anisomycin treatment. b) example section of LV-RFP expression in Lsi1 animal and example of LMT and steps for calculation of bassoon puncta with Imaris. c-e) Bassoon density expressed as fold change across the time course.(N=3-5 mice with atleast 50 LMTs per animal per time point).



2.2.3.2 Morphological characterization of pyramidal cells in mice with developmental blockade of nitric oxide signaling

Structural analysis of Presynaptic connectivity in CA3:

A detailed structural analysis was done in order to test if the altered synapse development would affect the selective connectivity in CA3 and CA1 in adult mice post nNOS blockade during development. The mean distances between consecutive LMTs were calculated in Lsi1 and Lsi2 in baseline and with L-NAME treatment at different synaptogenic window during development.



b

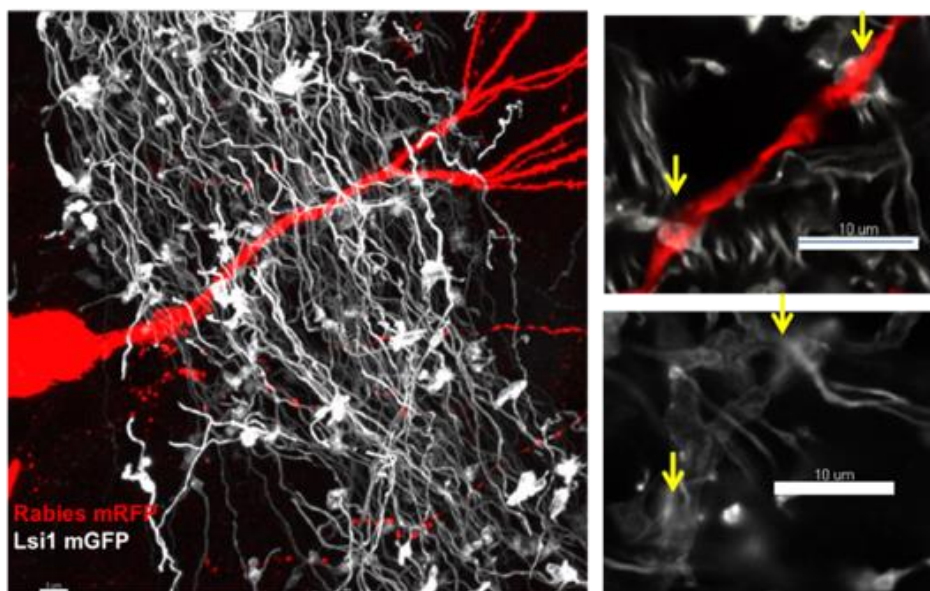
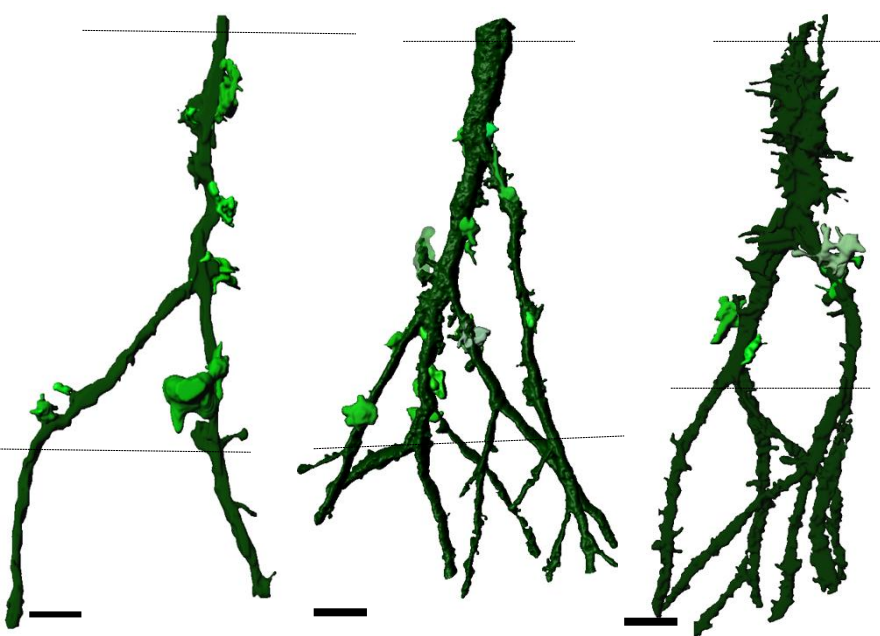
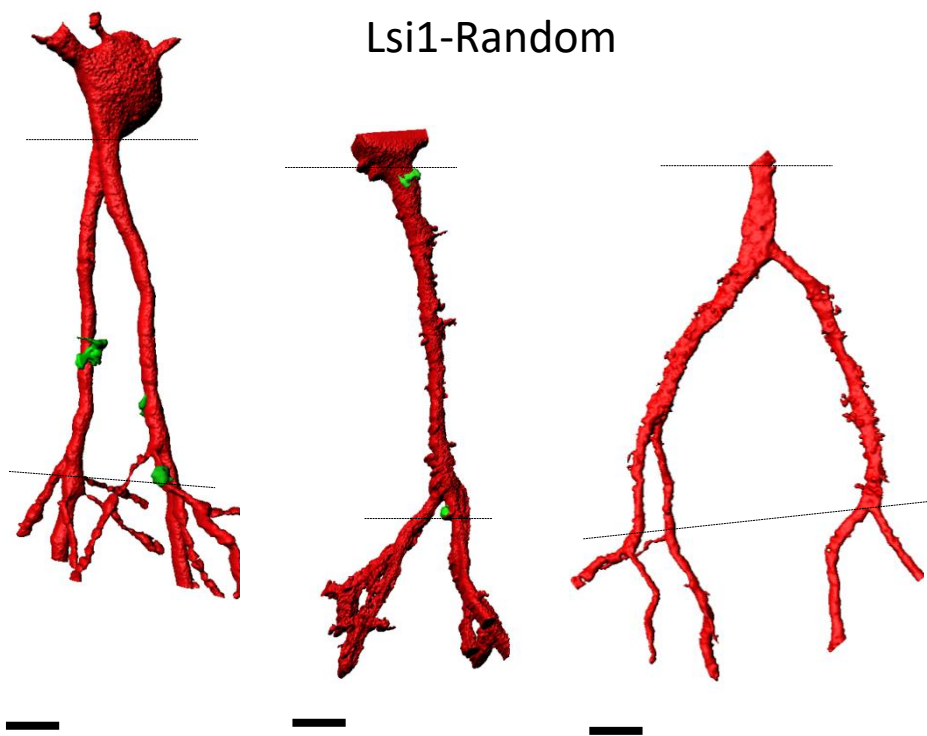


Figure 2.2.8 Connectivity analysis in adult post nNOS blockade during development. a) Hypothesis: Will Lsi1 be able to form synapses onto other subpopulation upon nNOS blockade during development. b) Example of randomly labelled CA3 cell. on the right top, example of randomly labelled dendrite with overlapping mGFP-LMTs (shown with arrows), example of mGFP+ dendrite with overlapping mGFP-LMTs. c) example reconstruction of Lsi1-Lsi1 and Lsi1-Random LMTs-CA3 from ventral hippocampus. LMTs are denoted in shades of light green, Lsi1 CA3 is represented by dark green, note dendritic projections are more complex in stratum lucidum (marked by dotted lines) of Lsi1 and not in random. Also the Lsi1 LMTs are clustered on to Lsi1 CA3 and rarely found on randomly labelled CA3.

Lsi1-Lsi1



Lsi1-Random



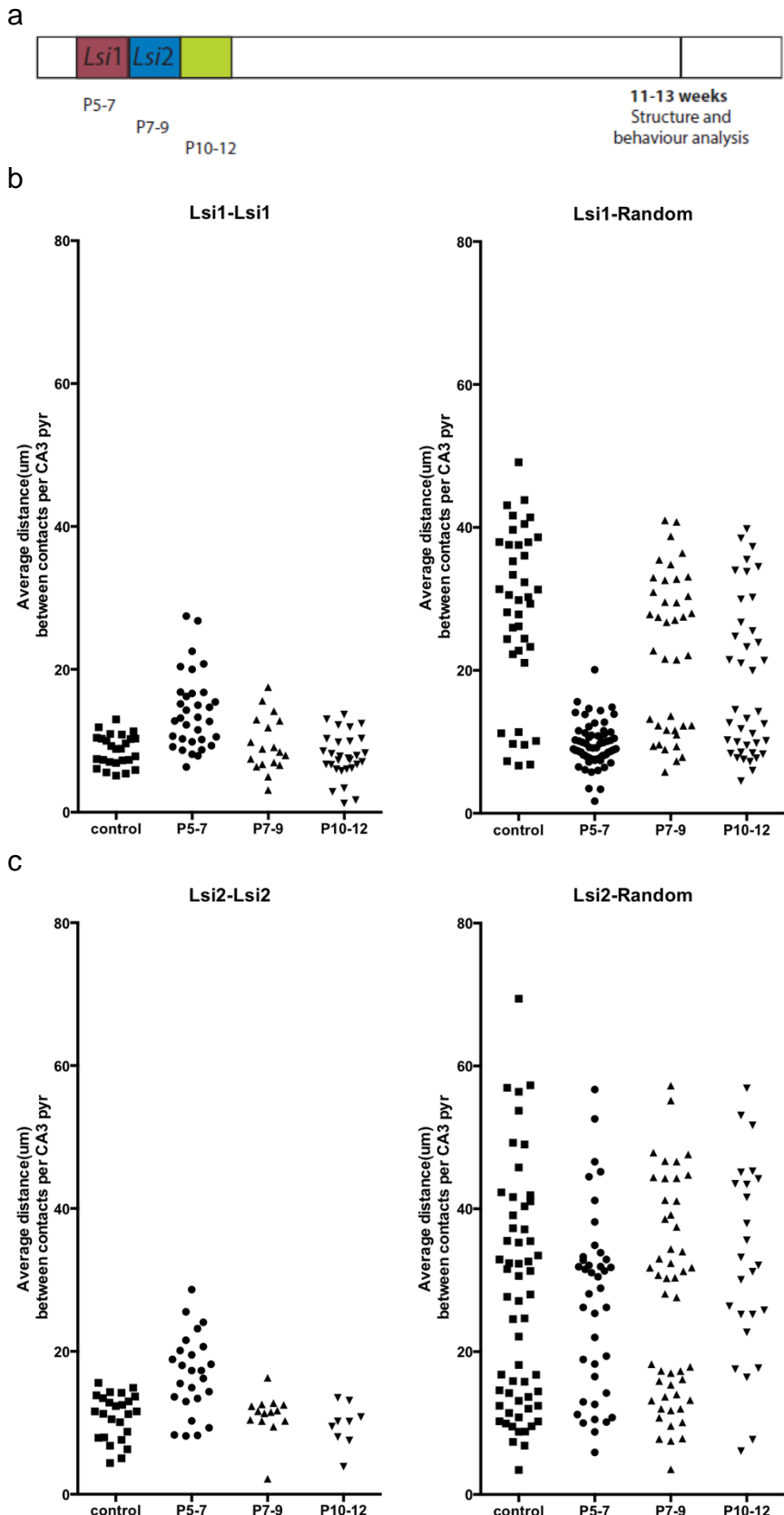


Figure 2.2.9 Connectivity analysis in adult post nNOS blockade during development. a) schema of DG-CA3 synaptogenic window of Lsi1, Lsi2 and next subpopulation and analysis in adult. b) Lsi1 connectivity analysis, each data point represents a single cell. Lsi1-Lsi1 and Lsi1-Random in baseline and P5-7 are

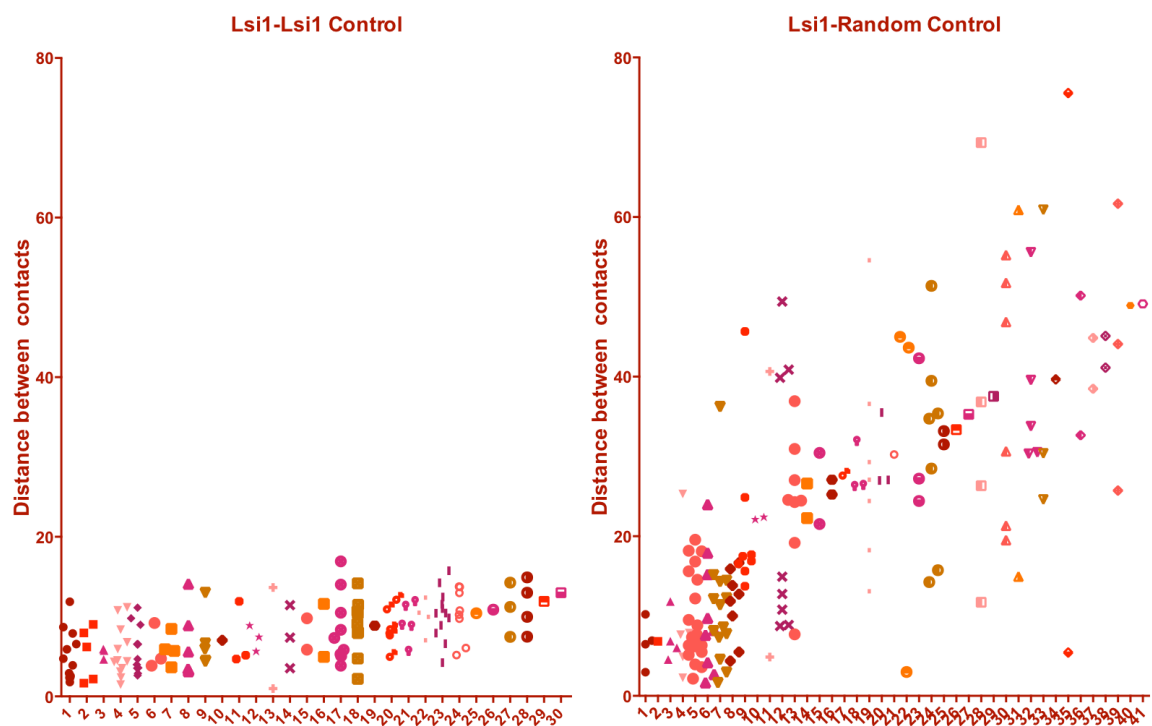
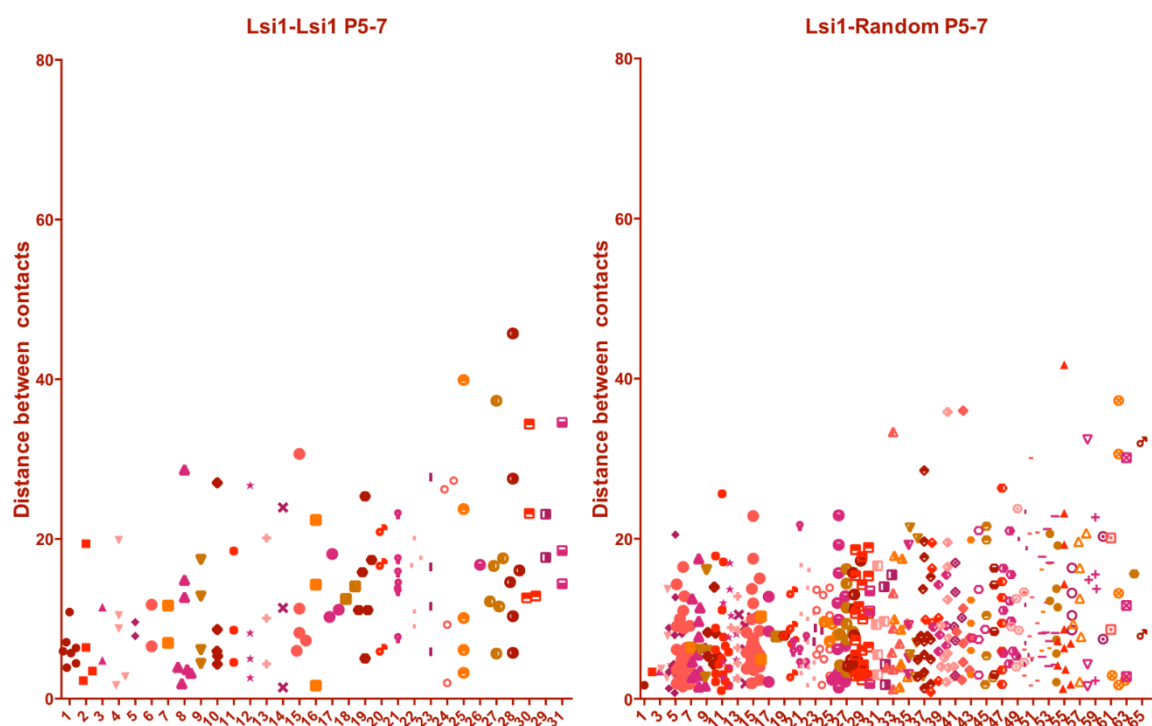
significantly different (p value <0.0001). However, L-NAME treatment in later windows does not seem to alter selective connectivity in Lsi1.c) Lsi2 connectivity analysis. Lsi2-Lsi2 is altered upon L-NAME P5-7 however, other combinations of Lsi2 remain unaffected. Note that in b and c there are two groups of cells with minimal average distance (putative Lsi1 in b, putative Lsi2 in c) and another which are more sparsely connected in Lsi1 (or) Lsi2 -randomly labelled CA3.

The synaptogenic windows for Lsi1 and Lsi2 are P5-7 and P7-9 respectively. As a control, effect of L-NAME treatment was done also in P10 - 12 outside the synaptogenic window of Lsi1 and Lsi2. All the analysis in this section was done in 3 month old mice. For this study, the cells were considered for analysis only if the entire dendritic tree was found in stratum lucidum.

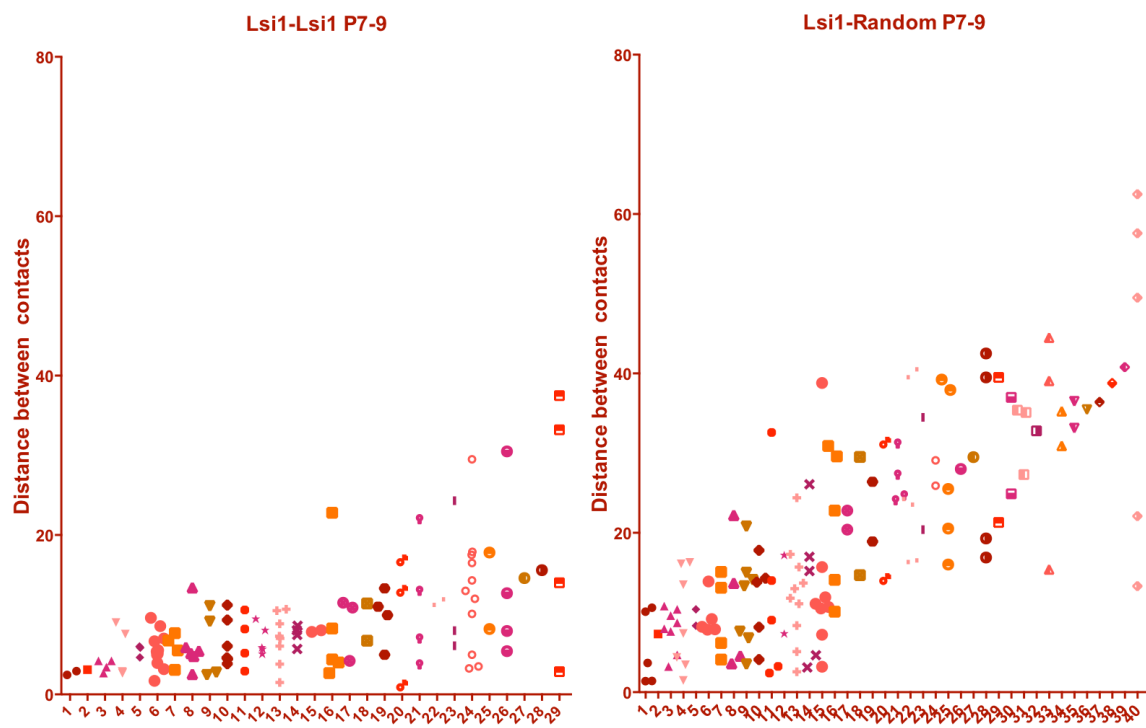
In baseline conditions, Lsi1-Lsi1 connectivity is clustered and sparser in Lsi1-random. 20% of random CA3 cells are the putative Lsi1 cells that exhibit clustered connectivity. Lsi2- Lsi2 synapses are not clustered like that of Lsi1, however there is also sparser Lsi2 –random CA3 cells. Upon L-NAME P5-7 treatment, Lsi1 synapses are found clustered onto random CA3 cells than on itself. Owing to this, there is also relatively sparser distribution of Lsi2 synapses. Otherwise, Lsi2 pre-synaptic connectivity is insensitive to L-NAME treatment in all the treatment windows.

In order to better understand the distribution of presynaptic terminals onto the CA3, the individual distance analyzed in each CA3 cell was plotted for each subpopulation. This clearly demonstrated the clustered connectivity in Lsi1. Although, from the mean distances the effect of P7-9 L-NAME in Lsi1 seems to have recovered, persistence of partial changes in individual distance is observed. However, the P10-12 window remains unaltered in connectivity.

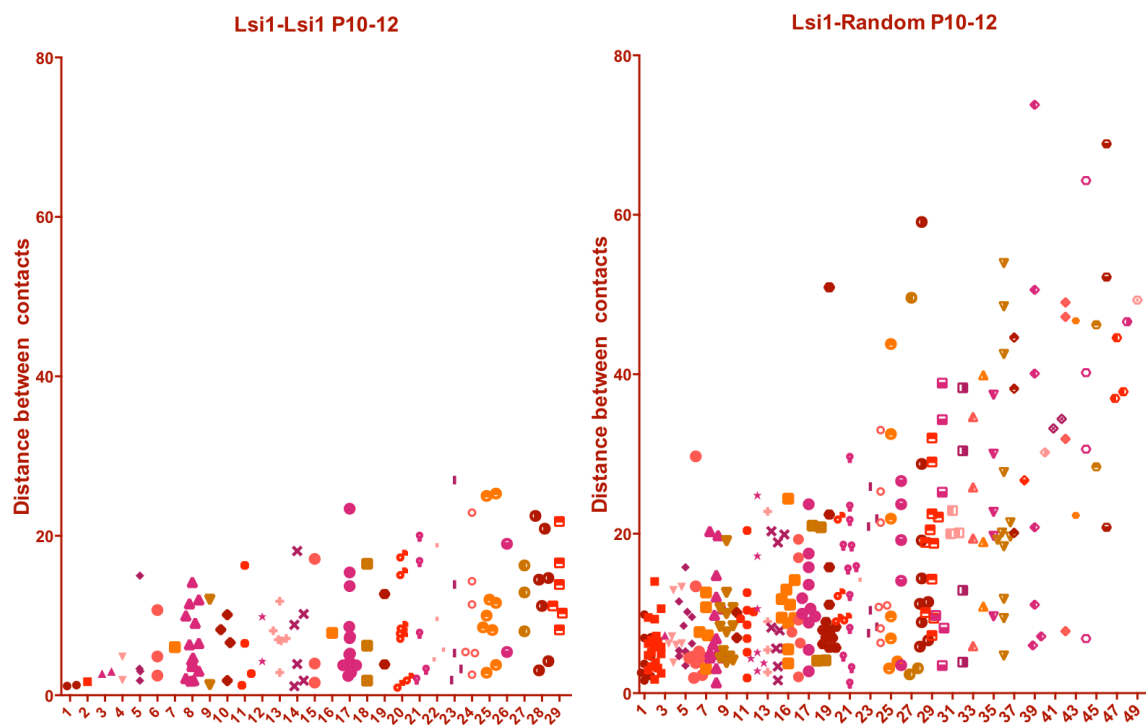
Figure 2.2.9 Individual cell analysis shows clearly the change in preferential connectivity in Lsi1. Each column in the graph represents a single CA3 cell and these are arranged in order of increasing mean distances between contacts(LMTs) (N= atleast 3 mice in each condition) a) Lsi1 in control mice has clustered connectivity on to Lsi1 CA3 and less frequent synapses onto randomly labeled CA3. Note that Lsi1- random CA3 has 20% clustered connectivity owing to putative Lsi1. b) Lsi1-Lsi1 connectivity in P5-7 L-NAME treated mice is altered and more spaced out. Lsi1 LMTs form more frequent contacts onto randomly labelled cells upon interference during its synaptogenic window P5-7. c) and d) shows that in P7-9 window there is still some remnant effect, however P10-12 is similar to baseline connectivity.

a**b**

C



d



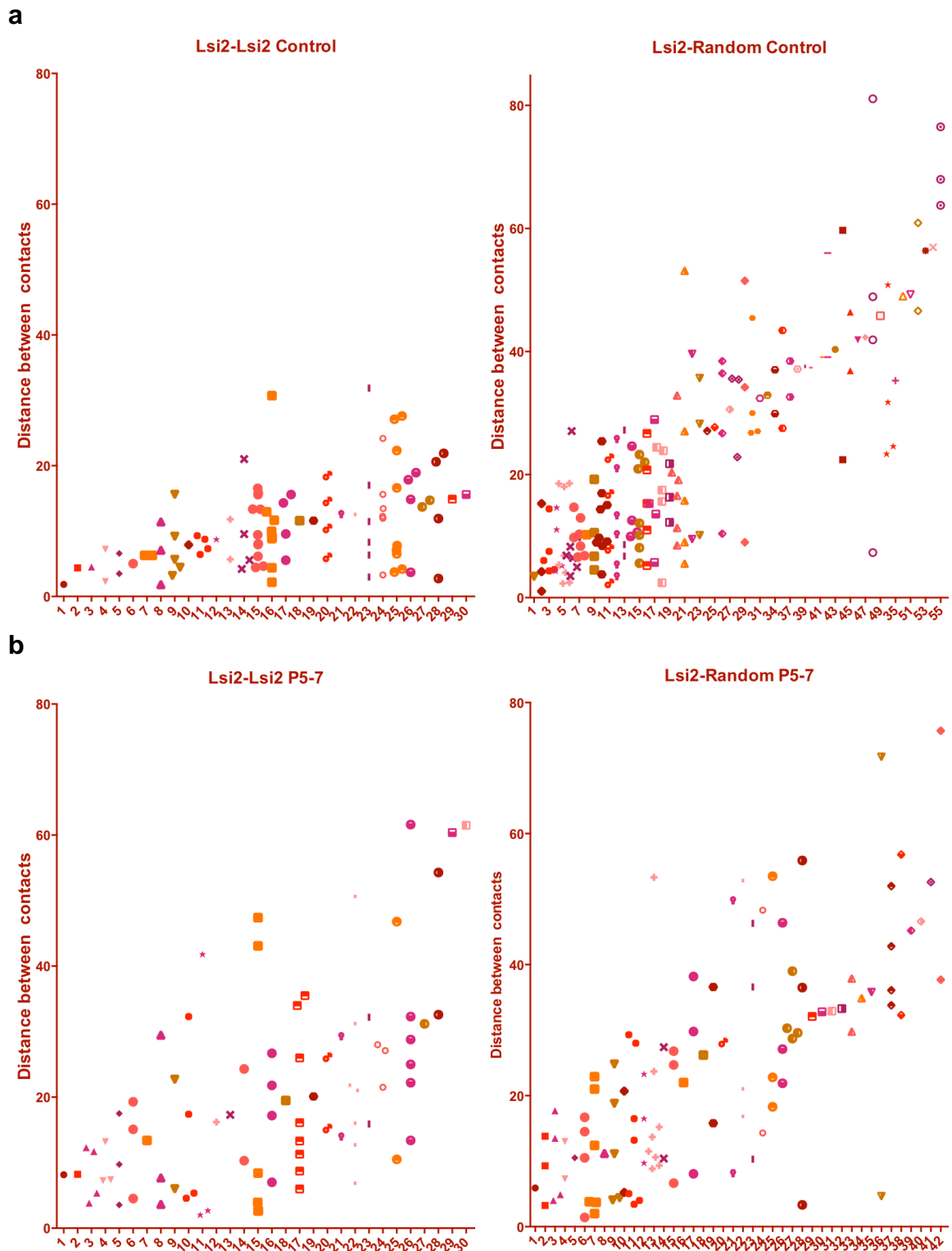
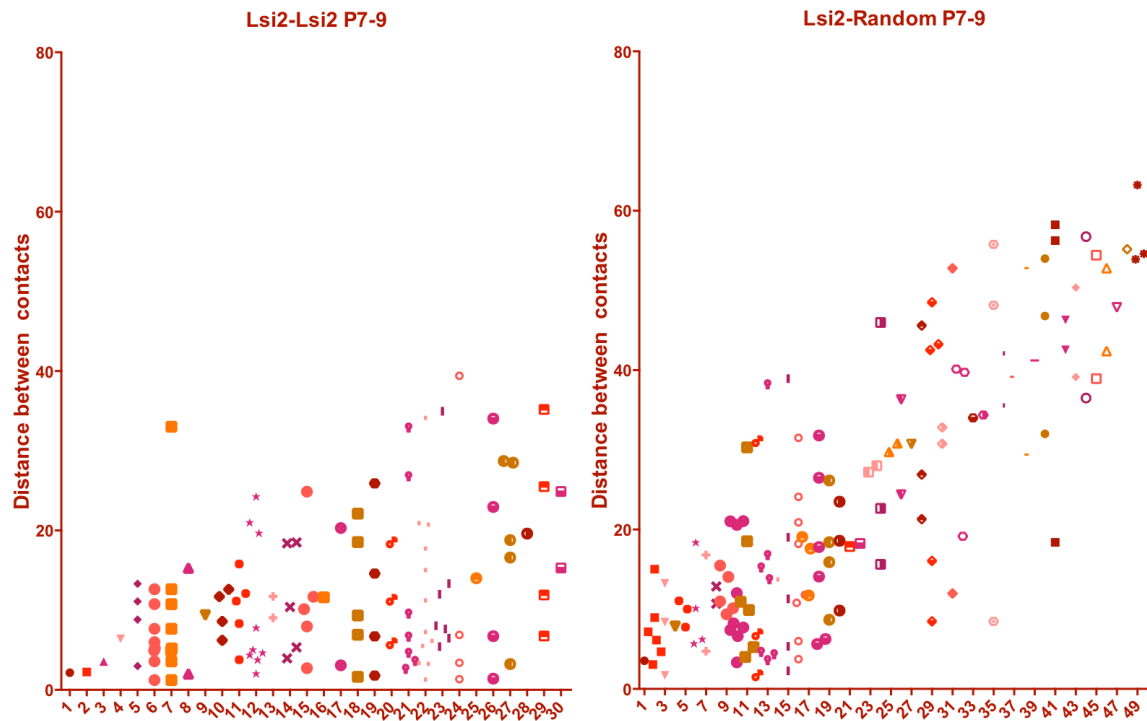


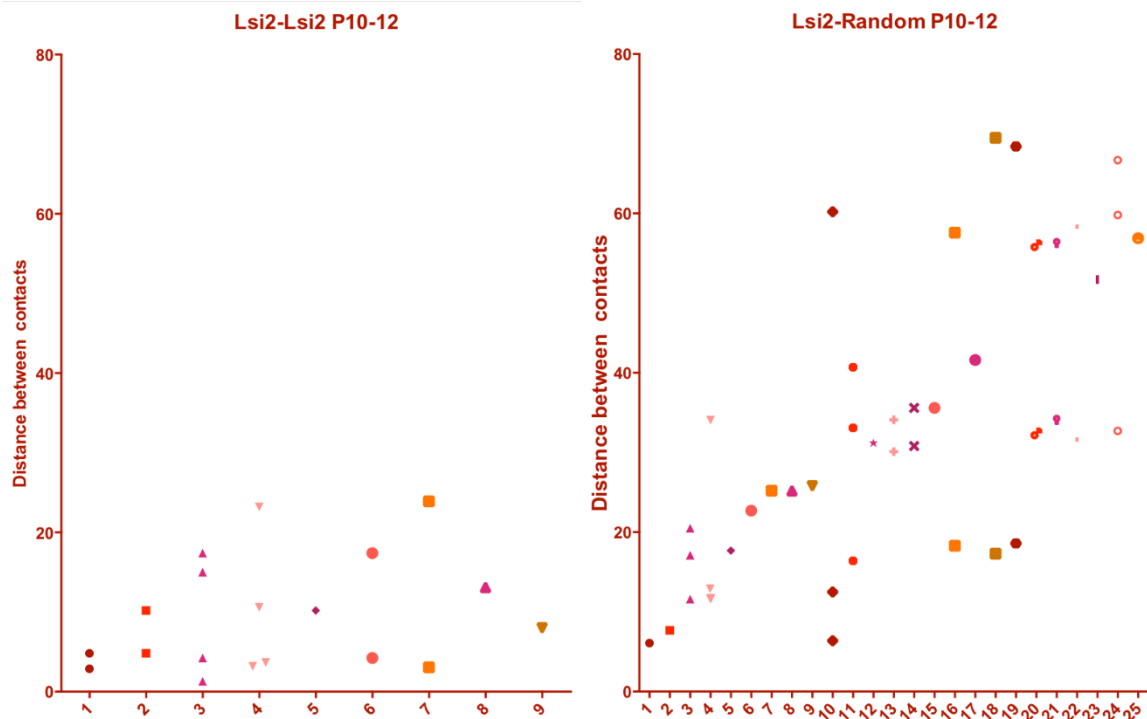
Figure 2.2.10 Individual cell analysis shows little or no alteration in Lsi2 connectivity. Each column in the graph represents a single CA3 cell and these are arranged in order of increasing mean distances between contacts(LMTs) (N= atleast 3 mice in each condition, N=2 for P10-12) a) Lsi2 LMTs are less clustered on Lsi2 CA3 in comparison with Lsi1.Lsi2 LMTs are sparsely connected to random CA3 b) Lsi2-Lsi2 connectivity in P5-7 L-NAME treated mice is altered and more spaced out. However Lsi2-random CA3 connectivity remains

unaffected c) and d) shows that there are no changes in the connectivity in P7-9 and P10-12 in Lsi2-Lsi2 connectivity as well as Lsi2-random connectivity.

c



d



In summary the Lsi1 preferential connectivity is severely altered in P5-7 L-NAME treated mice, partial persistence of this effect on P7-9 and no effect in P10-12 window whereas Lsi2 synapses are unaffected upon L-NAME treatment except a partial effect on Lsi2-Lsi2 connectivity in P5-7.

Characterization of postsynaptic architecture in CA3:

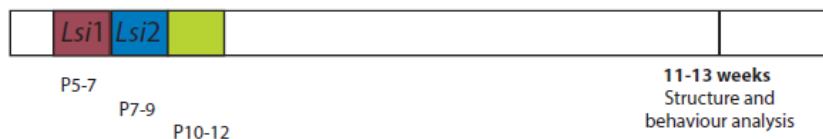
Since Lsi1 GC to Lsi1 CA3 is clustered at baseline, the corresponding postsynaptic architecture was studied in detail so as to understand the baseline differences in postsynaptic architecture if any. As mentioned in the introduction, LMTs make synapses on to CA3 through a specialized dendritic spine called thorny excrescences. There are around 42 excrescences per CA3 (Gonzales et al., 2001). Although the resolution of light microscopy is not suitable for analyzing dendritic structure in extreme details, we could identify the small and big clusters of excrescences and observe some single spines.

Generally, there was more thorny excrescence clusters in region CA3a and almost none of these clusters in CA3c. Hence, only cells from CA3b region was chosen for this study. In baseline, the large clusters were found both in Lsi1 and randomly labelled cells in dorsal whereas Lsi2 had almost no large clusters in both dorsal and ventral regions. In the ventral region, the large clusters were restricted to mainly Lsi1 (p value Lsi1 vs Lsi2 – 0.0001, Lsi1vs random- 0.0005). Upon P5-7 L-NAME treatment where Lsi1 forms more synapses on to random CA3 cell than onto itself, there is a rapid decrease in large thorny excrescence clusters (4.8 fold, P value =0.0006) in Lsi1, whereas this is distributed onto Lsi2 (6-fold increase in dorsal and 2 fold increase in ventral) and randomly labelled CA3 (2 fold increase in dorsal and 3 fold increase in ventral). Also the decrease in large clusters in Lsi1 is accompanied by increase in individual spines and single excrescences in Lsi1. The small clusters are not changed drastically like the other dendritic processes observed.

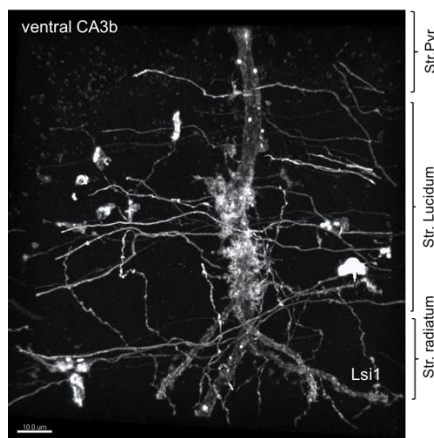
In P7-9 L-NAME treated mice, the predominant effect is the increased large clusters of Lsi2 in dorsal and ventral CA3b. There is a partial effect on Lsi1 as it does not lose all its large clusters like in the P5-7 window. P10-12 window does not show any change compared to the baseline.

In summary, the distribution of large TE clusters is always accompanied by clustering of Lsi1 pre-synapses both in baseline and in the different postsynaptic treatments.

a



b



c

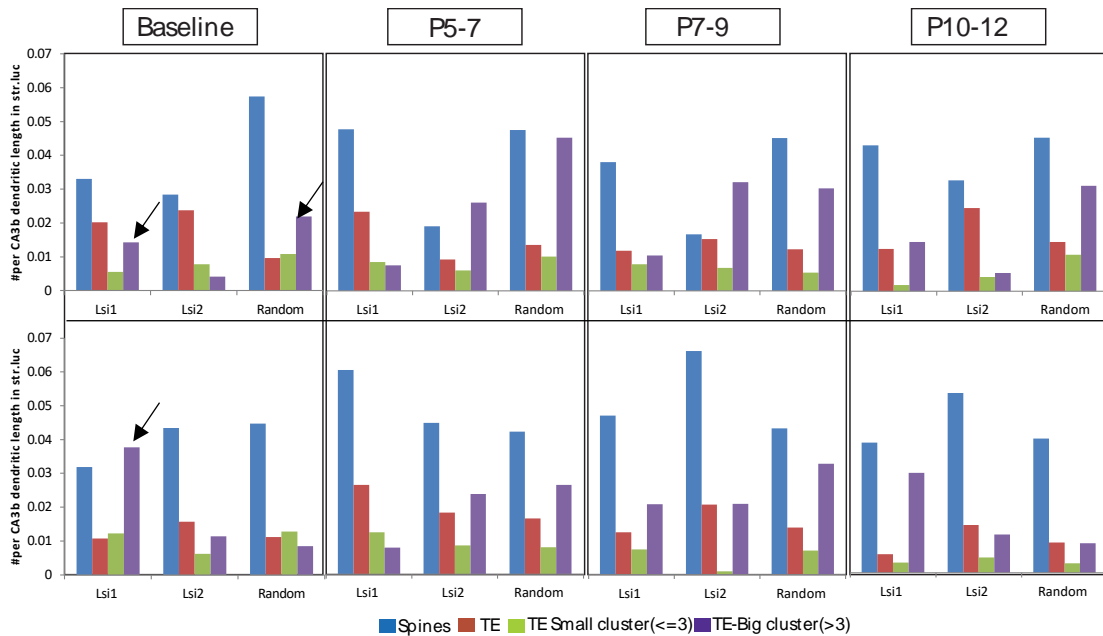


Figure 2.2.11 Postsynaptic structural analysis shows that there is increase in distribution of large thorny excrescence clusters in Lsi1 especially in ventral CA3b. a) Time line for the structural studies: Treatment with L-NAME

during early postnatal days and analysis at 11-13 weeks. b) example of ventral CA3b in Lsi1 with large thorny excrescence clusters in stratum lucidum. c) Quantification of number of single spines, single excrescences, small and big clusters of thorny excrescences normalized to length of dendrites in stratum lucidum. N=12-30 cells per condition.

Analysis of presynaptic connectivity in CA1:

Presynaptic connectivity analysis in CA3 has clearly elucidated the altered connectivity in P5-7 nitric oxide signaling blockade. To test whether this also affects the connectivity in CA1, the Schaffer collateral synapses were analyzed. For each CA1 cell be it Lsi1 or random , % of contacts with the boutons were quantified. In spite of significant changes in CA3 connectivity in P5-7, there was no corresponding change in CA1.

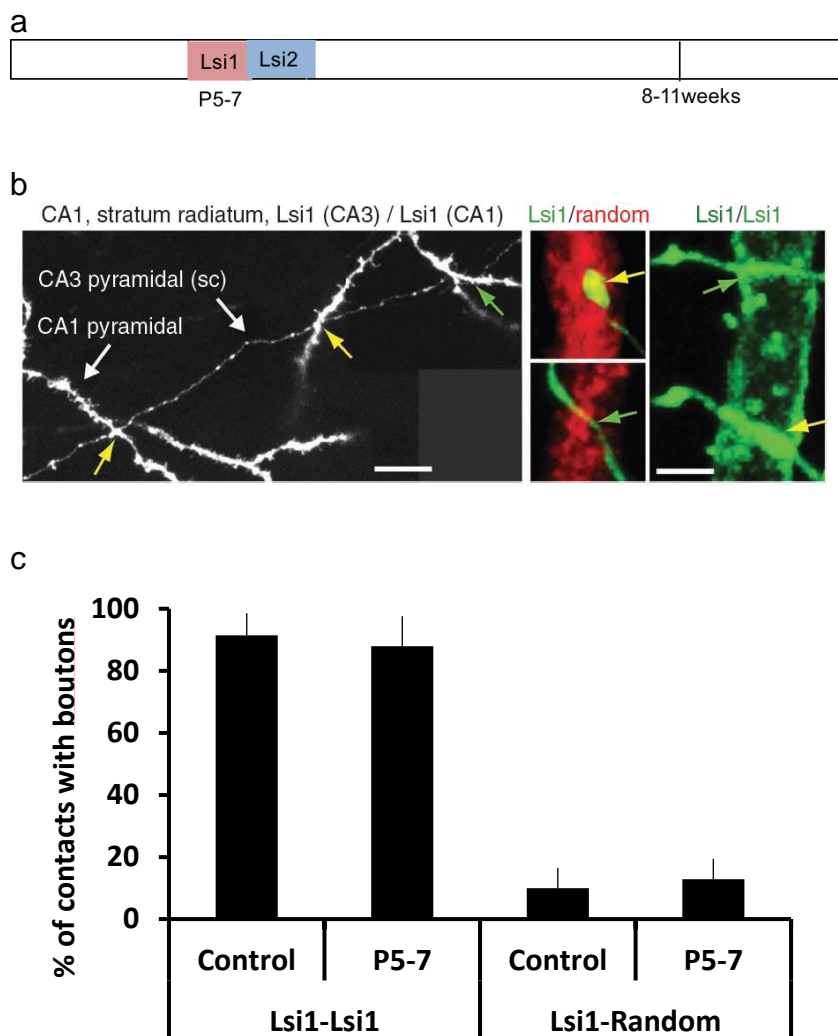


Figure 2.2.12 Selective connectivity analysis of Lsi1 in CA1 is not affected in P5-7 a) Time line for the structural studies: Treatment with L-NAME during P5-7 and analysis at 11-13 weeks. b) example of CA1 with Schaffer collaterals in stratum radiatum of CA1 c) Quantification of percentage of Schaffer collateral

boutons on Lsi1 or random CA1 pyramidal cell (N=3 mice per condition). Note that altered connectivity in CA3 upon P5-7 L-NAME treatment does not have an effect on CA1 connectivity.

2.2.3.3 Alteration in behavior and PV distribution upon developmental interference during principal neuron synaptogenesis

In order to test the effect of altered connectivity and developmental interference nitric oxide signaling on learning and memory, mice were subjected to various behavioral tasks and their inhibitory PV neuron distribution was quantified. Mice that underwent L-NAME treatment in different synaptogenic windows were tested for incidental memory by their ability to discriminate a novel object from a familiar object. Mice treated during Lsi1 window of synaptogenesis-P5-7 were very poor in this task (Discrimination ratio: 0.037, p<0.0001). In comparison to this, mice treated in Lsi2 synaptogenic window –P7-9 were better than the baseline (Discrimination ratio : 0.56, p value <0.0001). As a control, mice with P10-12 were tested and these were similar to the controls.

From earlier work in the lab, these opposite changes in the discrimination ratio were correlated to PV distribution in CA3b region (Donato et al., 2013). Hence, the distribution of PV interneurons in these mice were calculated. Mice that were poor learners had a high PV network configuration (p value – 0.0003) and mice that were better learners had low PV configuration (P value – 0.0039).

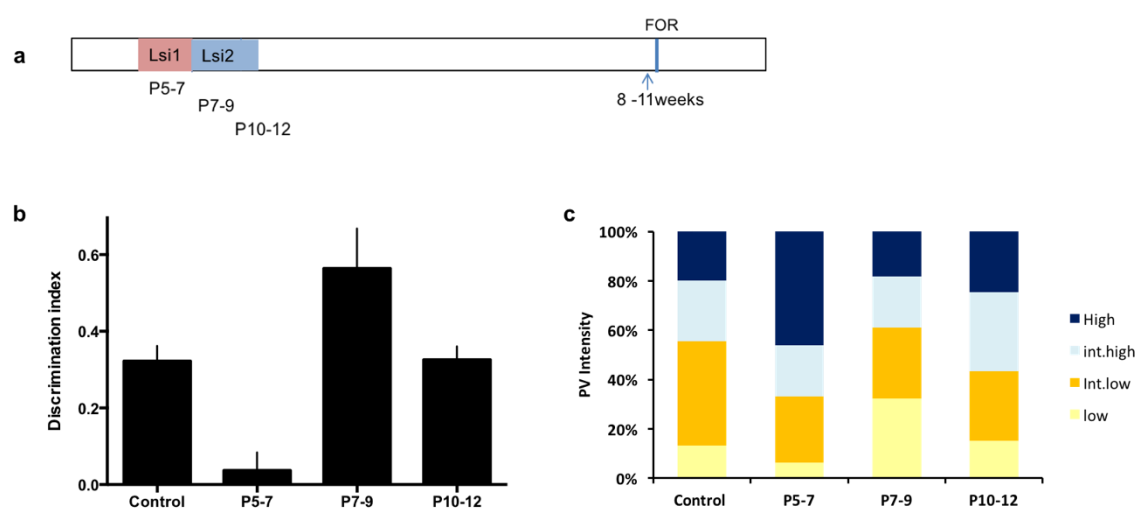
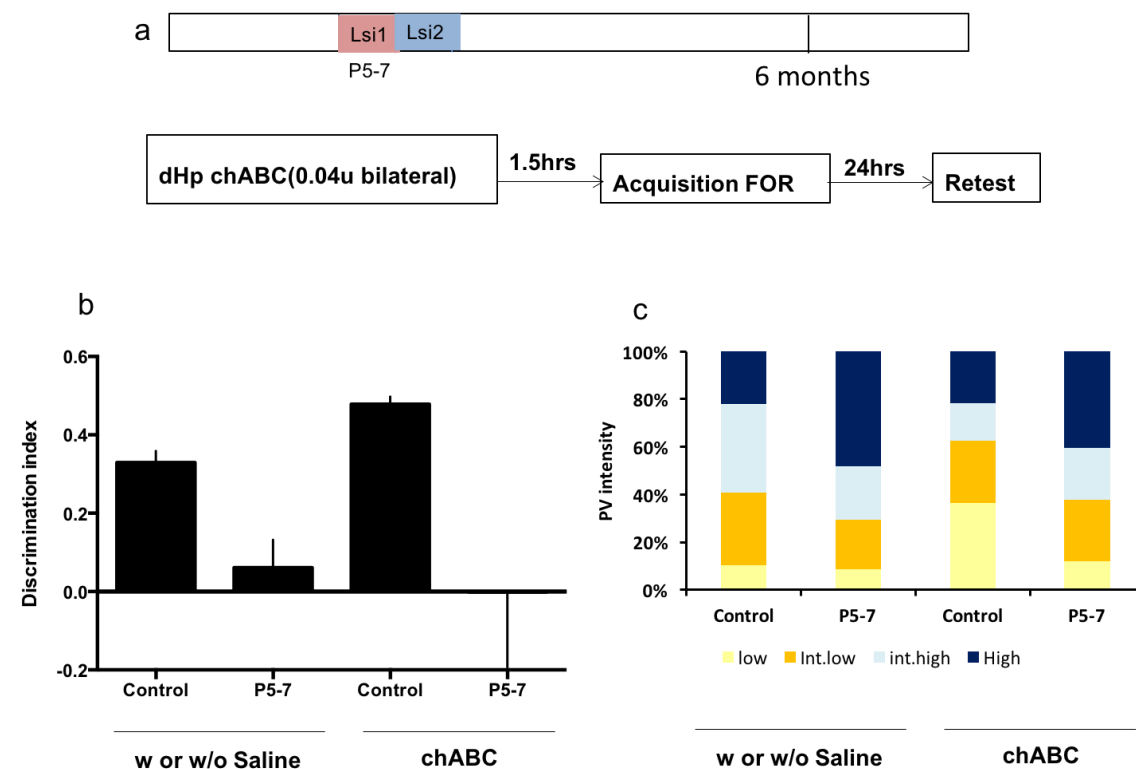


Figure 2.2.13 Familiar object recognition upon L-NAME treatment during development. a) Time line for the behavioral studies: Treatment with L-NAME during P5-7, P7-9 and P10-12 and analysis at 8-11weeks.b) Discrimination index of control and treated mice N= at least 7 mice per condition. Note that L-NAME treated mice shows opposing changes in discrimination index in P5-7 and P7-9

treatment, but no difference in P10-12 c) Distribution of PV cells in dorsal CA3b upon respective treatments (N= at least 5 mice per condition).

It has been shown that enzymatic digestion of PNNs (perineuronal nets) via topical application of Chondroitinase ABC can restore plasticity in the visual system of mice with developmental monocular deprivation during critical period of PV plasticity (Pizzorusso et al., 2002). In addition, treating with chondroitinase has been shown to change the PV configuration by increasing the low PV fraction (Donato et al., 2013). Also, behaviorally, environmental enrichment is known to increase the low PV network configuration. So, P5-7 L-NAME treated mice with high PV network configuration were subjected to both the biochemical and behavioral modification to test if the PV network there was plastic and if it is so, can it translate in the incidental learning task? Upon chondroitinase treatment, control mice showed better performance as well as increase in the low PV fraction. However, there was no increase in low PV fraction and no improvement in incidental memory in P5-7 L-NAME treated mice. Upon environmental enrichment for three weeks in P5-7 L-NAME treated mice, there was a decrease in high PV fraction (P value, 0.01), but there was no improvement in the behavior.



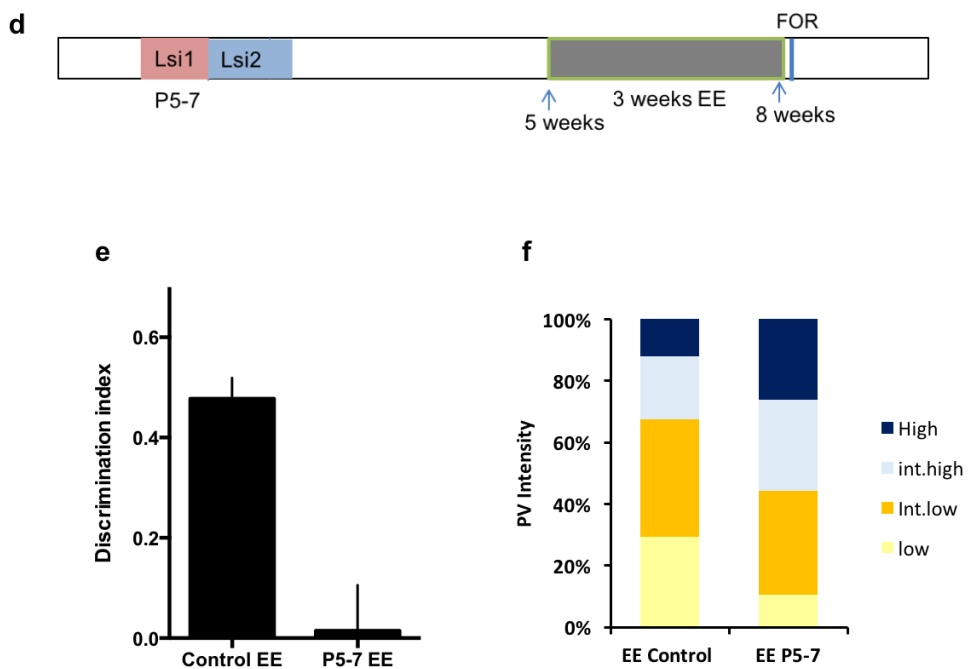


Figure 2.2.14 Biochemical or behavioral modification does not improve discrimination index in mice with altered connectivity in Lsi1 CA3. a) Time line for the behavioral studies: Treatment with L-NAME during P5-7 and protocol for chondroitinase treatment and FOR test. b) Discrimination index of control and treated mice N= 3 mice per condition. Note that L-NAME treated mice c) Distribution of PV cells in dorsal CA3b (N= 3). d) Time line for the behavioral studies: Treatment with L-NAME during P5-7 and protocol for FOR with environmental enrichment. e) Discrimination index of control and treated mice upon EE. (N= at least 10 mice per condition) f) Distribution of PV cells in dorsal CA3b (N= 5). Note that although PV distribution shows changes upon enrichment, there is no improvement in the behavior.

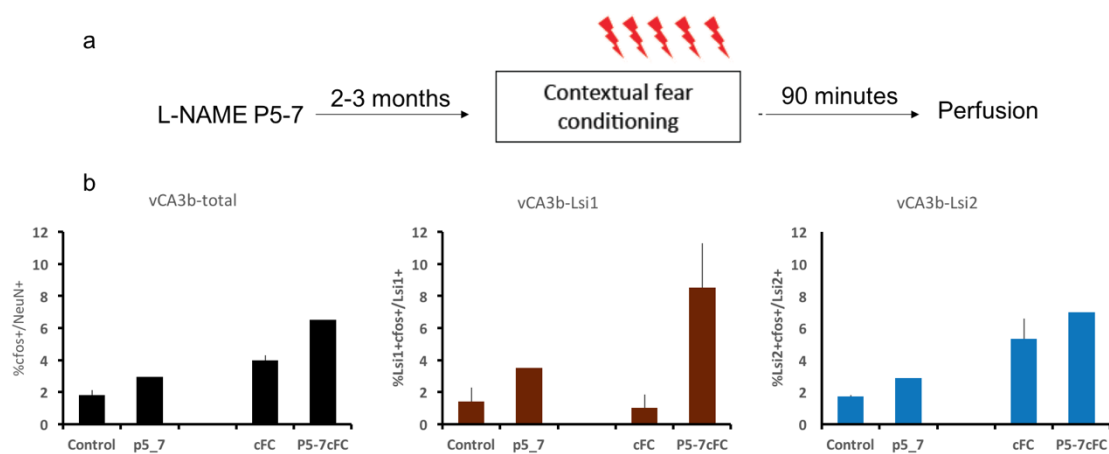


Figure 2.2.15 Analysis of c-fos upon cFC in control mice and mice with altered selective connectivity in Lsi1 shows abnormal induction of c-fos in Lsi1 cells. a) Protocol for behavior and c-fos analysis. b) Quantification of c-fos in ventral vCA3b (N=2-4 mice per condition)

Further, mice with altered synaptic connectivity in Lsi1 CA3 (L-NAME P5-7) were subjected to contextual fear conditioning task. These mice had reduced memory than their litter mate controls injected with saline (p value - 0.0091) when re-exposed to the training context. However, these mice were also generalizing the fear and was freezing more to the neutral context (p value, 0.0012) than the corresponding controls. Interestingly, t c-fos analysis post acquisition revealed an abnormal induction of c-fos in Lsi1 sub-population in ventral CA3b (P value- 0.0083).

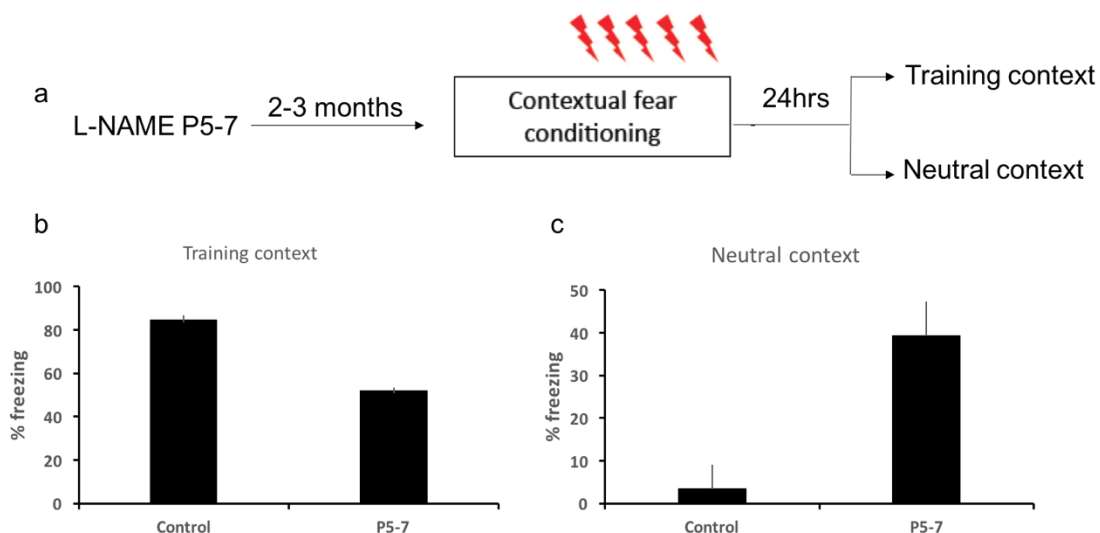


Figure 2.2.16 Behavioral analysis of mice with altered connectivity in Lsi1 shows poor learning in Lsi1. a) Protocol for behavior. b) % freezing time in training and neutral context (N= at least 4 mice per condition).

2.4 Discussion

Nitric oxide signaling allows selective access to hippocampal Lsi1 neuron function

Normally during development, multiple collaterals arise from the mossy fiber axons which then forms into LMT upon identifying the appropriate postsynaptic partner in CA3. This study demonstrates using organotypic slice cultures and pharmacology that blocking nitric oxide synthase during mossy fiber-CA3 synaptogenesis affects the stability of only Lsi1 both in *in vitro* and *in vivo*. The stability of Lsi2 LMTs remain unaffected. Nitric oxide and its receptors (soluble guanylyl cyclase) is known to be present early during development in hippocampus and is involved in regulating the synchronous activity between P5-8 even before GABA (Cserep et al., 2011). It is interesting that this timeline

overlaps with Lsi1 synaptogenic window. This could be a possible reason for Lsi1 LMTs to be affected by nNOS blockade. Anisomycin treatment was used to study the loss and recovery of putative active zones at LMTs *in vivo*. This treatment interrupts the supply of newly synthesized proteins post 9 hours in CA3 leading to a transient destabilization of synapses (Wanisch and Wotjak, 2008, Dieterich et al, 2010). This method has been previously used to study the behavior induced plasticity (Bednarek and Caroni, 2011, Donato et al., 2013). The synapses in pups (9hrs) recover much faster than in the adults (12hrs/24hrs). This could be due to differing mechanisms that exists during development and in a mature circuit. A very interesting finding in this study is the baseline difference in the synaptic plasticity between Lsi1 and Lsi2 in adults -- Lsi2 synapses turn over faster (12hrs) than Lsi1 synapses (24hrs). Additionally, even in adults, L-NAME affected only the Lsi1 synapses by rapidly increasing the turnover rate (6hrs) whereas Lsi2 remained unaltered.

Prevention of stability in Lsi1 during its synaptogenic window, could lead to competition for postsynaptic partners during the following (Lsi2) window of synaptogenesis which could then lead to alteration in connectivity in Lsi1 subpopulation. There have been previous observations that there could be structured connectivity in terms of synaptic density and clustering that are enhanced between temporally matched hippocampal neurons (Deguchi et al., 2011, Druckmann et al, 2014). So, the alternate connectivity hypothesis was tested using connectivity analysis in Lsi1 and Lsi2 by comparing the nature of synapses distribution on itself vs randomly labelled cells (Deguchi et al., 2011). Some of the very interesting findings from this study include the following. 1) The baseline distribution of Lsi1 GCs–Lsi1 CA3 cells were clustered but Lsi2-Lsi2 was not. 2) This also was accompanied by presence of large clusters of postsynaptic thorny excrescences (TE) in Lsi1 and not in Lsi2. 2) L-NAME in P5-7 window led to clustering of Lsi1 presynapses onto random cells instead onto itself. 3) Lsi2 remained largely unaffected by this treatment, 4) This connectivity change in CA3 did not affect the further change in connectivity in CA1.

As mentioned earlier an interesting correlation in this study is the presence of large clusters of TE in post synapse is always accompanied by the clustering in the Lsi1 presynapses. During the course of TE spinogenesis, there is a large increase in the spines per LMT at P14 after which the extra spines are pruned to

the adult state (Wilke SA, 2013). Additionally, around the same timeframe specification of terminal Arborization of LMTs happens in the CA3 (Galimberti et al., 2010). Further experiments in this direction could help to identify if Lsi1 LMTs/TAs are responsible for maintenance of the large clusters of TEs in adults.

Role of selective connectivity in learning

The P5-7 L-NAME treated mice were further used in different learning tasks as the severity in Lsi1 connectivity changes was much larger than the other treatment windows. Mice with altered connectivity in CA3 had poor memory in incidental learning task and contextual fear conditioning. These mice also had a marked increase in the baseline high PV fraction in CA3. Although this could explain the poor performance in FOR (Donato et al., 2013), it is interesting that biochemical modification could not change the PV network configuration. On the contrary, upon enrichment the PV network configuration could be altered to baseline levels. Intriguingly, this could not bring a change in performance of FOR in these mice. This could be due to an altered connectivity in Lsi1 in CA3. Individual scoring and analysis of the behavior also showed that these mice actively explore both the objects equally and their poor performance is not due to inactiveness or extended exploration of only the familiar object.

Further, these mice had a slightly higher c-fos levels in vCA3b even at baseline. However, upon acquisition of cFC, these mice not only had a slight increase in c-fos induction in general population but also had an abnormal increase of c-fos in the Lsi1 subpopulation. It is extremely interesting that the altered connectivity in Lsi1 allows for altered recruitment of Lsi1 subpopulation in learning. In addition, these mice also freeze less in the training context and generalizes the fear memory in a neutral context. In parallel, there is also an increased FFI in Lsi1 at baseline but no induction of FFI post learning. Previously it has been shown that altering the FFI connectivity post acquisition could lead to generalization of fear memory (Ruediger et al., 2011). Further study to understand if there are specific interneurons that are recruited by these different subpopulations in learning would be central to support the impact of these subpopulations in learning.

Hence by combining pharmacological, structural and behavioral approach, it is clear that alteration in Lsi1 connectivity leads to poor learning.

3.General Discussion and Outlook

Differential recruitment of principal neuron subpopulation in learning and the contribution of selective connectivity

The main goal of my thesis was to understand the role of segregated Lsi1 and Lsi2 pathways from DG to CA3 to CA1 in the hippocampus. The role of hippocampus in different learning paradigms have been earlier identified through lesion studies (Philips and Le doux, 1992; Kim and Fanselow, 1992). Later studies showed that memory traces could be recognized using immediate early genes (IEGs) like c-fos, arc, zif268 (Guzowski et al, 1999, Barot et al., 2008, Marrone et al., 2008). The results presented in this thesis provide evidence that these hippocampal parallel circuits (Lsi1 and Lsi2) are recruited differentially in different types of learning through c-fos and early activity markers post different types of learning. Lsi1 is recruited for transient learning (FOR, initial days of MWM and one trial massed extinction) and Lsi2 for definite learning paradigms (cFC and later stages of MWM). Interestingly, both the subpopulations are recruited post acquisition of massed extinction paradigm which ideally fits with the fact that this memory trace now has both the fear component and a new component encoding for extinction. Similar results have been earlier described in amygdala as fear and extinction neurons distinguished by their activity patterns and distinct connectivity across different brain regions (Herry et al, 2008). It could be interesting to know if such distinct connectivity patterns exist also for Lsi1 and Lsi2 subpopulations. Previous studies in the development of cortical circuitry have showed that neurons from the same progenitor tend to be interconnected and share similar responses to stimuli later as adults (Yu et al., 2009 , Li et al., 2012). The results presented in the first part of the thesis thus points that the hippocampus is not only organized in well defined microcircuits (Deguchi et al., 2011, Druckmann et al, 2014) but these are functionally different as well. Apart from this it has been shown that novelty detection relies on dopaminergic receptors in hippocampus during acquisition (Lemon and Manahan-Vaughan, 2012). So it could be interesting also to see if there is any difference in neuromodulatory response in these two subpopulations.

Recent advances have also led to selective tagging and manipulation of the c-fos expressing cells post learning (Liu et al., 2012, Garner et al., 2012, Ramirez et al, 2015). Although this method allows for selective tagging of c-fos cells it does have some contamination of both the subpopulations even at

baseline and is difficult to target just one subpopulation through this method. However, from experiments in organotypic slice cultures it was evident that nitric oxide signaling specifically alters Lsi1 synapse stability and allows for selective manipulation of this sub circuit. When the preferential connectivity in Lsi1 is altered, it leads to distorted recruitment of these circuits which further leads to poor learning and memory in mice. An interesting correlation is that the nitric oxide synthase is also regulated by FMRP (Fragile X mental retardation protein) (Kwan et al., 2012). The loss of function of FMRP is one of the leading monogenic cause of intellectual disability and autism (Rogers et al., 2001, Abbeduto et al., 2007, Willemsen et al., 2011). It could be interesting to further know if there is any relation to fragile X syndrome models especially with respect to Lsi1 subpopulation connectivity and function.

The recruitment of the principal neurons – Lsi1 and Lsi2 interestingly coincides with low and high PV mediated learning. Lsi1 is recruited for transitory and exploratory learning. This could possibly be mediated through the large clusters of synapses in CA3. As LMTs are detonator synapses, such clustering could further aid the information in reaching the CA3. On the other hand, when learning is definite, Lsi2 are recruited and Lsi1 are possibly actively inhibited by the high PV network configuration (paired recordings between Lsi1 and embryonically labeled PV neurons could help understand if this is the case). Whenever Lsi2 is active, the filopodia in Lsi1 is induced and the PV network configuration also is high. It is known that increase in FFI connectivity provides excitation to PV neurons thereby recruiting the early born PV neurons (Donato et al., 2015). This in turn could actively silence the Lsi1 principal neurons. In support of this hypothesis, in Lsi1 preferential connectivity altered mice shows no induction of filopodia upon fear conditioning and there is also recruitment of Lsi1 in c-fos ensemble. Additionally, there are basic structural differences in Lsi1 and Lsi2 that could further explain their differential participation in different learning tasks. For example, 1) the presynaptic LMT terminals are clustered in Lsi1 whereas Lsi2 has no clustering; 2) Lsi1 CA3b cells have higher number of large TE clusters whereas Lsi2 does not; 3) The FFI connectivity in baseline is already high in Lsi2 but Lsi1 has a low baseline which can be induced upon relevant behavioral tasks; 4) There are differences in recovery of synapses post

anisomycin where Lsi2 is faster than Lsi1.5) The distribution of highly plastic terminals TAs are different for different in Lsi1 and Lsi2 (Galimberti et al., 2010).

In conclusion, these results provide insight about the role of parallel circuits in hippocampus during different forms of learning and provides stronger evidence that hippocampal circuits use biased connectivity to extract and process specific types of information.

Outlook:

To understand the role of the parallel circuits in the hippocampus is not only important for knowing the machinery of hippocampal learning but also to get insight into basic rules of learning and memory. Therefore, the work from my thesis can be further used to study the role of these parallel circuits in recruiting specific interneuron populations during learning. This could further enhance the knowledge on how memory is encoded. Knowing if such parallel microcircuits exists in other parts of the brain would be central in understanding how these subpopulations described in this thesis could support learning in a generalized manner. Gaining genetic access to these subpopulations could be extremely useful in further interference of learning and memory by selectively activating or inhibiting these subpopulations. Such an approach could help in understanding the involvement of these subpopulations in both normal and pathological conditions like schizophrenia and autism. Recently a new technique to render Cre-recombinase activity to GFP+ cells (Tang JCY et al., 2015) have been developed that could possibly be used to modify these subpopulations and to know the functional connectivity patterns of these two subpopulations with other regions in the brain.

4.Materials and Methods

4.1 Mice

Transgenic mice expressing membrane-targeted GFP in a small subset of neurons (*Thy1-mGFP Lsi1* and *Thy1-mGFP Lsi2*) were used (De Paola et al., 2003; Galimberti et al., 2010). PV neurons labelling was achieved via breeding of a PV-cre line with Rosa-CAG-STOP-tdTomato (both as a kind gift from Silvia Arber, Basel).

Mice were kept in temperature-controlled rooms on a constant 12h light/dark cycle. Before the behavioral experiment, mice were housed individually for 2–3 days and provided with food and water ad libitum unless otherwise stated. All experiments were in accordance with institutional guidelines and were approved by the Cantonal Veterinary Office of Basel Stadt, Switzerland.

4.2 Behavioral experiments:

All behavioral experiments were carried out with mice that were 2-3 months old at the onset of the experiment.

4.2.1 Contextual fear conditioning- One time associative learning task:

The contextual fear conditioning experiment was carried out as described (Ruediger et al., 2011). Briefly, the conditioning chamber (rectangular in shape) was cleaned with 2% acetic acid before each session. Once placed inside the fear-conditioning chamber, mice were allowed to freely explore the apparatus for 2.5-3 min and then received five foot shocks (1 second duration and 0.8 mA each, inter-trial interval of ~30s). To test for contextual fear memory (recall), mice were re-introduced to the same conditioning chamber 24 hours later for 5 minutes but with no shock. For the extinction experiments, mice were re-introduced to the conditioned chamber 72 hours later but for 30 minutes. The freezing responses were quantified in 6 consecutive bins of five minutes each. In order to test for generalization of fear memory, mice were exposed to a neutral context (cylindrical in shape) for 5 minutes at~18 hours post acquisition and subsequently taken to the conditioning chamber for a recall experiment 5 hours later.

All the experiments - acquisition, recall, extinction and generalization sessions were digitally recorded and fear retention was measured as the percentage of time spent freezing excluding the first 2 minutes of exposure. Freezing was

defined as the complete absence of somatic mobility, except for respiratory movements.

4.2.2 Environmental Enrichment (EE):

For some initial experiments, 4-6 five-week-old mice were housed for 3 weeks in a large cage (rat cage) containing running wheels tunnels, houses and toys for exploration. The order of toys in the enrichment cage was changed after each week. For later experiments, 3-4 mice that are 7-8 weeks were kept in the enrichment cage for a week. Some of the above mentioned enriched animals subsequently were tested for familiar abject recognition.

4.2.3 Familiar object recognition (FOR)- Incidental memory task:

Mice explored two identical objects placed in a 30 × 50 cm arena (10 min exploration) on day one, returned to their home cage immediately after training and were tested for FOR 24 h later, when one of the two objects had been replaced with a new one (5 min exploration). Discrimination indices were calculated as $(t_{\text{novel}} - t_{\text{familiar}})/(t_{\text{novel}} + t_{\text{familiar}})$ where t_{novel} and t_{familiar} are time spent with novel and the familiar object respectively. To avoid discrimination of the objects based on odor, both the arena and the objects were thoroughly wiped with 70% ethanol before and after each trial.

4.2.4 Morris Water Maze (MWM) – Incremental learning task:

The Morris water maze experiment was carried out as stated in Ruediger et al., 2012. Briefly, the Morris water maze consists of a 140-cm pool filled with opaque water surrounded by three different objects placed as reference cues around the pool. The temperature of the water was kept constant at 23°C throughout the experiment. A circular escape platform (10 cm diameter) was either submerged above (0.5cm) or below the water surface for the visible and invisible trials respectively. Mice were trained to find the platform during four trials a day (1 minute each), with inter-trial intervals of 5 min. On day 1, mice underwent training with the visible platform and were guided to the platform if they were unable to find it. From second day on, invisible platform was used and was kept in the opposite quadrant for the subsequent training days across the trials. Swim controls were done with mice undergoing the same protocol but without any platform. Data collection and analysis from training sessions and probe trials were done using Viewer2 Software (Biobserve, Bonn, Germany).

4.3 Tissue preparation:

4.3.1 Slice cultures:

Hippocampal slice cultures of appropriate ages were prepared as described in Gogolla et al., 2006 from Lsi1 and Lsi2 pups. Briefly, 400 μ m hippocampal slices were cut and incubated for 30 minutes at 4°C in the dissection medium. Healthy slices were then plated on Millipore filters with culture medium in 6 well plates and incubated at 37°C thereafter. Further these slice cultures were used from div3 to div 6 for time-lapse imaging (Gogolla et al., (b), 2006).

4.3.2 Fixed tissue preparation:

Mice were transcardially perfused with cold 4%PFA (pH7.4) and the brains were collected and kept in 4%PFA overnight at 4°C. For c-fos analysis mice were perfused 90 minutes after the behavioral protocol. For pCREB and pERK analysis, mice were perfused 15 minutes after the behavioral protocol.

Structural analysis of the hippocampal pyramidal neurons and mossy fiber axons/terminals were done on transverse hippocampal sections. Hippocampi were dissected out, embedded in 3%agarose gel and sliced at ~100 μ m thickness transversally on a tissue chopper (McIlwain) along the entire dorsoventral axis so as to preserve the lamellar architecture for analysis. The same procedure was used for analysis of active zone density in the LMTs both in pups and adults.

For all other immunostaining, the brains post overnight fixation was kept in 30% sucrose overnight. 40 μ m coronal sections were then prepared using cryostat.

4.4 Immunohistochemistry:

Antibodies and its concentration used are as follows: primary antibodies chicken-anti GFP (abcam), 1:1000; mouse anti-Bassoon (Stressgen, clone SAP7F407) 1:200; goat anti-PSD95 (abcam) 1:200; Rabbit anti-RFP (Rockland) 1:1000 Goat anti-PV (Swant biotechnologies) 1:5000; rabbit anti-c-Fos (Santa Cruz), 1:7000; mouse anti-NeuN (Millipore), 1:1000; rabbit anti-pCREB (Cell signaling), 1:800; rabbit pERK (Cell signaling), 1:500; rat anti-BrdU(abcam)1:500.

The standard immunohistochemistry procedure was as follows: free floating transverse / coronal sections were blocked for an hour at room temperature with 3 % BSA in PBS-0.3%Triton X-100 (PBS-T) followed by incubation in primary antibody solution in 3%BSA, PBS-T overnight at 4°C, washed 3 times in PBS-T

for 20 minutes each, further incubated in secondary antibody solution in 3%BSA, PBS-T at room temperature for 2-3 hours and subsequently washed 3 times in PBS for 20 minutes each. Later, sections were mounted in Prolong Gold antifade reagent (Molecular probes), coverslipped and kept at room temperature overnight, sealed with transparent nail polish and stored at 4°C until imaging.

For Bassoon immunochemistry, the primary antibody incubation was done at room temperature and rest of the protocol was the same. For c-fos immunochemistry the initial blocking for 1 hour before primary antibody was done in PBS-T with 10 % BSA and the rest was the same.

BrdU labeling *in vivo* was as described (Wojtowicz and Kee,2006). Mice were injected with BrdU at defined times during embryonic development, and hippocampal sections were analyzed for BrdU labeling in the adult. Only strongly BrdU-labeled cells that did not undergo further rounds of DNA replication and cell division subsequent to BrdU incorporation were included in the analysis.

4.5 Drug delivery:

L-NAME (N^{ω} -Nitro-L-arginine methyl ester hydrochloride) (abcam Biochemicals) was injected subcutaneously at 60mg/kg bodyweight. For repeated injections the time interval between subsequent injections was 24 hours. Anisomycin (Applichem) was injected subcutaneously at 50mg/kg bodyweight. Slice cultures were treated with L-NAME (200 μ M) for the required number of days with 24 hours interval.

4.6 Stereotactic surgeries:

Lentiviral injections:

Lentiviral constructs were a generous gift from Pavel Osten (CSHL, Dittgen et al., 2004); cytosolic GFP was replaced in the expression cassette by the mGFP sequence (Bednarek and Caroni, 2011). It was used to randomly label the granule cells of the dentate. Stereotaxic coordinates used to target the dorsal DG are as follows: bregma -0.9 (posterior), 1.82 (lateral), 2.15 (down).

Mice were further used for pharmacologic treatment to test for synaptic plasticity with or without L-NAME 20 days later.

Rabies injections:

Rabies-mCherry was a generous gift from S.Arber and was used to randomly label the CA3 and CA1 pyramidal cells in 3 month old mice. The coordinates used are as follows: Dorsal CA3: bregma -1.8 (posterior), 2.4 (lateral), 2.15 (down); Ventral CA3: bregma -2.75 (posterior), 2.9 (lateral), 3.55 (down); CA1: bregma -2.18 (posterior), 2.7 (lateral), 1.45 (down).

Drug delivery:

Chondroitinase () was delivered topically to the dorsal CA3b (bregma -1.8 (posterior), 2.4 (lateral), 2.15 (down)) to dissolve the PNNs 1.5 hours before acquisition of familiar object recognition.

4.7 Imaging:

For imaging of organotypic slice cultures, slices were placed in 2ml of physiologic Tyrode salt solution (Gogolla et al., 2006) at 37°C and imaged using 40X water objective of Olympus Bx16 LSM Fluoview. To follow the synaptogenesis of mossy fiber synapses of Lsi1 and Lsi2, two different resolutions of time lapse imaging was done-1) 24 hrs interval for 3 days 2) 3 hours interval for 2 days.

For high resolution imaging of LMTs and thorny excrescences in fixed tissue, transverse sections were imaged in 63x oil immersion objective of Zeiss LSM 700 confocal microscope. CA3/CA1 pyramidal cells that were GFP+/mcherry + were imaged with all its branches in stratum lucidum/stratum radiatum respectively for further selective connectivity analysis. For all other imaging of fixed tissue, 40x oil immersion objective of Zeiss LSM 700 confocal microscope was used. All samples for further intensity analysis, belonging to the same experimental set were processed in parallel and acquired with the same settings.

4.8 Image analysis and data quantification:

All the image analysis was done using Imaris (Bitplane). XUV tools was used in order to stitch the images.

Individual GFP+ granule cell axons in CA3b obtained from time-lapse imaging of organotypic slice cultures were traced and the changes along the axons- collateral formation, transition of collateral to LMTs, disappearance of collaterals/LMTs across the time were arranged and further stability of the synapses and the number of collaterals were recorded.

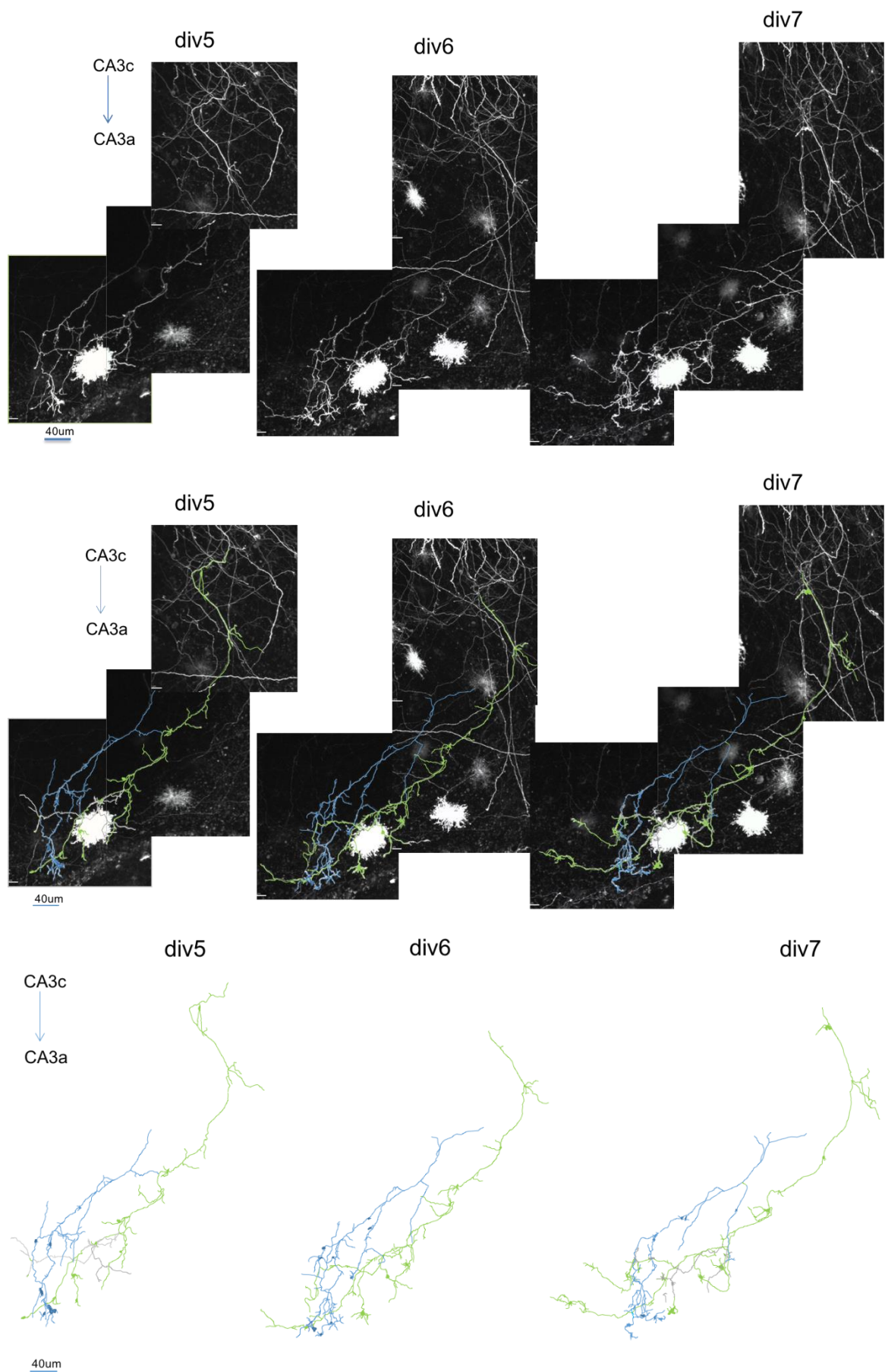


Figure 4.1 Example traces of time lapse imaging.

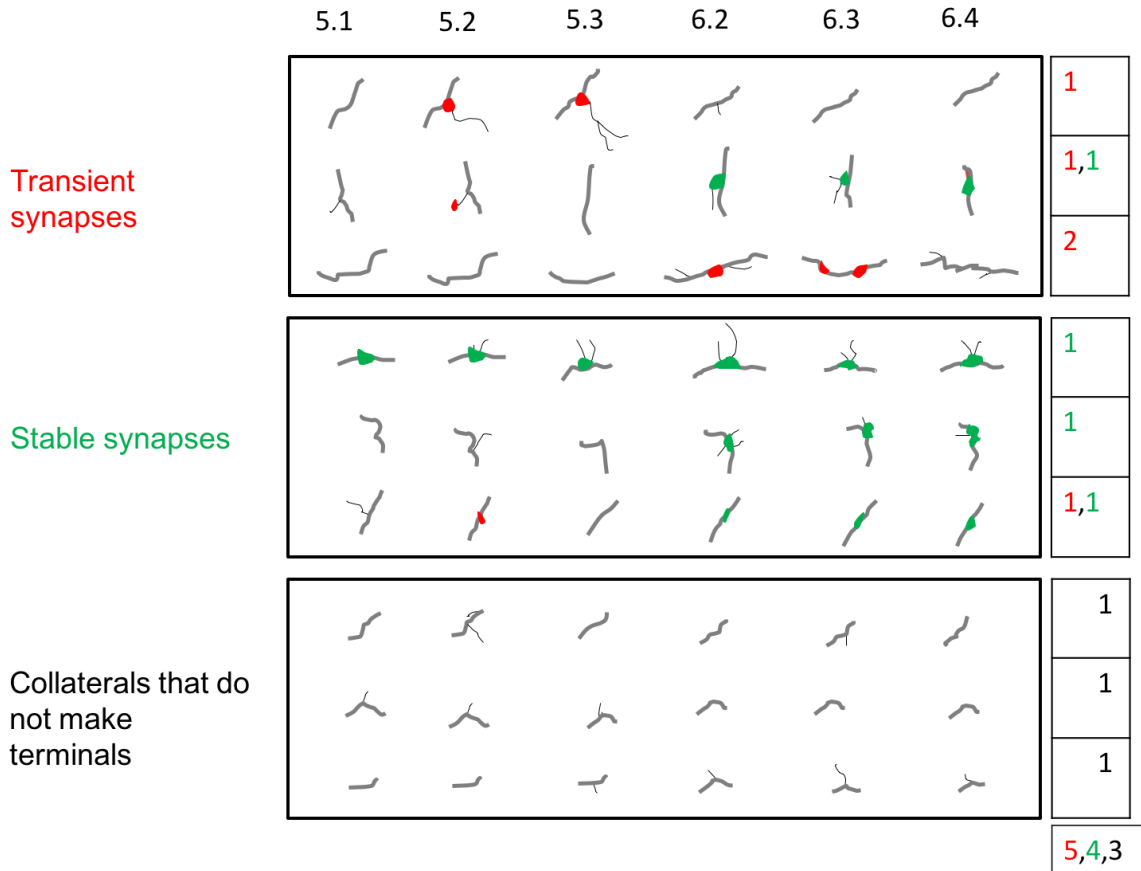


Figure 4.2 Example for quantification of transient and stable synapses and collaterals that do not make terminals.

For selective connectivity analysis between DG and CA3, the procedure was followed as in Deguchi et al., 2011. Briefly, contacts between presynaptic mGFP-positive Lsi1 (or Lsi2) mossy fiber terminals and mGFP+ and mCherry+ (randomly labeled) postsynaptic CA3 pyramidal neurons were analyzed. We considered as putative contact sites only events in which the distance between mossy fiber terminals ($>3 \mu\text{m}$ diameter) and pyramidal neuron dendrites was smaller than $0.2 \mu\text{m}$. Distance between consecutive contact sites in stratum lucidum was measured using Imaris for each CA3 pyramidal neuron. For further characterization of the postsynaptic CA3 dendritic architecture in CA3, dendritic components were classified as single spines, single thorny excrescences (TE), small clusters of TE (≤ 3 TE), large clusters of TE (>3 TE). Numbers of these processes along each CA3 pyramidal neuron analyzed were normalized to the length of its dendrites in stratum lucidum.

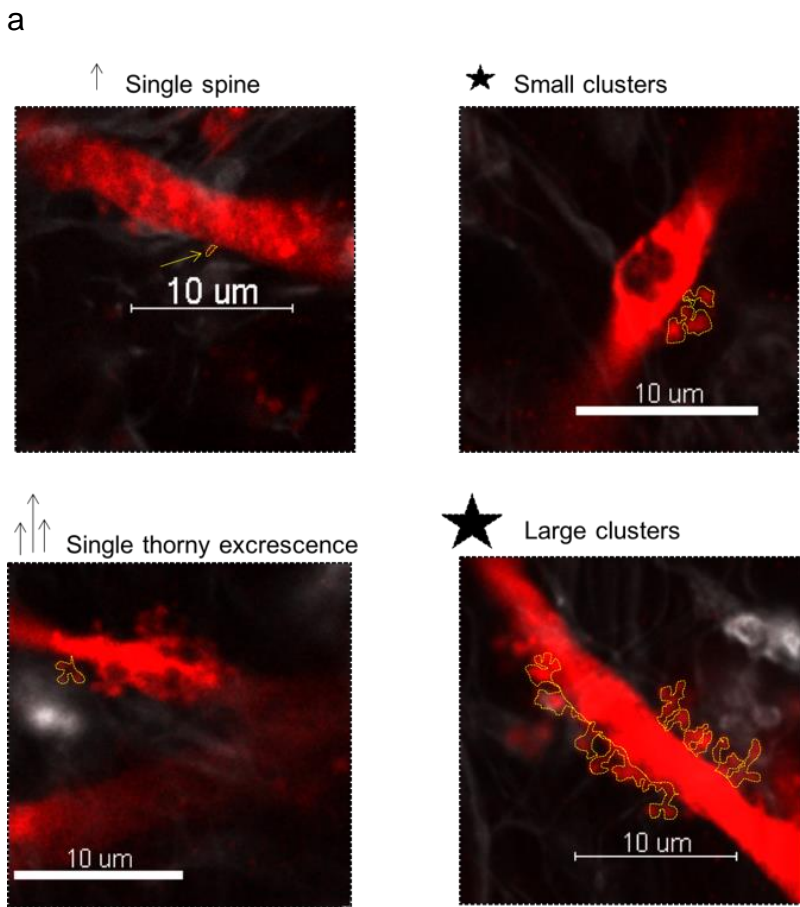


Figure 4.3 Example for characterization of postsynaptic architecture. Images in single confocal plane. Example for single spine, small clusters, small and big thorny excrescence clusters are shown.

For selective connectivity of CA3-CA1, the same procedure in Deguchi et al , 2011 was followed. Putative synaptic contacts between mGFP-positive Schaffer collaterals (the axons of CA3 pyramidal neurons) and mGFP-positive /m-cherry positive CA1 pyramidal neurons in stratum radiatum were analyzed.

These contact sites were defined as distances of less than 0.2μm (single confocal sections) and contacts were counted as synaptic when they involved an axonal bouton (varicosity) of at least 1μm diameter. Number of contacts and number of passes (axons at distances of less than 0.2μm from the dendrite) were calculated per CA1 cell (in stratum radiatum) that was mGFP+/mCherry+.

For c-fos analysis, fos+ cells were selected according to signal intensities using an automatic detection (spot detection in Imaris: expected radius,10μm) and binned as medium ($>550 < 750$) and high (>750) cfos cells. The number of

cfos + cells were normalized to total NeuN+ cells in the same section. Further, using the orthoslicer mode, in Imaris, each optical section was scanned to detect the mGFP + soma, and Fos+ (medium and high) GFP+ were quantified and normalized to the total GFP+ cells analyzed per region per mouse. Since the mGFP expression is variable from mouse to mouse, only when there could be at least 50 cells collected from CA1 and CA3 and 100 cells from DG from the ventral hippocampus, the mouse was taken for analysis.

pERK+ mGFP + cells were selected similar except that all pERK+ cells were used for quantification and were not binned. Since pCREB was present in all NeuN+ cells, the increase in intensity was quantified based on baseline expression of pCREB in cage controls. For each mGFP+ soma, pCREB intensities were quantified and the distribution were compared between the cage controls and post acquisition of contextual fear conditioning. A higher cut off was chosen for region CA3 as CA3 had already a very high baseline than CA1.

For active zone density calculation in LMTs, mGFP+ or mRFP+ LMT were cropped (Imaris) and each of these LMT isosurface (smoothness:0.2 μm) was masked and number of bassoon punctas were detected using semi-automatic spot detection(radius:0.5 μm) in Imaris and normalized by the volume of LMTs. Further the active zone turnover upon anisomycin treatment was expressed as a function of time and the values were expressed as fold changes over control values in the absence of anisomycin (Bednarek and Caroni, 2011).

Parvalbumin intensity analysis was done as in Donato et al., 2013. Briefly, the soma of PV neurons with optimal staining (dampening of intensity between the first and last confocal plane <15%) were isolated in three dimensions (Imaris). Three-dimensional isosurfaces (smoothness: 0.5 μm) were created around each PV-neuron soma and labeling intensities were quantified automatically in arbitrary units as the mean of all isolated pixels. The PV cells were then classified as low, intermediate low, intermediate high and high based on their intensities.

4.9 Statistical analysis:

All statistical analyses were performed using GraphPad Prism 6 (GraphPad Softwares). Unless otherwise stated, statistical groups were compared using unpaired, nonparametric Student's *t*-test (Mann–Whitney test). Average values are expressed as means \pm s.d

5. Bibliography

Abbeduto L, Brady N, Kover ST (2007). Language development and fragile X syndrome: Profiles, syndrome-specificity, and within-syndrome differences. *Mental Retardation and Developmental Disabilities Research Reviews*. **13**(1): 36-46.

Acsady L, Kamondi A, Sik A, Freund T, Buzsáki G (1998). GABAergic cells are the major postsynaptic targets of mossy fibers in the rat hippocampus. *Journal of Neuroscience*. **18**(9): 3386-3403.

Amaral DG (1978). A golgi study of cell types in the hilar region of the hippocampus in the rat. *The Journal of Comparative Neurology*. **182**(5): 851-914.

Amaral DG, Dent JA (1981). Development of the mossy fibers of the dentate gyrus: I. A light and electron microscopic study of the mossy fibers and their expansions. *The Journal of Comparative Neurology*. **195**(1): 51-86.

Amaral DG, Ishizuka N, Claiborne B (1990). Neurons, numbers and the hippocampal network. *Progress in Brain Research* **83**: 1-11.

Amilhon B, Huh Carey YL, Manseau F, Ducharme G, Nichol H, Adamantidis A, Williams S (2015). Parvalbumin interneurons of hippocampus tune population activity at theta frequency. *Neuron*. **86**(5): 1277-1289.

Anderson SA (1997). Interneuron migration from basal forebrain to neocortex: Dependence on dlx genes. *Science*. **278**(5337): 474-476.

Bannerman DM, Sprengel R, Sanderson DJ, McHugh SB, Rawlins JNP, Monyer H, Seeburg PH (2014). Hippocampal synaptic plasticity, spatial memory and anxiety. *Nature Reviews Neuroscience*. **15**(3): 181-192.

Barot SK, Kyono Y, Clark EW, Bernstein IL (2008). Visualizing stimulus convergence in amygdala neurons during associative learning. *Proceedings of the National Academy of Sciences*. **105**(52): 20959-20963.

Barrett LF, Kensinger EA (2010). Context is routinely encoded during emotion perception. *Psychological Science*. **21**(4): 595-599.

Baumann O, Mattingley JB (2013). Dissociable representations of environmental size and complexity in the human hippocampus. *Journal of Neuroscience*. **33**(25): 10526-1053.

Bednarek E, Caroni P (2011). B-adducin is required for stable assembly of new synapses and improved memory upon environmental enrichment. *Neuron*. **69**(6): 1132-1146.

Ben-Ari Y, Cherubini E, Corradietti R, Gaiarsa JL (1989). Giant synaptic potentials in immature rat ca3 hippocampal neurones. *The Journal of Physiology*. **416**(1): 303-325.

Ben-Ari Y, Spitzer NC (2010). Phenotypic checkpoints regulate neuronal

development. *Trends in Neurosciences*. **33**(11): 485-492.

Blackstad TW (1956). Commissural connections of the hippocampal region in the rat, with special reference to their mode of termination. *The Journal of Comparative Neurology*. **105**(3): 417-537.

Blackstad TW (1958). On the termination of some afferents to the hippocampus and fascia dentata. *Acta Anatomica*. **35**(3): 202-214.

Buzsáki G (2010). Neural syntax: Cell assemblies, synapsembles, and readers. *Neuron*. **68**(3): 362-385.

Chen JL, Nedivi E (2013). Highly specific structural plasticity of inhibitory circuits in the adult neocortex. *The Neuroscientist*. **19**(4): 384-393.

Chicurel ME, Harris KM (1992). Three-dimensional analysis of the structure and composition of CA3 branched dendritic spines and their synaptic relationships with mossy fiber boutons in the rat hippocampus. *The Journal of Comparative Neurology*. **325**(2): 169-182.

Clark RE, West AN, Zola SM, Squire LR (2001). Rats with lesions of the hippocampus are impaired on the delayed nonmatching-to-sample task. *Hippocampus*. **11**(2): 176-186.

Cobb SR, Buhl EH, Halasy K, Paulsen O, Somogyi P (1995). Synchronization of neuronal activity in hippocampus by individual gabaergic interneurons. *Nature*. **378**(6552): 75-78.

Cremer H, Chazal G, Goridis C, Represa A (1997). NCAM is essential for axonal growth and fasciculation in the hippocampus. *Molecular and Cellular Neuroscience*. **8**(5): 323-335.

Cserep C, Szonyi A, Veres JM, Nemeth B, Szabadits E, de Vente J, Hajos N, Freund TF, Nyiri G (2011). Nitric oxide signaling modulates synaptic transmission during early postnatal development. *Cerebral Cortex*. **21**(9): 2065-2074.

De Paola V, Arber S, Caroni P (2003). AMPA receptors regulate dynamic equilibrium of presynaptic terminals in mature hippocampal networks. *Nature Neuroscience*. **6**(5): 491-500.

Debiec J, LeDoux JE, Nader K (2002). Cellular and systems reconsolidation in the hippocampus. *Neuron*. **36**(3): 527-538.

Deguchi Y, Donato F, Galimberti I, Cabuy E, Caroni P (2011). Temporally matched subpopulations of selectively interconnected principal neurons in the hippocampus. *Nature Neuroscience*. **14**(4): 495-504.

Dieterich DC, Hodas JJL, Gouzer G, Shadrin IY, Ngo JT, Triller A, Tirrell DA, Schuman EM (2010). *In situ* visualization and dynamics of newly synthesized proteins in rat hippocampal neurons. *Nature Neuroscience*. **13**(7): 897-905.

Dittgen T, Nimmerjahn A, Komai S, Licznerski P, Waters J, Margrie TW, Helmchen F, Denk W, Brecht M, Osten P (2004). Lentivirus-based genetic manipulations of cortical neurons and their optical and electrophysiological monitoring in vivo. *Proceedings of the National Academy of Sciences*. **101**(52): 18206-18211.

Donato F, Chowdhury A, Lahr M, Caroni P (2015). Early- and late-born parvalbumin basket cell subpopulations exhibiting distinct regulation and roles in learning. *Neuron*. **85**(4): 770-786.

Donato F, Rompani SB, Caroni P (2013). Parvalbumin-expressing basket-cell network plasticity induced by experience regulates adult learning. *Nature*. **504**(7479): 272-276.

Druckmann S, Feng L, Lee B, Yook C, Zhao T, Magee Jeffrey C, Kim J (2014). Structured synaptic connectivity between hippocampal regions. *Neuron*. **81**(3): 629-640.

Eisenberg M (2003). Stability of retrieved memory: Inverse correlation with trace dominance. *Science*. **301**(5636): 1102-1104.

Fanselow MS (1990). Factors governing one-trial contextual conditioning. *Animal Learning and Behavior*. **18**(3): 264-270.

Fanselow MS, Dong H-W (2010). Are the dorsal and ventral hippocampus functionally distinct structures? *Neuron*. **65**(1): 7-19.

Freund TF, Katona I (2007). Perisomatic inhibition. *Neuron*. **56**(1): 33-42.

Galimberti I, Bednarek E, Donato F, Caroni P (2010). EphA4 signaling in juveniles establishes topographic specificity of structural plasticity in the hippocampus. *Neuron*. **65**(5): 627-642.

Galimberti I, Gogolla N, Alberi S, Santos AF, Muller D, Caroni P (2006). Long-term rearrangements of hippocampal mossy fiber terminal connectivity in the adult regulated by experience. *Neuron*. **50**(5): 749-763.

Garner AR, Rowland DC, Hwang SY, Baumgaertel K, Roth BL, Kentros C, Mayford M (2012). Generation of a synthetic memory trace. *Science*. **335**(6075): 1513-1516.

Gogolla N, Galimberti I, DePaola V, Caroni P (2006). Preparation of organotypic hippocampal slice cultures for long-term live imaging. *Nat Protoc*. **1**(3): 1165-1171.

Gogolla N, Galimberti I, DePaola V, Caroni P (2006). Long-term live imaging of neuronal circuits in organotypic hippocampal slice cultures. *Nat Protoc*. **1**(3): 1223-1226.

Gonzales RB, DeLeon Galvan CJ, Rangel YM, Claiborne BJ (2001). Distribution of thorny excrescences on CA3 pyramidal neurons in the rat hippocampus. *The*

Journal of Comparative Neurology. **430**(3): 357-368.

Graves Austin R, Moore Shannon J, Bloss Erik B, Mensh Brett D, Kath William L, Spruston N (2012). Hippocampal pyramidal neurons comprise two distinct cell types that are counter modulated by metabotropic receptors. *Neuron.* **76**(4): 776-789.

Groenewegen HJ, der Zee EV-V, te Kortschot A, Witter MP (1987). Organization of the projections from the subiculum to the ventral striatum in the rat. A study using anterograde transport of *Phaseolus vulgaris* leucoagglutinin. *Neuroscience.* **23**(1): 103-120.

Gu L, Kleiber S, Schmid L, Nebeling F, Chamoun M, Steffen J, Wagner J, Fuhrmann M (2014). Long-term *in vivo* imaging of dendritic spines in the hippocampus reveals structural plasticity. *Journal of Neuroscience.* **34**(42): 13948-13953.

Guenthner Casey J, Miyamichi K, Yang Helen H, Heller HC, Luo L (2013). Permanent genetic access to transiently active neurons via TRAP: Targeted Recombination in Active Populations. *Neuron.* **78**(5): 773-784.

Guzowski JF, McNaughton BL, Barnes CA, Worley PF (1999). Environment-specific expression of the immediate-early gene Arc in hippocampal neuronal ensembles *Nat. Neurosci.* **2**(12): 1120-1124.

Hafting T, Fyhn M, Molden S, Moser M-B, Moser EI (2005). Microstructure of a spatial map in the entorhinal cortex. *Nature.* **436**(7052): 801-806.

Hamlyn LH (1962). Fine Structure of Mossy Fibre Endings in Hippocampus of Rabbit. *Journal of Anatomy* **96**(Pt 1): 112-20.

Hangya B, Pi H-J, Kvitsiani D, Ranade SP, Kepcs A (2014). From circuit motifs to computations: Mapping the behavioral repertoire of cortical interneurons. *Current Opinion in Neurobiology.* **26**(117-124).

Hensch TK (2005). Critical period plasticity in local cortical circuits. *Nature Reviews Neuroscience.* **6**(11): 877-888.

Henze DA, Urban NN, Barrionuevo G (2000). The multifarious hippocampal mossy fiber pathway: A review. *Neuroscience.* **98**(3): 407-427.

Herry C, Ciocchi S, Senn V, Demmou L, Müller C, Lüthi A (2008). Switching on and off fear by distinct neuronal circuits. *Nature.* **454**(7204): 600-606.

Holtmaat A, Svoboda K (2009). Experience-dependent structural synaptic plasticity in the mammalian brain. *Nature Reviews Neuroscience.* **10**(9): 647-658.

Hong W, Mosca TJ, Luo L (2012). Teneurins instruct synaptic partner matching in an olfactory map. *Nature.* **484**(7393): 201-207.

Imamura F, Ayoub AE, Rakic P, Greer CA (2011). Timing of neurogenesis is a

determinant of olfactory circuitry. *Nature Neuroscience*. **14**(3): 331-337.

Isshiki T, Pearson B, Holbrook S, Doe CQ (2001). Drosophila neuroblasts sequentially express transcription factors which specify the temporal identity of their neuronal progeny. *Cell*. **106**(4): 511-521.

Iwata J, LeDoux JE (1988). Dissociation of associative and nonassociative concomitants of classical fear conditioning in the freely behaving rat. *Behavioral Neuroscience*. **102**(1): 66-76.

Josselyn S (2010). Continuing the search for the engram: Examining the mechanism of fear memories. *Journal of Psychiatry & Neuroscience*. **35**(4): 221-228.

Kamondi A, Acsády L, Wang X-J, Buzsáki G (1998). Theta oscillations in somata and dendrites of hippocampal pyramidal cells *in vivo*: Activity-dependent phase-precession of action potentials. *Hippocampus*. **8**(3): 244-261.

Karunakaran S, Chowdhury A and Caroni P (2015). Submitted

Kepecs A, Fishell G (2014). Interneuron cell types are fit to function. *Nature*. **505**(7483): 318-326.

Kim J, Fanselow M (1992). Modality-specific retrograde amnesia of fear. *Science*. **256**(5057): 675-677.

Kishi T, Tsumori T, Yokota S, Yasui Y (2006). Topographical projection from the hippocampal formation to the amygdala: A combined anterograde and retrograde tracing study in the rat. *The Journal of Comparative Neurology*. **496**(3): 349-368.

Kjelstrup KB, Solstad T, Brun VH, Hafting T, Leutgeb S, Witter MP, Moser EI, Moser MB (2008). Finite scale of spatial representation in the hippocampus. *Science*. **321**(5885): 140-143.

Klausberger T, Somogyi P (2008). Neuronal diversity and temporal dynamics: The unity of hippocampal circuit operations. *Science*. **321**(5885): 53-57.

Kohara K, Pignatelli M, Rivest AJ, Jung H-Y, Kitamura T, Suh J, Frank D, Kajikawa K, Mise N, Obata Y, Wickersham IR, Tonegawa S (2013). Cell type-specific genetic and optogenetic tools reveal hippocampal CA2 circuits. *Nature Neuroscience*. **17**(2): 269-279.

Kwan KY, Sestan N, Anton ES (2012). Transcriptional co-regulation of neuronal migration and laminar identity in the neocortex. *Development*. **139**(9): 1535-1546.

Lapray D, Lasztoczi B, Lagler M, Viney TJ, Katona L, Valenti O, Hartwich K, Borhegyi Z, Somogyi P, Klausberger T (2012). Behavior-dependent specialization of identified hippocampal interneurons. *Nature Neuroscience*. **15**(9): 1265-1271.

Lavenex P, Banta Lavenex P, Amaral DG (2007). Postnatal development of the

primate hippocampal formation. *Developmental Neuroscience*. **29**(1-2): 179-192.

Lawrence JJ, Grinspan ZM, McBain CJ (2004). Quantal transmission at mossy fibre targets in the CA3 region of the rat hippocampus. *The Journal of Physiology*. **554**(1): 175-193.

Lawrence JJ, McBain CJ (2003). Interneuron diversity series: Containing the detonation – feedforward inhibition in the CA3 hippocampus. *Trends in Neurosciences*. **26**(11): 631-640.

LeDoux JE (2000). Emotion circuits in the brain. *Annu. Rev. Neurosci.* **23**(1): 155-184.

Lee S-H, Marchionni I, Bezaire M, Varga C, Danielson N, Lovett-Barron M, Losonczy A, Soltesz I (2014). Parvalbumin-positive basket cells differentiate among hippocampal pyramidal cells. *Neuron*. **82**(5): 1129-1144.

Legault M, Rompre, PP & Wise RA (2000). Chemical stimulation of the ventral hippocampus elevates nucleus accumbens dopamine by activating dopaminergic neurons of the ventral tegmental area. *Journal of Neuroscience* **20**(4): 1635-42.

Lemon N, Manahan-Vaughan D (2011). Dopamine D1/D5 receptors contribute to *de novo* hippocampal LTD mediated by novel spatial exploration or locus coeruleus activity. *Cerebral Cortex*. **22**(9): 2131-2138.

Li Y, Lu H, Cheng P-I, Ge S, Xu H, Shi S-H, Dan Y (2012). Clonally related visual cortical neurons show similar stimulus feature selectivity. *Nature*. **486**(7401): 118-121.

Liu X, Ramirez S, Pang PT, Puryear CB, Govindarajan A, Deisseroth K, Tonegawa S (2012). Optogenetic stimulation of a hippocampal engram activates fear memory recall. *Nature*. **484**(7394): 381-385.

Lohmann C, Bonhoeffer T (2008). A role for local calcium signaling in rapid synaptic partner selection by dendritic filopodia. *Neuron*. **59**(2): 253-260.

Magarinos AM, McEwen BS, Sabouret M, Pevet P (2006). Rapid and reversible changes in intrahippocampal connectivity during the course of hibernation in european hamsters. *Proceedings of the National Academy of Sciences*. **103**(49): 18775-18780.

Makino H, Komiyama T (2015). Learning enhances the relative impact of top-down processing in the visual cortex. *Nature Neuroscience*. **18**(8): 1116-1122.

Manns JR, Hopkins RO, Squire LR (2003). Semantic memory and the human hippocampus. *Neuron*. **38**(1): 127-133.

Margolis SS, Salogiannis J, Lipton DM, Mandel-Brehm C, Wills ZP, Mardinly AR, Hu L, Greer PL, Bikoff JB, Ho H-YH, Soskis MJ, Sahin M, Greenberg ME (2010). EphB-mediated degradation of the RhoA GEF Ephexin5 relieves a developmental brake on excitatory synapse formation. *Cell*. **143**(3): 442-455.

Marissal T, Bonifazi P, Picardo MA, Nardou R, Petit LF, Baude A, Fishell GJ, Ben-Ari Y, Cossart R (2012). Pioneer glutamatergic cells develop into a morpho-functionally distinct population in the juvenile CA3 hippocampus. *Nature Communications*. **3**:1316.

Marrone DF, Schaner MJ, McNaughton BL, Worley PF, Barnes CA (2008). Immediate-early gene expression at rest recapitulates recent experience. *Journal of Neuroscience*. **28**(5): 1030-1033.

Miles R, Tóth K, Gulyás AI, Hájos N, Freund TF (1996). Differences between somatic and dendritic inhibition in the hippocampus. *Neuron*. **16**(4): 815-823.

Mizuseki K, Diba K, Pastalkova E, Buzsáki G (2011). Hippocampal CA1 pyramidal cells form functionally distinct sublayers. *Nature Neuroscience*. **14**(9): 1174-1181.

Morris RGM, Garrud P, Rawlins JNP, O'Keefe J (1982). Place navigation impaired in rats with hippocampal lesions. *Nature*. **297**(5868): 681-683.

Moser MB, Moser EI, Forrest E, Andersen P, Morris RG (1995). Spatial learning with a minislab in the dorsal hippocampus. *Proceedings of the National Academy of Sciences*. **92**(21): 9697-9701.

Muller JF, Mascagni F, McDonald AJ (2005). Coupled networks of Parvalbumin-immunoreactive interneurons in the rat basolateral amygdala. *Journal of Neuroscience*. **25**(32): 7366-7376.

Mumby DG, Pinel JPJ (1994). Rhinal cortex lesions and object recognition in rats. *Behavioral Neuroscience*. **108**(1): 11-18.

Murray AJ, Peace AG, Shewan DA (2009). cGMP promotes neurite outgrowth and growth cone turning and improves axon regeneration on spinal cord tissue in combination with cAMP. *Brain Research*. **1294**:12-21.

Myers KM, Davis M (2002). Behavioral and neural analysis of extinction. *Neuron*. **36**(4): 567-584.

Nader K (2003). Memory traces unbound. *Trends in Neurosciences*. **26**(2): 65-72.

Nemanic S, Alvarado MC, Bachevalier J (2004). The hippocampal/parahippocampal regions and recognition memory: Insights from visual paired comparison versus object-delayed nonmatching in monkeys. *Journal of Neuroscience*. **24**(8): 2013-2026.

Neves G, Cooke SF, Bliss TVP (2008). Synaptic plasticity, memory and the hippocampus: A neural network approach to causality. *Nature Reviews Neuroscience*. **9**(1): 65-75.

Nikonenko I, Boda B, Steen S, Knott G, Welker E, Muller D (2008). PSD-95

promotes synaptogenesis and multiinnervated spine formation through nitric oxide signaling. *The Journal of Cell Biology*. **183**(6): 1115-1127.

Nitz D, Mc Naughton B (2004). Differential modulation of CA1 and dentate gyrus interneurons during exploration of novel environments. *Journal of Neurophysiology*. **91**(2): 863-872.

Ogilvie P, Schiling K, Billinsley ML, Schmidt HHW (1995). Induction and variants of neuronal nitric oxide synthase type 1 during synaptogenesis. *FASEB Journal* **9**(9): 799-806.

Ojo B, Davies H, Rezaie P, Gabbott P, Colyer F, Kraev I, Stewart MG (2013). Age-induced loss of mossy fibre synapses on CA3 thorns in the CA3 stratum lucidum. *Neuroscience Journal*. **2013**.

Pedreira MaE, Maldonado H (2003). Protein synthesis subserves reconsolidation or extinction depending on reminder duration. *Neuron*. **38**(6): 863-869..

Petrovich GD, Canteras NS, Swanson LW (2001). Combinatorial amygdalar inputs to hippocampal domains and hypothalamic behavior systems. *Brain Research Reviews*. **38**(1-2): 247-289.

Phelps EA, Delgado MR, Nearing KI, LeDoux JE (2004). Extinction learning in humans. *Neuron*. **43**(6): 897-905.

Phillips RG, LeDoux JE (1992). Differential contribution of amygdala and hippocampus to cued and contextual fear conditioning. *Behavioral Neuroscience*. **106**(2): 274-285.

Pikkarainen M, Rönkkö S, Savander V, Insausti R, Pitkänen A (1999). Projections from the lateral, basal, and accessory basal nuclei of the amygdala to the hippocampal formation in rat. *The Journal of Comparative Neurology*. **403**(2): 229-260.

Pitkänen A, Pikkarainen M, Nurminen N, Ylinen A (2000). Reciprocal connections between the amygdala and the hippocampal formation, perirhinal cortex, and postrhinal cortex in rat: A review. *Annals of the New York Academy of Sciences*. **911**(1): 369-391.

Pizzorusso T, Medini P, Berardi N, Sabrina C, Fawcett JW, Maffei L (2002). Reactivation of ocular dominance plasticity in the adult visual cortex. *Science*. **298**(5596): 1248-1251.

Pleasure SJ, Anderson S, Hevner R, Bagri A, Marin O, Lowenstein DH, Rubenstein JLR (2000). Cell migration from the ganglionic eminences is required for the development of hippocampal GABAergic interneurons. *Neuron*. **28**(3): 727-740.

Ramirez S, Liu X, MacDonald CJ, Moffa A, Zhou J, Redondo RL, Tonegawa S (2015). Activating positive memory engrams suppresses depression-like

behaviour. *Nature*. **522**(7556): 335-339.

Reed JM, Squire LR (1997). Impaired recognition memory in patients with lesions limited to the hippocampal formation. *Behavioral Neuroscience*. **111**(4): 667-675.

Rogers SJ, Wehner EA, Hagerman R (2001). The behavioral phenotype in fragile x: Symptoms of autism in very young children with fragile x syndrome, idiopathic autism, and other developmental disorders. *Journal of Developmental & Behavioral Pediatrics*. **22**(6): 409-417.

Royer S, Zemelman BV, Losonczy A, Kim J, Chance F, Magee JC, Buzsáki G (2012). Control of timing, rate and bursts of hippocampal place cells by dendritic and somatic inhibition. *Nature Neuroscience*. **15**(5): 769-775.

Ruediger S, Spirig D, Donato F, Caroni P (2012). Goal-oriented searching mediated by ventral hippocampus early in trial-and-error learning. *Nature Neuroscience*. **15**(11): 1563-1571.

Ruediger S, Vittori C, Bednarek E, Genoud C, Strata P, Sacchetti B, Caroni P (2011). Learning-related feedforward inhibitory connectivity growth required for memory precision. *Nature*. **473**(7348): 514-518.

Sandi C, Davies HA, Cordero MI, Rodriguez JJ, Popov VI, Stewart MG (2003). Rapid reversal of stress induced loss of synapses in CA3 of rat hippocampus following water maze training. *European Journal of Neuroscience*. **17**(11): 2447-2456.

Sargolini F, Fyhn M, Hafting T, McNaughton BL, Witter MP, Moser MB, Moser EI (2006). Conjunctive representation of position, direction, and velocity in entorhinal cortex. *Science*. **312**(5774): 758-762.

Scoville WB, Milner B (1957). Loss of recent memory after bilateral hippocampal lesions. *Journal of Neurology, Neurosurgery & Psychiatry*. **20**(1): 11-21.

Sheng M, Greenberg ME (1990). The regulation and function of c-fos and other immediate early genes in the nervous system. *Neuron*. **4**(4): 477-485.

Solstad T, Boccara CN, Kropff E, Moser MB, Moser EI (2008). Representation of geometric borders in the entorhinal cortex. *Science*. **322**(5909): 1865-1868.

Stark E, Koos T, Buzsáki G (2012). Diode probes for spatiotemporal optical control of multiple neurons in freely moving animals. *Journal of Neurophysiology*. **108**(1): 349-363.

Stewart MG, Davies HA, Sandi C, Kraev IV, Rogachevsky VV, Peddie CJ, Rodriguez JJ, Cordero MI, Donohue HS, Gabbott PLA, Popov VI (2005). Stress suppresses and learning induces plasticity in CA3 of rat hippocampus: A three-dimensional ultrastructural study of thorny excrescences and their postsynaptic densities. *Neuroscience*. **131**(1): 43-54.

Stirling RV and Bliss TV(1978). Hippocampal mossy fiber development at the

ultrastructural level. *Progress in Brain Research* **48**: 191-198.

Strange BA, Witter MP, Lein ES, Moser EI (2014). Functional organization of the hippocampal longitudinal axis. *Nature Reviews Neuroscience*. **15**(10): 655-669.

Suzuki A, Josselyn SA, Frankland PW, Masushige S, Silvia AJ, Kida S (2004). Memory reconsolidation and extinction have distinct temporal and biochemical signatures. *Journal of Neuroscience*. **24**(20): 4787-4795.

Szabadics J, Soltesz I (2009). Functional specificity of mossy fiber innervation of GABAergic cells in the hippocampus. *Journal of Neuroscience*. **29**(13): 4239-4251.

Tang JCY, Rudolph S, Dhanda OS, Abraira VE, Choi S, Lapan SW, Drew IR, Drokhlyansky E, Huberman AD, Regehr WG, Cepko CL (2015). Cell type-specific manipulation with GFP-dependent Cre recombinase. *Nature Neuroscience*. **18**(9): 1334-1341.

Thompson CL, Pathak SD, Jeromin A, Ng LL, MacPherson CR, Mortrud MT, Cusick A, Riley ZL, Sunkin SM, Bernard A, Puchalski RB, Gage FH, Jones AR, Bajic VB, Hawrylycz MJ, Lein ES (2008). Genomic anatomy of the hippocampus. *Neuron*. **60**(6): 1010-1021.

Torborg CL, Nakashiba T, Tonegawa S, McBain CJ (2010). Control of CA3 output by feedforward inhibition despite developmental changes in the excitation-inhibition balance. *Journal of Neuroscience*. **30**(46): 15628-15637.

Trifilieff P, Herry C, Vanhoutte P, Caboche J, Desmedt A, Riedel G, Mons N, Micheau J (2006). Foreground contextual fear memory consolidation requires two independent phases of hippocampal ERK/CREB activation. *Learning & Memory*. **13**(3): 349-358.

Tripodi M, Stepien AE, Arber S (2011). Motor antagonism exposed by spatial segregation and timing of neurogenesis. *Nature*. **479**(7371): 61-66.

Tronson NC, Wiseman SL, Neve RL, Nestler EJ, Olausson P, Taylor JR (2012). Distinctive roles for amygdalar CREB in reconsolidation and extinction of fear memory. *Learning & Memory*. **19**(5): 178-181.

Tsamis K, Mytilinaios D, Njau S, Fotiou D, Glaftsi S, Costa V, Baloyannis S (2010). Properties of CA3 dendritic excrescences in Alzheimer's disease. *CAR*. **7**(1): 84-90.

Tulving E (1972). Organization of Memory. 381-403.

Wanisch K, Wotjak CT (2008). Time course and efficiency of protein synthesis inhibition following intracerebral and systemic anisomycin treatment. *Neurobiology of Learning and Memory*. **90**(3): 485-494.

Wilke SA, Antonios JK, Bushong EA, Badkoobehi A, Malek E, Hwang M, Terada

M, Ellisman MH, Ghosh A (2013). Deconstructing complexity: Serial block-face electron microscopic analysis of the hippocampal mossy fiber synapse. *Journal of Neuroscience*. **33**(2): 507-522.

Willemse R, Levenga J, Oostra BA (2011). CGG repeat in the fmr1 gene: Size matters. *Clinical Genetics*. **80**(3): 214-225.

Witton J, Padmashri R, Zinyuk LE, Popov VI, Kraev I, Line SJ, Jensen TP, Tedoldi A, Cummings DM, Tybulewicz VLJ, Fisher EMC, Bannerman DM, Randall AD, Brown JT, Edwards FA, Rusakov DA, Stewart MG, Jones MW (2015). Hippocampal circuit dysfunction in the Tc1 mouse model of down syndrome. *Nature Neuroscience*. **18**(9): 1291-1298.

Wojtowicz JM, Kee N (2006). Brdu assay for neurogenesis in rodents. *Nat Protoc*. **1**(3): 1399-1405.

Yoshihara Y, De Roo M, Muller D (2009). Dendritic spine formation and stabilization. *Current Opinion in Neurobiology*. **19**(2): 146-153.

Yu Y-C, Bultje RS, Wang X, Shi S-H (2009). Specific synapses develop preferentially among sister excitatory neurons in the neocortex. *Nature*. **458**(7237): 501-504.

Zola SM, Squire LR, Teng E, Stefanacci L, Buffalo EA, Clark RE (2000). Impaired recognition memory in monkeys after damage limited to the hippocampal region. *The Journal of Neuroscience*. **20**(1): 451-463.

Zola-Morgan S, Squire LR, Ramus SJ (1995). The role of the hippocampus in declarative memory: A reply to nadel. *Hippocampus*. **5**(3): 235-239